

Regulation and Quaternary Structure of Human Equilibrative Nucleoside Transporter 1

by

Xenia Cravetchi

This thesis is submitted in partial fulfillment of the requirements for the degree of

Master of Science

Department of Pharmacology

University of Alberta

© Xenia Cravetchi, 2016

ABSTRACT

Equilibrative nucleoside transporter 1 (ENT1) is an ubiquitously expressed membrane transporter in mammalian cells responsible for the transmembrane flux of endogenous nucleosides such as adenosine, as well as chemotherapeutic, anti-viral, and anti-parasitic nucleoside analogues. The present studies were designed to: 1) assess whether changes in ENT1 trafficking to the plasma membrane are responsible for enhanced uptake function observed in response to stimulation at adenosine receptor 1 (A₁AR) or protein kinase C (PKC) activation, and 2) determine whether ENT1 forms a multimeric protein complex.

Immunofluorescence co-localization and cell surface biotinylation studies were conducted to quantify changes in plasma-membrane localized ENT1 in response to phorbol 12-myristate 13-acetate (PMA), a PKC activator, and 2-chloro-N(6)-cyclopentyladenosine (CCPA), an A₁AR stimulator. It was found that an increase in ENT1 trafficking to the plasma membrane in response to PKC stimulation partially accounts for enhanced uptake function; however, intermediate factors may be involved as in PK15-S281A-hENT1 cells, an increase in plasma membrane expression is not reflected by an increase in uptake function. Stimulation of A₁AR did not have an effect on ENT1 localization at the plasma membrane; therefore, the CCPA-induced increase in uptake activity is achieved by changes to ENT1 already at the plasma membrane. These findings provide some insight into regulation of ENT1 activity.

Co-immunoprecipitation and proximity ligation assays showed that, in intact cells, ENT1 proteins interact. Moreover, mass spectrometry and proximity ligation studies identified Na⁺/K⁺-ATPase as a potential binding partner of ENT1. We conclude that hENT1 exists as a dimer in intact cells and potentially interacts with other membrane proteins.

The findings of this thesis open new avenues of research relating to regulation of transporter activity, including the influence of quaternary structure and binding partners on transport function and ligand binding.

Keywords: nucleoside transport, ENT1, trafficking, oligomerization, complex

PREFACE

Some of the research in this thesis has been published. Rationale for pursuing some of the work in this thesis comes from research by Scott J. Hughes, previously a student in the Hammond laboratory, and is summarized in Chapter 2. At the time of Scott's work, the Hammond laboratory was in the Department of Physiology and Pharmacology at Western University in London, Ontario. The uptake assays with PMA were replicated in the lab here at the University of Alberta. My original work in chapter 4.1 of this thesis, were published as X. Cravetchi and S. Hughes, J. Vilas, J.R. Hammond, "Adenosine A1 receptor activation modulates human equilibrative nucleoside transporter 1 (hENT1) activity via PKC-mediated phosphorylation of serine-281," *Cellular Signaling*, vol. 27, issue 5, 1008-1018. In this publication, Scott Hughes and I are listed as co-first authors. G. Vilas contributed key radioligand binding and uptake experiments as well as shRNA work to the publication, and was a key player in manuscript compilation and editing. I also participated in writing the relevant methods and materials, results, and discussion sections of the manuscript as well as editing the final work. J.R. Hammond was the supervisory author and was involved in concept formulation, manuscript composition and submission.

ACKNOWLEDGEMENTS

Thank you Dr. Hammond for having me as a member of your laboratory, your support of my work and growth as a professional outside the laboratory. Thank you to my advisory committee, Dr. Andy Holt, Dr. Jim Young, and Dr. Nicolas Touret, for your advice and great questions during committee meetings. Huge thank you to Dr. Gonzalo Vilas and Catherine Compston, completing our small lab crew, for scientific mentorship, “tough love” in editing and commenting on my work, laughs, and always having my back. I also cannot thank Greg Plummer and Stephen Ogg enough for training me on the confocal microscope and being there when things went awry, as they often did. To Dr. Andrew Simmonds and all the members of his lab, thank you for sharing your IMARIS program and expertise with me, and even more importantly thank you for your lively, positive company during the many hours I spent working in your lab. Thank you to Dr. Sampath Loganath for your scientific advice and providing access to equipment. Thanks to Jaclyn Hutchinson, Shelynn Hui, Logan Smith and Chantal Allan for your company in the summers! Dr. Frances Plane and Dr. Paul Kerr, thank you for your support both personal and academic. Stephanie Lunn and Ran Wei, I am so glad that you were just down the fall from me, thank you for everything. Thank you to my mom and dad, Olga and Igor Cravetchi, for being shining examples of brilliant scientists, listening to my experimental dilemmas and pushing me along to complete this program! I can’t thank my friends enough for always being there to listen, laugh, and even edit bits of my work right when it mattered. Huge thank you to the “find and replace” feature developers for Microsoft Word, without whom the final revisions of this document would have taken a little longer. Finally, Luke, thank you for keeping me sane and supporting me unconditionally through this journey.

LIST OF FIGURES

Figure 1.1 Nucleosides	3
Figure 1.2 Signaling Through Adenosine Receptors	4
Figure 1.3 Predicted Eleven-Transmembrane Domain Topology for hENT1.....	9
Figure 2.1 Initial rate of uptake of [³ H]2-Chloroadenosine following PKC activation in PK15-hENT1 and PK15-S281A-hENT1 cells	31
Figure 2.2 Initial rate of uptake of [³ H]2-Chloroadenosine following A ₁ AR stimulation in PK15-hENT1 and PK15-S281A-hENT1 cells	32
Figure 2.3 Changes in V _{max} of PK15-hENT1 Cells.....	33
Figure 2.4 Graphical representation of Objective 1: Regulation of hENT1 expression at the plasma membrane	34
Figure 4.1 PK15-hENT1 Cells, +/- 100 nM PMA Treatment	51
Figure 4.2 PK15-S281A-hENT1 Cells, +/- 100 nM PMA Treatment.....	53
Figure 4.3 PK15-hENT1 Cells, +/- 100 nM CCPA Treatment	55
Figure 4.4 PK15-S281A-hENT1 Cells, +/- 100 nM CCPA Treatment.....	57
Figure 4.5 Quantifying colocalization of hENT1 with plasma membrane marker, GPI-GFP	59
Figure 4.6 Representative Western Blots of cell surface processing experiments	62
Figure 4.7 Quantifying hENT1 at the plasma membrane	64
Figure 4.8 Co-Immunoprecipitation Western Blot	68
Figure 4.9 Chemical cross-linking of PK15-hENT1 cells	71
Figure 4.10 Chemical cross-linking of HEK293 cells expressing MYC- and HA- hENT1	73
Figure 4.11 Proximity Ligation Assay Images Showing hENT1 Monomer Interaction	75
Figure 4.12 Quantitation of Proximity Ligation Assay	77

Figure 4.13 Proximity Ligation Assay of PK15-hENT1_{FLAG} with Na⁺/K⁺-ATPase..... 80

LIST OF TABLES

Table 1.1 Equilibrative Nucleoside Transporter Family, Substrate Selectivity, and Distribution . 6

Table 1.2 Inhibitors of hENT1 23

Table 1.3 Selection of Nucleoside Analog Drugs 26

Table 4.1 Mass Spectrometry In-Gel ID Results..... 78

LIST OF ABBREVIATIONS

4 α -PMA; 4 α -phorbol 12-myristate 13-acetate
A1AR; adenosine A1 receptor
A_{2a}AR; adenosine 2a receptor
A_{2b}AR; adenosine 2b receptor
A₃AR; adenosine 3 receptor
A; alanine
AE1; anion exchanger 1
ANOVA; analysis of variance
ATP; adenosine triphosphate
BLAST; basic local alignment search tool
BLASTP; basic local alignment search tool protein
CAII; carbonic anhydrase II
cAMP; cyclic adenosine monophosphate
CCPA; 2-chloro-N(6)-cyclopentyladenosine
CD39; 5'-ectonucleotidase
cDNA; complementary deoxyribonucleic acid
CKII; Casein Kinase II
CNT; concentrative nucleoside transporter
Co-IP; co-immunoprecipitation
CORUM; comprehensive resource of mammalian protein complexes
CSP; cell surface processing
CTS; cationic steroids
DAPI; 4',6-diamidino-2-phenylindole
DDM; dodecyl maltoside
DIP; database of interacting proteins
Dilazep; (N,N'-bis[3-(3,4,5-trimethoxybenzyloxy)propyl]-homo-piperazine)

Dipyridamole; [2,6-bis (diethanolamino)-4,8-dipiperidinopyrimido-[5,4-d]pyrimidine]
DMSO; dimethyl sulfoxide
DNA; deoxyribonucleic acid
D-PBS; Dulbecco's phosphate buffered saline
DPCPX; 8-Cyclopentyl-1,3-dipropylxanthine
Draflazine; [2-(aminocarbonyl)-4-amino-2,6-dichlorophenyl]-4-[5,5-bis(4-fluorophenyl) pentyl]-1-piperazine acetamide 2HCl]
DSP; dithiobis [succinimidylpropionate]
DTSSP; 3,3'-dithiobis [sulfosuccinimidylpropionate]
DTT; dithiothreitol
ENT1; equilibrative nucleoside transporter subtype 1
ERK; extracellular signal-regulated kinase
FLAG; DYKDDDDK amino acid tag
G; glycine

GAPDH; glyceraldehyde-3-phosphate dehydrogenase
Gö6983; 3-[1-[3-(dimethylamino)propyl]-5-methoxy-1*H*-indol-3-yl]-4-(1*H*-indol-3-yl)-1*H*-pyrrole-2,5-dione
GLUT; glucose transporter
GPCR; G-protein coupled receptor
GPI-GFP; glycosylphosphatidyl-inositol-anchored green fluorescent protein
h; human
HA; protein tag, YPYDVPDYA amino acids
HIF; hypoxia inducible factor
IF; immunofluorescence
K; lysine
m; mouse
mAB; monoclonal antibody
MAP; mitogen activated protein
MDCK; Madin-Darby canine kidney cells
MYC; protein tag, EQKLISEEDL amino acids
MEM; Modified Eagle Medium
mRNA; messenger ribonucleic acid
Na⁺/K⁺-ATPase; sodium potassium ATPase
NBMPR; nitrobenzylmercaptapurine riboside
NPS; network protein sequence analysis
NT; nucleoside transporter
Pf; *P. falciparum*
PK15-NTD; nucleoside transport deficient pig kidney epithelial cells derived from the PK15 cell line
PKA; protein kinase A
PKC; protein kinase C
PLA; proximity ligation assay
PMA; phorbol 12-myristate 13-acetate
PMAT; plasma membrane monoamine transporter
r; rat
RNA; ribonucleic acid
ROI; region of interest
S; serine
SDS-PAGE; sodium dodecyl sulfate polyacrylamide gel electrophoresis
SEM; standard error of mean
SLC; solute carrier family
TMD; transmembrane domain
t-RNA; transfer RNA
V_{max}; maximum transport rate
WT; wild-type

Table of Contents

ABSTRACT.....	ii
PREFACE.....	iv
ACKNOWLEDGEMENTS.....	v
LIST OF FIGURES.....	vi
LIST OF TABLES.....	vii
LIST OF ABBREVIATIONS.....	viii
CHAPTER 1. INTRODUCTION.....	1
1.1 Nucleosides.....	1
1.2 Nucleoside Transporters.....	5
1.3 Equilibrative Nucleoside Transporter Subtype 1, ENT1.....	6
1.3.1 Molecular Properties of ENT1.....	7
1.3.2 Trafficking and Localization of ENT1.....	11
1.3.3 Transport Mechanism of ENT1.....	13
1.3.4 Regulation of ENT1.....	15
1.3.5 Oligomerization of ENT1.....	19
1.4 Clinical Relevance.....	21
1.4.1 ENT1 Inhibitors.....	23
1.4.2 Nucleoside Analog Drugs.....	26
CHAPTER 2. RATIONALE FOR RESEARCH OBJECTIVES.....	29
2.1 Rationale and Hypothesis for Objective 1: Regulation of hENT1.....	29
2.2 Rationale and Hypothesis for Objective 2: hENT1 Complex.....	35
2.3 Specific Goals.....	39
CHAPTER 3. MATERIALS AND METHODS.....	40
3.1 Materials.....	40
3.2 Immunofluorescence Analysis of FLAG-ENT1 Colocalized to the Plasma Membrane.....	41
3.3 Cell Surface Processing by Biotinylation.....	43
3.4 Co-Immunoprecipitation Analysis.....	44
3.5 Extracellular Chemical Cross-Linking with DTSSP and Zinc Formalin.....	44
3.6 Proximity Ligation Assay.....	45
3.7 Mass Spectrometry Analysis Sample Preparation.....	46
3.8 Data Analysis.....	47
CHAPTER 4. RESULTS.....	49

4.1 Regulation of hENT1 by PKC Activation and A ₁ AR Stimulation.....	49
4.1.1 Immunofluorescence Analysis of hENT1 Localization	50
4.1.2 Cell Surface Processing by Biotinylation	61
4.2 Multimeric hENT1 Complex	66
4.2.1 Co-Immunoprecipitation in HEK293 Cells.....	66
4.2.2 PK15-hENT1 Cells Did Not Show Cross-Linking of ENT1	70
4.2.3 Proximity Ligation Assay in PK15-hENT1 Cells	74
4.2.4 Mass Spectrometry In-Gel ID	78
4.2.5 Proximity Ligation of hENT1 and Na ⁺ /K ⁺ -ATPase	79
CHAPTER 5. DISCUSSION.....	81
5.1 A PKC-Mediated Mechanism is Partially Responsible for Increasing ENT1 Expression at The Plasma Membrane	81
5.2 hENT1 Forms Dimers in Intact Cells	86
5.2.1 Interacting Partners of hENT1.....	92
5.3 Conclusions	96
REFERENCES.....	98
APPENDICES	109

CHAPTER 1. INTRODUCTION

Nucleoside transporters mediate the flux of nucleosides which are otherwise unable to pass across semi-permeable membranes due to their hydrophilicity and size. Adequate intracellular and extracellular nucleoside concentrations are necessary for various cell functions; nucleosides serve as building blocks for energy carrier molecules and nucleic acids and nucleosides also have cell signaling functions. Changes to expression levels and function of these transport systems can result in both deleterious or constructive cellular responses under hypoxic conditions or in certain cancers, for example. Equilibrative nucleoside transporter 1 (ENT1) is an ubiquitously expressed nucleoside transporter and the subject of this thesis. The important biological functions of nucleosides and their transport systems are discussed in Section 1.1 and 1.2. The molecular properties of ENT1, ENT1 trafficking and ENT1 regulation are discussed in Section 1.3. Section 1.4 addresses the clinical and pharmacological relevance of ENT1.

1.1 Nucleosides

Nucleoside molecules have a glucosylamine structure that consists of a nitrogenous base attached to a five-carbon sugar (either ribose or deoxyribose) by a beta-glycosidic linkage. The nitrogenous bases of nucleosides fall into one of two categories: purine and pyrimidine. Pyrimidine bases are composed of one six-sided di-nitrogenous ring structure with various functional groups, while purine bases have two rings. Some examples of nucleosides, adenosine, guanosine, cytidine, uridine, thymidine and inosine are shown in Figure 1.1.

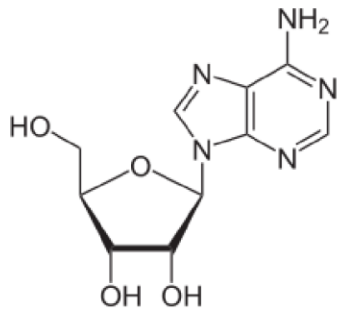
Nucleosides have many physiological functions, and they serve as building blocks for many important biological molecules including deoxyribonucleic acids needed for DNA replication. They also make up energy carrier molecules such as adenosine tri-phosphate (ATP) and guanylate tri-phosphate (GTP). Therefore, their abundance in cells is necessary for normal cellular function. In most cells, nucleosides can be produced *de novo* by multi-enzyme complexes; however, under conditions of high metabolic stress, rapid growth, or in cells incapable of *de novo* synthesis, the salvage pathway is also used to retrieve nucleosides from extracellular environments. In humans, tissues vary in their dependence on *de novo* versus salvage pathways; for example, enterocytes, leukocytes, and bone marrow cells are incapable of *de novo* synthesis of nucleosides¹.

Nucleosides also act as signaling molecules. Extracellular adenosine, specifically, stimulates purinergic receptors on the cell surface. There are four subtypes of these G-protein coupled receptors: A₁AR, A_{2a}AR, A_{2b}AR, and A₃AR. These receptors vary in their tissue distribution and also in the types of cell signaling cascades their stimulation initiates, as is shown in Figure 1.2².

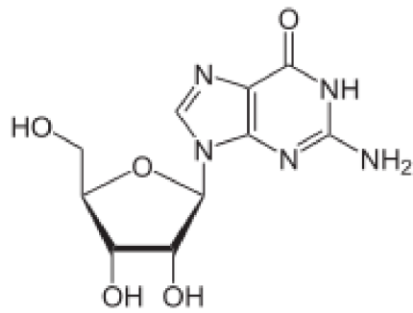
Through actions at these receptors, adenosine is a neuromodulator, an anti-inflammatory agent, has vasodilatory effects, and regulates cardiomyocytes in response to ischemia³⁻⁶.

Due to their size and hydrophilicity, nucleosides are unable to move passively across cell membranes and require specialized transporters to facilitate their movement.

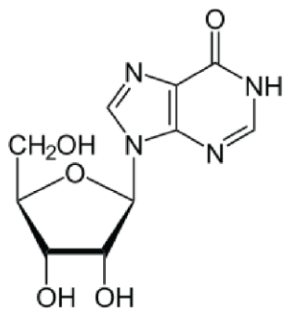
Figure 1.1 Nucleosides
Purines



Adenosine

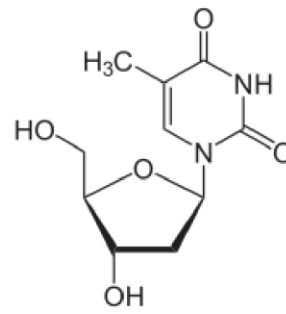


Guanosine

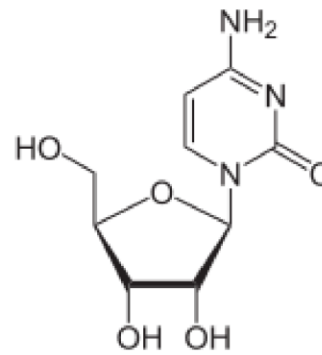


Inosine

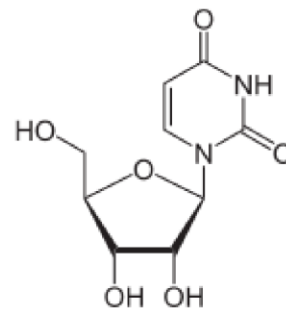
Pyrimidines



Thymidine



Cytidine



Uridine

Figure 1.2 Signaling Through Adenosine Receptors ¹

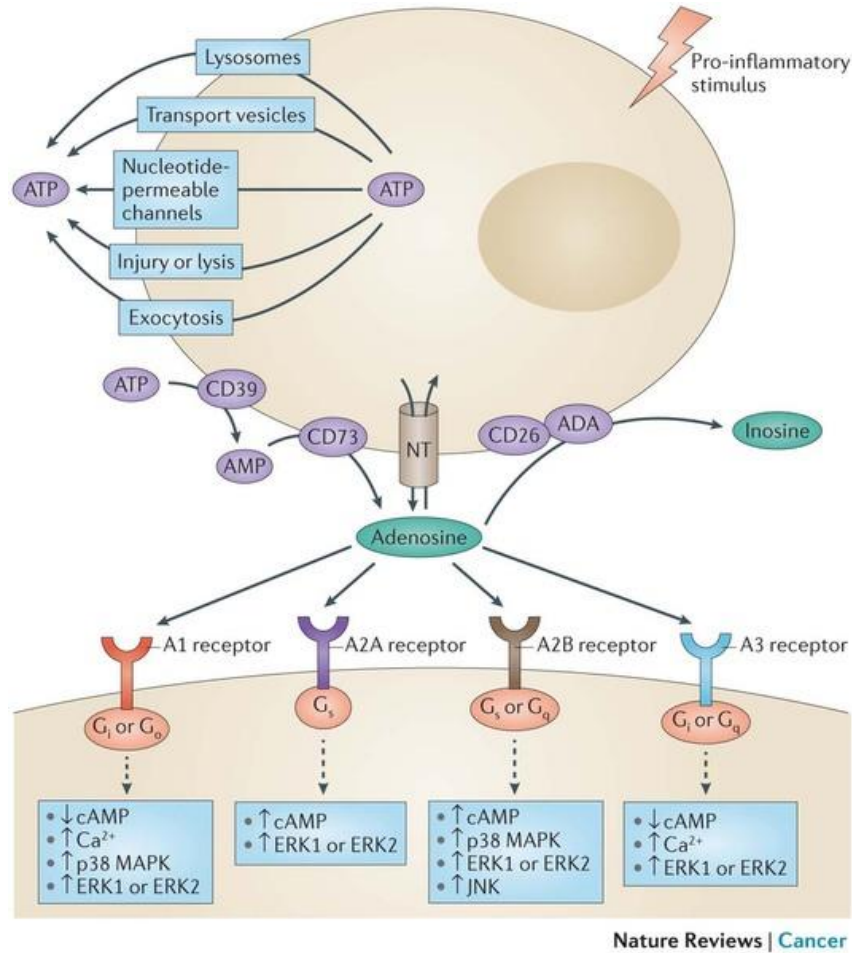


Figure 1.2: Signaling pathways through adenosine receptors following stimulation by adenosine. Adenosine can be formed in the extracellular space or inside the cell and transported to the extracellular milieu by ENT1. CD39 is the 5'-ectonucleotidase which converts ATP to AMP, and CD73 is a phosphatase converting AMP to adenosine. Clearance of adenosine from the extracellular space can be accomplished by uptake through nucleoside transporters (NT) or metabolism into inosine by adenosine deaminase (ADA). Stimulation of G-protein coupled adenosine receptors leads to the changes in secondary messengers, c-AMP and intracellular calcium ions (Ca²⁺) levels as well as activation of several kinases including mitogen activated protein kinase 38 (p38-MAPK), extracellular signal regulated kinases 1 and 2 (ERK1, ERK2), and c-Jun N-terminal kinase (JNK).

¹ Reprinted by permission from Macmillan Publishers Ltd on behalf of Cancer Research UK: Antonioli, Luca; Blandizzi, Corrado; Pacher, Pal; Hasko, Gyorgy. Immunity, inflammation, and cancer: a leading role for adenosine. *Nature Publishing Group, a division of Macmillan Publishers Limited. All Rights Reserved. Vol. 13 (12) p. 844, Figure 1.*

1.2 Nucleoside Transporters

There are two families of nucleoside transporters (NTs) that facilitate the movement of nucleosides across cell membranes: concentrative nucleoside transporters (CNTs), encoded by the SLC28 genes on human chromosomes 9 and 15, and the equilibrative nucleoside transporters (ENTs), encoded by SLC29 genes on human chromosomes 6, 7, 10, 11. These nucleoside transporters belong to a diverse family of solute carrier (SLC) proteins. The main difference between CNTs and ENTs is that CNTs facilitate the active transport of their substrate, relying on a sodium or proton gradient, whereas equilibrative nucleoside transporters are passive/ion-independent transporters that are driven solely by the substrate concentration gradient.

There are three members of the SLC28 family: CNT1, CNT2 and CNT3. hCNT1 (human CNT1) and hCNT2 facilitate unidirectional flux of nucleosides from extracellular milieu into the cell by a sodium-dependent mechanism^{7,8}. hCNT3 can use both a sodium or proton gradient to facilitate transport of a broad range of substrates, also into the cell. CNTs are primarily expressed in epithelial cells of tissues responsible for high quantities of absorption and secretion processes, such as in the small intestine, kidneys, and liver⁹. A crystal structure of the CNT structure from *V. cholera* has been elucidated¹⁰. The *V. cholera* CNT has 39% sequence homology to hCNT3. The prokaryotic CNT also transports substrates with the use of a sodium gradient, and although lacking three of the predicted eleven transmembrane domains of hCNT3, the model is a useful tool for predicting the possible structure of the human protein.

The equilibrative nucleoside transporters (ENTs) ENT1, ENT2, ENT3 and ENT4 are encoded by the SLC29 gene family (Table 1.2)¹¹. ENT1 and ENT2 are responsible for passive, bidirectional

transport of purine and pyrimidine nucleosides (and, with varying affinities, some nucleobases) across the plasma membrane¹². Historically, these two transporters have been identified by their sensitivity to an inhibitor, S-(4-Nitrobenzyl)-6-thioinosine (NBMPR), and are known as *es* (ENT1 is sensitive to NBMPR) and *ei* (ENT2 is insensitive to NBMPR)¹³. Both proteins are ubiquitously expressed. ENT3 is an intracellular transporter, localized to the lysosome, and therefore active at acidic pH¹⁴. Its expression has been deemed necessary for proper lysosome function, macrophage homeostasis, as well as mitochondrial function^{15,16}. ENT4 is also known as plasma membrane monoamine transporter (PMAT)¹⁷. It is predominantly expressed in the brain and heart and transports monoamines such as dopamine at neutral pH. It has been shown to transport adenosine under acidic conditions¹⁸.

Table 1.1 Equilibrative Nucleoside Transporter Family, Substrate Selectivity, and Distribution

ENT FAMILY MEMBER	TISSUE DISTRIBUTION	SUBSTRATE SELECTIVITY
SLC29A1, ENT1	Ubiquitous	Purine & pyrimidine nucleosides
SLC29A2, ENT2	Ubiquitous	Purine & pyrimidine nucleosides and nucleobases
SLC29A3, ENT3	Ubiquitous, localized to lysosomes (intracellular)	Purine & pyrimidine nucleosides, some nucleobases
SLC29A4, ENT4	Most abundant in the brain	Monoamine neurotransmitters at neutral pH; adenosine at acidic pH

1.3 Equilibrative Nucleoside Transporter Subtype 1, ENT1

Protein purification and ion exchange chromatography from erythrocytes of various species, including human, sheep, and pig, were used to identify Band 4.5 polypeptides. Band 4.5 was primarily composed of nucleoside and glucose transporters¹⁹. Human erythrocyte membranes

have an approximate 20:1 ratio of glucose to nucleoside transporters, whereas the pig erythrocytes lack cytochalasin B-sensitive glucose transport and rely on inosine for energy production²⁰. Therefore, pig erythrocytes were ideal for NBMPR-sensitive (es) nucleoside transporter isolation. Availability of systems for study, such as pig erythrocytes, and also the abundant expression of ENT1 across various cell types and tissues, led to ENT1 being the most well-studied member of the SLC29 family²¹. Furthermore, it was determined that adenosine has the highest affinity for ENT1, over other transporters²². This provided the physiological imperative to further study ENT1 in the context of adenosine mediated signaling, which is involved in coronary vasodilation, renal vasoconstriction, neurotransmission, platelet aggregation and lipolysis^{23,24}.

1.3.1 Molecular Properties of ENT1

SLC29A1 codes for several transcript variants of ENT1 which are translated into the same 456 amino acid-length protein. Hydrophobicity studies, N-linked glycosylation site mutagenesis, and antibody scanning studies have predicted an eleven-transmembrane (TM) helix topology, as shown in Figure 1.3²⁵. hENT1 is predicted to have a large intracellular loop between TMD's 6 and 7, intracellular N and extracellular C termini, and a large extracellular loop containing a glycosylation site between TM regions 1 and 2²⁶. Human, mouse, and rat ENT1 are frequently expressed in cell culture systems for structural and functional studies. The sequence homology of ENT1 among mammalian species is relatively high: human and mouse ENT1 have 79% sequence homology, and human and rat have 78% sequence homology. The sequence differences between these species have been exploited in ENT1 studies, including chimeric

studies to identify regions vital for substrate binding or uptake activity, regulation by cellular enzymes, and trafficking of ENT1 to various cell compartments. This will be discussed here and in sections 1.3.2 and 1.3.3.

The N-terminal region of ENT1 was identified as important for substrate binding by use of rENT1 and hENT1 chimeras expressed in *Xenopus* oocytes²⁷. The first TM helix, TM 1, was also found to be important for binding of inhibitors dilazep and dipyridamole²⁸. Chimeras of rENT1 and rENT2 also showed that TM 3-6 regions are important for the sensitivity of rENT1 to NBMPR²⁹. Glycine 154 on the exofacial side of TM 4 was determined to be necessary for NBMPR, draflazine, and dipyridamole binding and substrate transport across the membrane³⁰. Mutations of glycine residues G179 and G184 showed that these specific amino acids are important for transport activity. Any mutation of G184 abolished functional activity; the same was observed for G179L, G179C, and G179V (but not G179A, G179S)³¹. Cells expressing hENT1 containing mutations of cysteine residues revealed that TMs 9 to 11 and the intracellular loop regions in between are also important for inhibitor binding and substrate uptake³².

Figure 1.3 Predicted Eleven-Transmembrane Domain Topology for hENT1

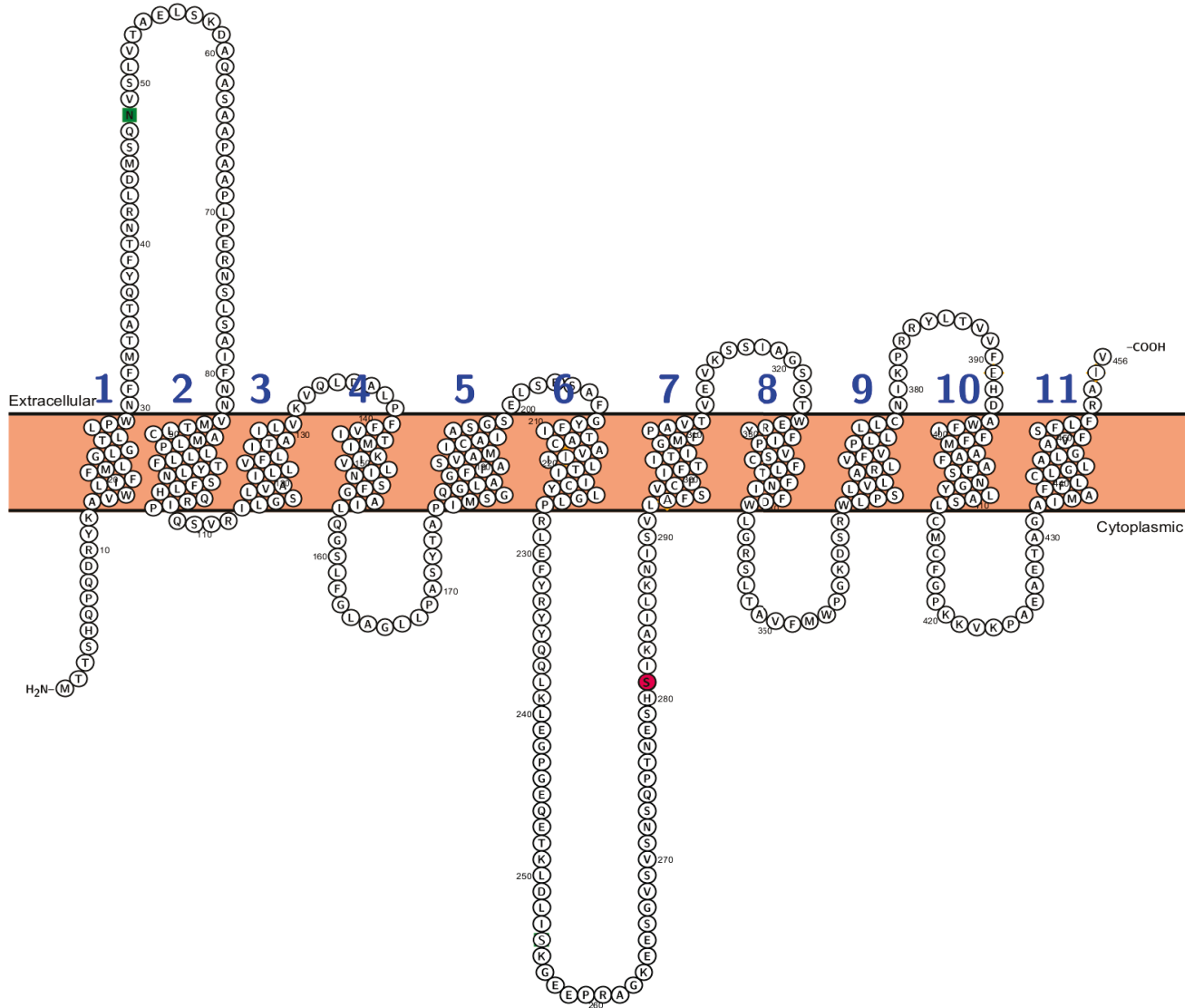


Figure 1.3: This image of hENT1 was designed using Protter web application². Human ENT1 has an eleven-transmembrane domain topology, an intracellular N-terminus and extracellular C-terminus. There is one large extracellular loop between TMD1 and TMD2 which contains the only glycosylation site, Asparagine 48, shown in green. Serine 281, highlighted in pink, shows the location of a putative protein kinase C phosphorylation site discussed in this thesis.

² Protter Web Application: <http://wlab.ethz.ch/protter/>

Despite advances in X-ray crystallography and the multitude of proteins with known 3D structure, no crystal structure exists for ENT1. The hydrophobic nature of membrane proteins makes them difficult to isolate as they are prone to hydrophobic collapse and aggregation. This can be somewhat overcome by finding a solubilizing reagent that maintains protein integrity. Studies reconstituting mENT1 from Ehrlich cell plasma membranes into liposomes identified decylmaltoside (DCM) and dodecyl maltoside (DDM) as optimum in both reagent stability and ability to isolate functionally-stable mENT1 for reconstitution in liposomes³³. Recently, the *Arabidopsis thaliana* ENT7 was isolated using DDM as the solubilizing reagent and reconstituted in *Xenopus laevis* oocytes, where it was able to transport nucleosides bidirectionally³⁴. Moreover, high yields of hENT1 have also been purified from Sf9 insect cells³⁵. The isolation and reconstitution of ENT protein in high quantities point to a promising future for an ENT crystal structure.

hENT1 has a predicted molecular mass of 50.2 kDa. However, by Western Blot analysis the non-glycosylated protein appears at 45 kDa and the glycosylated protein appears as a diffuse band around 55 kDa, indicating varying degrees of glycosylation^{36,22}. Several publications have also reported an ENT1 degradation product at 37 kDa³⁷. Analyses of molecular mass by various methods, including photoaffinity labelling, radiation inactivation, and Western blot, yield varying results. This variability in apparent molecular mass is largely species dependent, as glycosylation patterns on membrane proteins are species dependent³⁸. For example, glycosylated ENT1 from pig erythrocytes appears as a diffuse band just below 66 kDa³⁶. Photoaffinity labelling studies of cells from various species including human, pig, guinea pig, mouse, rat, and sheep drew varied estimates of ENT1 molecular mass. Multiple peaks, a lower

peak between 40-50 kDa and secondary peaks between 60-80 kDa were observed^{20,39-43}.

Section 2.2 discusses how these findings and other observations made in our laboratory led to hypothesis 2 addressed in this thesis.

1.3.2 Trafficking and Localization of ENT1

As a plasma membrane protein, properly folded ENT1 is processed in the Golgi before translocating to the plasma membrane. Therefore, ENT1 has been observed in endoplasmic reticulum (ER), the Golgi apparatus, at the plasma membrane, and along the secretory pathway. Furthermore, ENT1 has also been found in the mitochondrial membrane⁴⁴.

In one of the few studies addressing ENT1 trafficking and recycling, it was shown in COS-7/MCF-7 cells transfected with GFP-hENT1 that hENT1 travels along microtubules from the Golgi to the plasma membrane, where it is anchored by actin filaments, for a total life cycle of 14 hours⁴⁵.

Interestingly, a portion of ENT1 was observed in intracellular compartments that were neither the endoplasmic reticulum, nor the Golgi, nor part of the trafficking pathway leading to the plasma membrane. These unidentified internal pools have also been observed in earlier publications⁴⁶. One hypothesis with regards to these unidentified pools is that they exist in preparation for rapid translocation requirements in response to extra- or intracellular signals⁴⁵.

A system such as this one has been observed for glucose transporter GLUT4, which responds rapidly to changes in insulin concentration by translocating to the plasma membrane⁴⁷. Studies using cultured chromaffin cells (a neural cell population) suggests that ENT1 undergoes two trafficking cycles. ENT1 is localized to the plasma membrane for the initial 5 hours, followed by an endocytosis and subsequent partial return to the plasma membrane for a total maximum of

34 hours following translation⁴⁸. Not all internalized protein is cycled back to the plasma membrane, suggesting the presence of multiple populations of ENT1. These results are similar to observations of the Na⁺/H⁺ exchanger, NHE3, which is distributed at the plasma membrane in two populations, a mobile and immobile pool⁴⁹. These pools of NHE3 undergo differential trafficking in response to various associating factors. Although regulation of trafficking of ENT1 by various factors, including protein kinases, has been suggested, it has largely gone unaddressed^{48,50}. Therefore, effects of cellular stimuli on hENT1 expression at the plasma membrane is a topic addressed in this thesis.

Only a properly folded and, in some cases, appropriately modified membrane protein will successfully be translocated to the plasma membrane. Glycosylation is an important post-translational modification that affects the plasma membrane translocation of some solute carrier (SLC) proteins⁵¹. The glycosylation site on ENT1 is at Asparagine 48, between transmembrane domains 1 and 2²⁵. While it has been shown that an analogous site on ENT2 must be glycosylated for proper transporter localization and function, removal of Asn48 from ENT1 or in-situ de-glycosylation of the protein does not affect trafficking or function^{27,52}. Other regions of ENT1 have also been identified as crucial for either proper folding, translocation, or both. Transmembrane domain regions at the N and C termini are necessary for proper translocation. Specifically, a PWN sequence at the N-terminus and a positively charged group at the C-terminus have been identified^{27,53}. Site directed mutagenesis has been used to identify other important residues for protein folding and membrane translocation. Within the same region, mutations of glycines 179 and 184 have different effects. Any mutation to G184, but not

G179, abolished plasma membrane trafficking³¹. It has not yet been determined why this particular glycine is important to trafficking.

hENT1 is also localized to the mitochondrial membrane and has a mitochondrial signaling sequence, ⁷¹PExN⁷⁴; however, mENT1 and rENT1 do not^{44,54}. This was discovered when fialuridine (FIAU), a drug used for hepatitis B treatment that is taken up into the cell by ENT1, resulted in several cases of fatal liver toxicity in humans that were not observed during trials with rodents. These findings prompted a study which determined that human ENT1 can be localized to the mitochondria, in addition to the plasma membrane, and FIAU accumulation in the mitochondria induced cell death⁵⁴. In mice and rodents, this area (⁷¹PExN⁷⁴) is not conserved and mENT1 has a PAXN in that region instead. When the human ENT1 is mutated to PAXN, mitochondrial translocation is abolished while a mutation to PEXN in mENT1 induced mitochondrial translocation (although the protein did not retain transport function)^{44,54}.

1.3.3 Transport Mechanism of ENT1

ENT1 transport mechanics are believed to follow the 'simple carrier' or 'alternating access' model. The simple carrier model is supported because kinetic parameters for zero-*trans* influx and efflux are similar, suggesting that there is directional symmetry of permeant movement (although this symmetry was specific to fresh erythrocytes and lost in outdated blood samples suggesting changes in protein function with time after isolation)⁵⁵. According to the alternating access model, the transporter exposes its substrate binding site interchangeably to the extracellular and intracellular faces of the membrane (these are referred to as the outward and inward facing states). Binding of a permeant to one side, induces a conformational change so

that the binding site is opened on the other side of the membrane and the permeant can be released. The rate of conformational change of ENT1, or rate of transport, depends on the permeant⁵². For example, uridine-bound ENT1 was observed to undergo this conformational change six times faster than an unbound transporter at 22°C²². Inhibitor binding by NBMPR to the outward facing ENT1 protein appears to greatly reduce conformational changes, effectively 'locking' ENT1 in a particular conformation (NBMPR is cell permeable and is able to bind intracellular protein that is found in the right conformation- one that exposes its outward facing binding site)⁵⁶. NBMPR binding is competitive with nucleoside permeant binding and transport, therefore, it was proposed that the high affinity NBMPR binding site is either the same as, or significantly overlaps with, the permeant binding site⁵⁷. There is numerous evidence of the presence of an allosteric binding site on ENT1. Nucleosides and transport inhibitors modify the rate of NBMPR dissociation from its binding site, and this effect varies based on whether a nucleoside or transport inhibitor is present²². Nucleosides were shown to accelerate NBMPR dissociation; however, transport inhibitors such as dipyridamole and dilazep either inhibited/slowed dissociation or had no effect^{57,22}. The potencies of these nucleosides or transport inhibitors to modify NBMPR dissociation are less than their affinities for inhibiting NBMPR binding in a competition assay suggesting that there is an allosteric binding site^{22,57}. However, this evidence does not address the possibility of NBMPR binding affecting the conformation of the transporter, which may account for the change in affinities of nucleosides or inhibitors and therefore, weaken the evidence for an allosteric site⁵⁸. Studies of NBMPR dissociation from Ehrlich cell membranes in the presence of NBTGR provide further evidence for the presence of an allosteric site. In this case, the effect on dissociation rates of NBMPR

from ENT1 in the presence of a variety of nucleoside substrates and ENT1 inhibitors was measured in the presence of saturating concentrations of NBTGR⁵⁸. Therefore, following dissociation of NBMPPR, the permeant binding site was occupied by NBTGR and the effects on dissociation rate caused by added nucleosides or ENT1 inhibitors must occur through changes to the transporter through interaction with an allosteric site and not due to competition for the (NBTGR-occupied) permeant binding site⁵⁸. Furthermore, pseudo Hill-coefficients of greater than 1 have been calculated for the binding of lidoflazine analogs to ENT1 in human erythrocyte and calf lung membranes as well as for L-adenosine enantiomer transport in bovine chromaffin cells^{58,59}. All of this evidence suggests that a low affinity, broad specificity allosteric binding site modulates the high affinity site.

1.3.4 Regulation of ENT1

A membrane transporter such as ENT1 can be regulated in a variety of ways: through modulation of gene expression, mRNA transcript degradation or stabilization, post-translational modification, and protein trafficking and degradation. For example, the folate carrier (RFC), a member of the SLC19A family, can be post-translationally modified in response to environmental folate excess or deficiency. In response to substrate quantity changes, RFC targeting to the plasma membrane, regulation of trafficking, and mRNA transcript stability are all affected⁶⁰. How endogenous and exogenous factors, such as kinase activation and drugs, respectively, can affect the production and activity of a protein such as hENT1 is important to discern in order to develop appropriate assays, biomarkers, dosing mechanisms and to understand drug resistance.

Specific cellular conditions, such as metabolic stress and hypoxia, influence ENT1 activity. During hypoxia, the transcription factor hypoxia inducible factor 1 (HIF-1) is upregulated; HIF-1 subsequently modifies SLC29A gene expression and represses ENT1 transcription^{61–63}. In immortalized murine cardiomyocytes (HL-1), mENT1 mRNA expression and mENT1-dependent adenosine uptake are reduced following chronic hypoxia⁶⁴. Another study of cardiovascular preconditioning and ischemic injury noted that, in HL-1 cells, hypoxic challenge leads to an efflux of adenosine which acts on adenosine receptors (A_1AR and A_3AR in this case) in order to activate ENT1 through a $PKC\epsilon$ -mediated mechanism⁶⁵. PKC and other kinases have been implicated in regulating ENT1 in several studies and this is further discussed in Section 1.3.4.1- Regulation of ENT1 by Phosphorylation.

Endocrine factors also affect ENT1 expression. In rat intestinal epithelial cells, proliferative agents such as epidermal growth factor (EGF) and transforming growth factor ($TGF\alpha$) induced an increase in rENT1 activity and mRNA levels⁶⁶. EGF and $TGF\alpha$ use two different signal transduction pathways; however, there may be overlapping downstream factors that associate and modify ENT1. Growth-factor induced increase in ENT1 expression is suggested to aid proliferating cells through enhanced uptake of nucleosides necessary for DNA and RNA formation. ENT1 activity and mRNA levels were also enhanced by transforming growth factor- β_1 in renal tubular cells, suggesting a role for the nucleoside transporter in the epithelial-to-mesenchymal transition of tubular epithelial cells and therefore renal fibrosis⁶⁷.

ENT1 expression and activity aids rapidly proliferating cells, such as cancer cells, therefore it may seem counter-intuitive that high levels of ENT1 expression are actually associated with positive responses to many anti-cancer therapies. ENT1 expression in certain tissues is fairly

consistent from healthy individual to individual; however, changes in ENT1 expression in tumor tissue have been observed, contributing to the varied response of individuals to cytotoxic nucleoside analog drugs²¹. In fact, expression levels of hENT1 have been cited as reproducible markers for determining the prognosis of patients receiving gemcitabine –based chemotherapy for pancreatic cancer (see Table 1.3)⁶⁸. Chronic use of anti-cancer nucleoside analog drugs is correlated to a drop in ENT1 expression in some patients, therefore understanding regulation of ENT1 is particularly important in solving problems regarding drug resistance⁶⁹. For example, in CCRG-CEM cells (a leukemic cell line), induced resistance to the anti-cancer drug cytarabine was marked by a sharp decrease in ENT1 gene expression⁷⁰. In yet another mouse myeloid leukemic cell line, stress-activation of c-Jun N-terminal kinase (JNK) resulted in a rapid loss of mENT1 function and mRNA expression⁷¹. Wild-type c-Jun binds to an ENT1 promoter region, regulating ENT1 at the pre-transcription level. In summary, ENT1 expression is modified in cancer cells and is also further regulated by use of anti-cancer drugs, many of which are dependent on ENT1 for cell entry. There is much value in further study of ENT1 regulation in order to identify appropriate patients for ENT1-mediated therapies, design better drugs, and increase response in drug-resistant cells (as seen in tumours).

1.3.4.1 Regulation of ENT1 by Phosphorylation

Phosphorylation, the addition of a phosphoryl (PO_3^{2-}) group to a serine, threonine, or tyrosine amino acid side chain, is a post-translational modification that affects 30% of all proteins⁷².

Specific enzymes, known as kinases, recognize amino acid sequences surrounding these particular residues and transiently interact with the peptide to transfer the phosphoryl group.

Phosphorylation and the reverse reaction, dephosphorylation, can have many different effects

on a protein. This modification turns enzymes “on” or “off” such as in the well-documented case of p53. Phosphorylation also affects the accessibility of binding partner domains such as in the case of cystic fibrosis transmembrane conductance regulator (CFTR), it can facilitate endocytosis as in the case of the dopamine transporter, as well as induce the translocation to the plasma membrane as in the case of aquaporin⁷³⁻⁷².

Computational modeling studies with mENT1 and hENT1 suggested that ENT1 is modified by PKA, PKC, and CKII in the intracellular loop region between TM 6 and 7⁷⁸. Because several sites were identified within the same region of ENT1, this suggests the possibility of multisite cooperative phosphorylation, which is the phosphorylation of one site leading to hierarchical phosphorylation of other sites. Cooperative phosphorylation has been noted in many transport systems, such as the serotonin transporter (SERT) and human norepinephrine transporter (hNET)^{79,80}.

Several studies have suggested that ENT1 is regulated by these kinases. For example, ENT1 inhibition by ethanol requires PKA activity⁸¹. ENT1 expression is suppressed in diabetic patients, and studies on rat cardiac fibroblasts demonstrated that this suppression is due to elevated glucose concentrations which signals through various kinase pathways (PKC ζ , Raf-1, MEK, and p38 MAPK)⁸². So far, PKC ϵ , PKC δ , and PKC ζ isoforms have been reported to be responsible for regulating ENT1. In our laboratory, shRNA silencing experiments showed that PKC δ is responsible for modifying hENT1 activity through changes at a canonical PKC phosphorylation site surrounding Serine 281⁸³. Casein kinase 2 (CKII) has also been identified as a potential modifier of hENT1, as hENT1 contains a canonical phosphorylation site surrounding Serine 254. This site was first studied in mice, which express two splice variants of mENT1. mENT1b is

similar to hENT1 in that it contains a Serine at positions 254, whereas mENT1a has the Serine replaced with Arginine and is missing a Lysine at position 255, and Glycine at position 256. mENT1a is therefore missing a strong consensus sequence at Ser254 for CKII modification. Studies on stable PK15 cells expressing mENT1a or mENT1b treated with a CKII inhibitor, 4,5,6,7-tetrabromo-2-azabenzimidazole (TBB), confirmed that CKII has an effect on mENT1b through Ser254⁸⁴. Other studies with CKII and hENT1 have shown increases in ENT1 expression and function following CKII inhibition⁸⁵. Further, unpublished, work in our laboratory suggests that the effects of CKII regulation through the Serine 254 region are indirect. The intermediate modifier of ENT1 has yet to be identified.

Although canonical phosphorylation sites have been identified, and knock-downs of certain kinases have suggested that they regulate ENT1, more work is required to know how phosphorylation alters protein structure or function. Some modifications may directly alter the transport activity of ENT1 already at the plasma membrane by changing the structure of the protein into one more favorable for either influx or efflux of substrate^{50,86}. However, transporter activity may also be regulated through phosphorylation-induced changes in trafficking, recycling, or degradation.

1.3.5 Oligomerization of ENT1

Radiation inactivation of inhibitor-bound nucleoside-transporter complexes was used to estimate the molecular mass of ENT1 as 122 kDa in one publication, and 110 ± 12 kDa in another⁸⁷⁻⁸⁹. Several previously mentioned studies identified ENT1 by other methods, such as photoaffinity labelling, at molecular masses higher than the 50.2 kDa monomeric form³⁹⁻⁴¹.

Moreover, data from Frances Cunningham's thesis, examining ENT1 by Blue Native Electrophoresis located hENT1 protein at 130 kDa⁹⁰. These observations led to the hypothesis that ENT1 forms a multimeric complex at the plasma membrane or exists as an oligomer, which is addressed in this thesis.

Dimerization of ENT1 has also been hypothesized due the presence of GxxxG motifs in the ENT1 sequence. A motif refers to a specific pattern of amino acids; this pattern, through recognition by cellular machinery, direct cellular localization or determined other properties of the protein.

Using site directed mutagenesis of glycoporphin A (GpA), a motif that is necessary for GpA's dimerization was identified: GxxxG⁹¹. Further study, including computational modeling and solution NMR, has produced a body of literature that suggests that the GxxxG motif and surrounding hydrophobic residues provide the optimum interface for strong Van der Waals forces and support the formation of a stable interaction between two alpha-helices⁹²⁻⁹⁴.

GxxxG motifs occur in over 80% of interacting protein isolates, therefore their very presence suggests potential for ENT1 dimerization⁹⁴. Preliminary studies on mutants of two hENT1-GxxxG motifs were published in Frances Cunningham's thesis⁹⁰. G163L and G445L mutant constructs were designed, but only the G163L mutant could be expressed in PK15 cells. PK15-G163L-hENT1 had lower expression levels than PK15-hENT1 wild-type, and there was no difference in their apparent molecular mass by Blue Native Gel Electrophoresis. The G445L mutant was not expressed at all⁹⁰. These findings are inconclusive, and as suggested in Cunningham's thesis, modifying G163 and G445 to alanine or serine residues for further study may be more fruitful, as leucine (G163L, G445L) has a bulky side chain which may be too disruptive and resulted in non-viable or improperly folded ENT1 protein⁹⁰.

The presence of GxxxG motifs and observation of high apparent molecular mass of ENT1 provide strong preliminary data for further exploration of ENT1 oligomerization. It is important to know whether ENT1 forms oligomers or not because it is possible that populations of ENT1 with different oligomeric states will have altered transport kinetics, as seen in the case of GLUT1⁹⁵, or the relative amounts of oligomer populations could have an impact on the function of ENT1, as seen with GPCR heterodimerization⁹⁶.

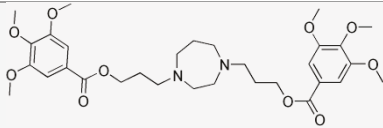
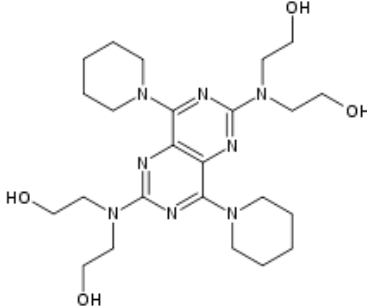
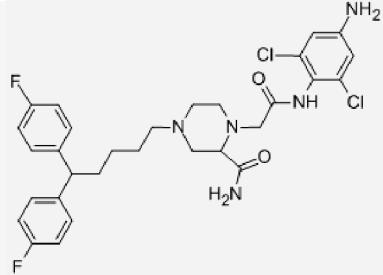
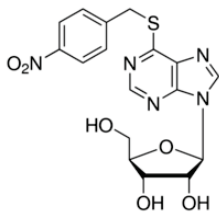
1.4 Clinical Relevance

ENT1 activity is relevant in many clinical areas, for example, ENT1 inhibitors are used to modulate endogenous systems and have been specifically studied with regards to adenosine signaling. These compounds are listed in Table 1.2 and discussed further in Section 1.4.1. Furthermore, as mentioned briefly in section 1.3.3, anti-cancer and anti-viral nucleoside analog drugs, which enter cells through ENT1, are frequently used in the clinic. Cytotoxic nucleoside analogs are listed in Table 1.3 and discussed further in Section 1.4.2.

There are areas of clinical study where ENT1 activity regulation has been identified as important, but no relevant ENT1-based therapies exist. Many of these observations have been made in ENT1 knockout mice. The ENT1 knockout mouse model was created by targeted deletion of 425 of the 1,380 base pairs in the coding region of SLC29A⁹⁷. These mice have normal reproductive behaviour and there are few obvious physiological differences between wild type and ENT1-null mice. One such difference is that ENT1-null mice have a slightly lower body weight than their litter-mates⁹⁷. In addition, several behavioural differences have been observed. For example, ENT1-null mice do show sex-specific differences in alcohol tolerance

and consumption⁹⁷. ENT1-null mice exhibited fewer anxiety behaviours which has sparked interest in studying the inhibition of ENT1 in the amygdala region of the brain as a possible target for anxiety disorders⁹⁸. Recent findings have also identified neuronal-ENT1 to be involved in the regulation of glutamatergic signaling, which is relevant to elderly people with Schizophrenia as well as for attenuating epileptic seizures^{99,100}. Further study of the cross-talk between excitatory amino acid transport 1 (EAAT2) and ENT1 activity or expression is needed. Aberrant effects of ENT1 deletion have also been observed outside of the central nervous system (CNS). ENT1 knockout mice develop an arthritic condition in later stages of life that is similar to human diffuse idiopathic skeletal hyperostosis (DISH); however, changes in ENT1 have not yet been linked to human patients with DISH¹⁰¹. Erythrocytes of β -thalassemia major patients show a decrease in uridine uptake that is tied to a significant drop in hENT1 expression compared to controls¹⁰². The functional implications of these findings with regards to disease progression have not yet been determined. Lastly, in the developing heart, mis-regulation of nucleoside transport and metabolism leads to the development of arrhythmias¹⁰³. These are just a few examples of conditions where ENT1 activity appears to be relevant. It must be better understood whether murine conditions reflect human disease and what changes to ENT1 in humans are responsible for producing such phenotypes. There is great need for a basic understanding of hENT1 regulation, trafficking, and substrate binding and transport mechanics in order to analyze and treat potential pathologies.

Table 1.2 Inhibitors of hENT1

DRUG	STRUCTURE	USE
DILAZEP		Coronary vasodilator
DIPYRIDAMOLE		Coronary vasodilator
DRAFLAZINE		Coronary vasodilator
NBMPR		Inosine analog, no clinical use

1.4.1 ENT1 Inhibitors

There are several clinically relevant ENT1 inhibitors, as shown in Table 1.2, many of which function as coronary vasodilators. Therapeutic benefits of ENT1 inhibition by drugs such as dilazep, dipyridamole, and draflazine are due to potentiation of endogenous adenosine

signaling by blocking re-uptake of adenosine into cells and therefore maintaining an increased extracellular level of adenosine¹⁰⁴. Adenosine signaling protects cardiovascular, intestinal, kidney and lung tissues from ischemic injury through stimulation of adenosine receptors at the cell surface¹⁰⁵.

Ischemic heart disease, also known as coronary artery disease or coronary heart disease, is one of the main contributors to mortality world-wide¹⁰⁶. Ischemia is defined as an inadequate supply of blood, and therefore oxygen, to tissue. A cardioprotected phenotype can be produced by exposing cardiac tissue to short period of ischemia, known as preconditioning; this limits the extent of ischemia-reperfusion injury, which paradoxically results from the rapid oxygenation of hypoxic tissue upon reperfusion. ENT1 is believed to play an important role in response to ischemia and cardioprotection. In wild type mice, 30 minutes of ischemia reduces ENT1 expression in cardiomyocytes to levels similar to ENT1-null mice¹⁰⁷. ENT1-null mice have a permanent cardioprotected phenotype as a result of elevated levels of circulating adenosine¹⁰⁵. Inhibiting ENT1 has similar protective effects and has been used during procedures such as coronary angioplasty to limit infarct size¹⁰⁸.

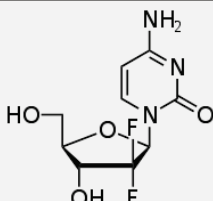
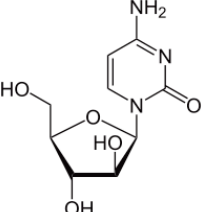
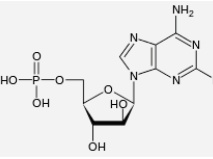
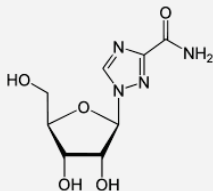
Temporary inhibition of adenosine re-uptake has been shown to be therapeutic; however, chronic inhibition of nucleoside uptake has deleterious effects. For example, pulmonary fibrosis has been associated with chronic purinergic signaling through excess extracellular adenosine, an effect that is exacerbated when nucleoside transport was blocked by dipyridamole¹⁰⁹.

Furthermore, lungs of asthmatic subjects have increased levels of adenosine in the extracellular space which is associated with bronchoconstriction¹¹⁰. These are conditions in which an increase in adenosine uptake from the extracellular space, as opposed to inhibition of re-

uptake, may have an appropriate therapeutic effect. Currently, there are no drugs that selectively enhance ENT1 transport activity. Because ENT1 is responsible for bidirectional movement of adenosine, enhancing or inhibiting ENT1 activity must be temporally regulated depending on the acute or chronic condition being treated.

ENT1 inhibition has also been reported as an off-target effect of other drugs, such as protein kinase inhibitors and P2Y₁₂ receptor (a purinergic receptor targeted on platelet cell surface for anti-coagulant therapy) antagonists. Multi-target tyrosine kinase inhibitors are used as therapies for many solid tumors, and several of these kinase inhibitors also inhibit ENT1¹¹¹. This poses a problem for drug regimens that include these kinase inhibitors as well as nucleoside-analog anti-cancer drugs such as gemcitabine, which can also be used against solid tumors¹¹². The use of Ticagrelor, anti-coagulant by its antagonism of platelet P2Y₁₂ receptors, resulted in unexpected vasodilatory effects such as increased coronary blood flow as well as shortness of breath in patients¹⁰⁴. These effects have been associated with an increase in extracellular adenosine levels through ENT1 inhibition¹⁰⁵. A recent study in human subjects concluded that at clinically relevant concentrations, Ticagrelor does not have the same effects on adenosine transport as it does *in vitro*¹¹⁵. Further studies are necessary to make conclusions on Ticagrelor use and mechanism of action. More research must be done to improve the selective inhibition of ENT1, and the understanding of off-target effects of other drugs on ENT1 activity.

Table 1.3 Selection of Nucleoside Analog Drugs

DRUG	STRUCTURE	USE
GEMCITABINE		Carcinomas- pancreatic, lung, bladder and breast cancer.
CYTARABINE		White blood cell cancers- acute myeloid leukemia, non-Hodgkin's lymphoma.
FLUDARABINE		Hematological malignancies- leukemias and lymphomas.
RIBAVIRIN		Anti-viral; used for hepatitis C, severe respiratory syncytial infection.

1.4.2 Nucleoside Analog Drugs

Nucleoside analog drugs, drugs that have a structure derived from endogenous nucleosides, are used as anti-cancer and anti-viral therapies. For these drugs, their primary mode of entry into cells is through nucleoside transporters. Synthetic nucleoside analogs are active once they are metabolized inside the cell. Their incorporation into DNA and RNA and inhibition of polymerases, kinases, and other cellular enzymes leads to the cell undergoing apoptosis, or programmed cell death¹¹⁶. A serious clinical complication to off-target effects by drugs is organ failure and is often the result of over-dosing. Over dosing can easily occur when there is a lack of knowledge of the affinity of drugs for their target, such as ENT1, or the regulation of ENT1

expression. This is especially the case for cells undergoing rapid division, such as fetal cells, bone marrow, hair follicles, and the lining of the digestive system. Recent advances in nucleoside analog development have focused on modifying current compounds to improve their efficacy. Some methods of doing this are by modifying the base and sugar moieties or making liposomal formulations^{116,117}.

1.4.2.1 Anti-Cancer Drugs

Nucleoside analogs have been used as treatment for lymphoproliferative disorders, blood cancers, as well as solid tumors. Cytarabine is a front line leukemia drug, fludarabine and cladribine are used for lymphoma, and gemcitabine is a well-studied pancreatic cancer drug. There are several compounds currently in the clinical trial pipeline that are based on these original molecules with modifications for improved targeting and efficacy¹¹⁶. Cytarabine and gemcitabine efficacy has been directly correlated with expression levels of hENT1; individuals with low expression of ENT1 have a poor response to these drugs^{68,118}. ENT1 levels may therefore act as a biomarker for appropriate drug prescription and dosage¹¹⁹. Moreover, regulation of hENT1 expression has become an important component of drug resistance to these agents.

1.4.2.2 Anti-Viral Medications

Over 25 approved anti-viral nucleoside analog drugs are available on the market today¹¹⁶. Their mechanism of action includes incorporation into viral DNA and RNA, as well as inhibition of various metabolizing enzymes. In general, because these drugs can be designed to selectively inhibit viral enzymes, they are less toxic to humans than the nucleoside analogs used in anti-

cancer treatment. One of these drugs is Ribavirin, a guanosine analog pro-drug, used by patients with Hepatitis C as well as HIV and is primarily taken up into cells by ENT1^{120,121}. Another area of possible drug development regarding ENT1's is against malaria. The parasite responsible for over 70% of malarial infections, *P. falciparum* expresses a PfENT1. The parasite relies on PfENT1 for nucleoside/nucleotide salvage as it cannot synthesize purines *de novo*. For this reason, PfENT1 has been identified as an excellent potential target for anti-malarial inhibitors. New drugs must be developed as NBMPR, draflazine, dipyridamole and dilazep (known inhibitors of hENT1) fail to inhibit PfENT1¹²². Due to the differences between hENT1 and PfENT1, perhaps it will be possible to develop a parasite-selective inhibitor or one with higher affinity for PfENT1 than hENT1, therefore reducing side effects for patients.

CHAPTER 2. RATIONALE FOR RESEARCH OBJECTIVES

2.1 Rationale and Hypothesis for Objective 1: Regulation of hENT1

The first hypothesis addressed in this thesis is that activation of PKC, or stimulation of the adenosine receptor 1 (A₁AR), enhanced hENT1 uptake activity by inducing an increase in the amount of transporter at the plasma membrane. This is graphically represented in Figure 2.3. Zero-*trans* influx studies of radiolabelled ENT1 substrate (substrate applied extracellularly to achieve a near infinite inward-directed gradient) were performed in the laboratory using cells treated with drugs that stimulate/antagonize A₁AR and activate/inhibit PKC. These drugs resulted in altered mediated uptake kinetics of the substrate by ENT1. Pig kidney epithelial cells (PK-15) cell mutants which are nucleoside transport deficient (NTD), were used to stably express wild type hENT1 and hENT1 containing a mutation in a canonical PKC phosphorylation site, at Serine 281^{123,124}. Under conditions of PKC activation with PMA, PK15-hENT1 cells displayed increase uptake of 2-chloroadenosine (See Figure 2.1 A). Treatment with PMA led to changes in V_{max} of uptake by ENT1, but with no change in K_m ; in PK15-S281A-hENT1 cells there was no change in V_{max} or K_m between the PMA-treated and control cells (Figure 2.1 B). This change in V_{max} suggests an increase in the number of available transporters at the plasma membrane or an enhancement in translocation efficiency; no change in K_m implies that the affinity of the transporter for its substrate did not change.

Cross-talk between hENT1 and adenosine receptors has been observed under conditions of ischemic stress¹²⁵. A₁AR receptors have a high affinity for adenosine and the signal transduction pathway can lead to the activation of PKC^{126–128}. Therefore, cross-talk between A₁AR and

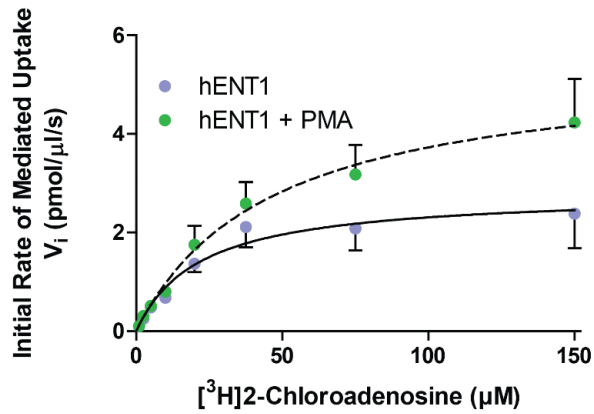
hENT1 and the involvement of PKC was also investigated by stimulating adenosine receptor 1 (A₁AR) with 2-chloro-N⁶-cyclopentyladenosine (CCPA). This resulted in an increase in 2-chloroadenosine uptake in PK15-hENT1 but not PK15-S281A-hENT1 cells (Figure 2.2 A and B, respectively).

There are several possible reasons for an increase in transport function following the stimulation of PKC. One possibility is that a post-translational modification at Serine 281 changes the conformation of hENT1 to one that favors inward movement of substrate. Alternatively, a conformational change may increase substrate binding affinity. Changes to uptake activity could also be a result of enhanced translation efficiency of this protein or stabilization of the mRNA transcripts. The other possibility, which is addressed in this thesis, is that an increase in the amount of transporter localized to the plasma membrane contributes to enhanced substrate uptake. This phenomenon has been observed for dopaminergic signaling: PKC β was found to affect the plasma membrane localization and subsequently activity of the D₂-like dopamine autoreceptor¹²⁹.

Immunocytochemical and biochemical experiments were designed to address whether changes to plasma membrane localization of hENT1 contribute to the increase in uptake activity following A₁AR stimulation and PKC activation.

Figure 2.1 Initial rate of uptake of [³H]2-Chloroadenosine following PKC activation in PK15-hENT1 and PK15-S281A-hENT1 cells

A.



B.

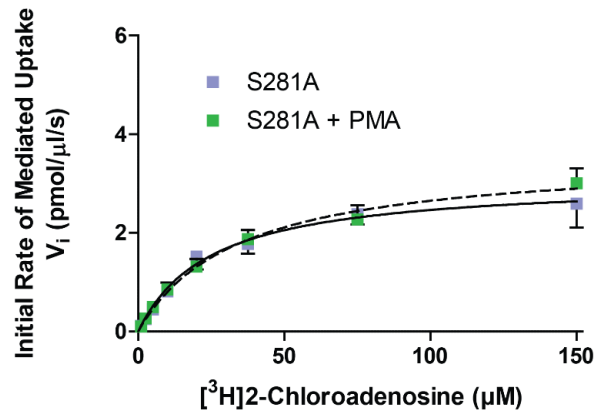
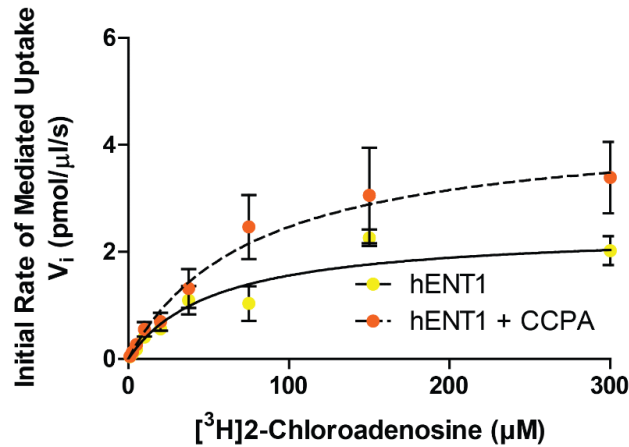


Figure 2.1: PK15-hENT1 (Panel A) and PK15-S281A-hENT1 (Panel B) cells were incubated for 10 min with 0.1% DMSO (control) or 100 nM PMA prior to the measurement of [³H]2-chloroadenosine uptake. Cells were incubated with a range of concentrations of [³H]2-chloroadenosine for 5 seconds, and curves were fitted to the initial rate of mediated uptake (pmol/μl/s) versus concentration using a Michaelis-Menten model. Mediated uptake was calculated as the difference between total uptake and non-mediated uptake, where non-mediated uptake was defined as cell-associated radiolabel in the presence of 5 μM NBMPR and 5 μM dipyridamole. PK15-hENT1 cells, but not PK15-S281A-hENT1 cells, showed an increase in uptake function following PMA treatment. Each point represents the mean ± SEM from 5 independent experiments.

Figure 2.2 Initial rate of uptake of [³H]2-Chloroadenosine following A₁AR stimulation in PK15-hENT1 and PK15-S281A-hENT1 cells

A.



B.

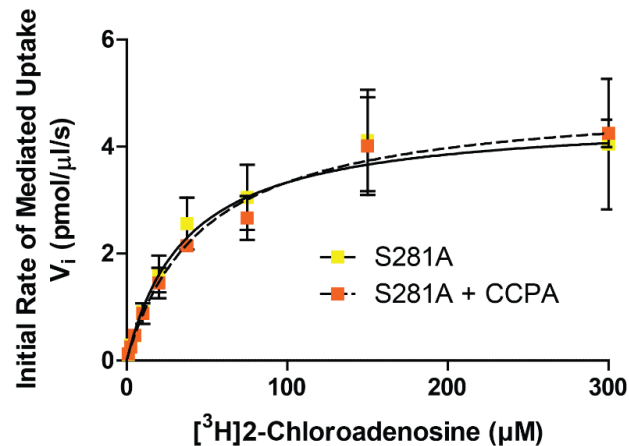


Figure 2.2: PK15-hENT1 (Panel A) and PK15-S281A-hENT1 (Panel B) cells were incubated for 10 min with 0.1% DMSO (control) or 100 nM CCPA prior to the measurement of [³H]2-chloroadenosine uptake. Cells were incubated with a range of concentrations of [³H]2-chloroadenosine for 5 seconds, and curves were fitted to the initial rate of mediated uptake (pmol/μl/s) versus concentration using a Michaelis-Menten model. Mediated uptake was calculated as the difference between total uptake and non-mediated uptake, where non-mediated uptake was defined as cell-associated radiolabel in the presence of 5 μM NBMPR and 5 μM dipyridamole. PK15-hENT1 cells, but not PK15-S281A-hENT1 cells, showed an increase in uptake function following CCPA treatment. Each point represents the mean ± SEM from 5 independent experiments.

Figure 2.3 Changes in V_{max} of PK15-hENT1 Cells

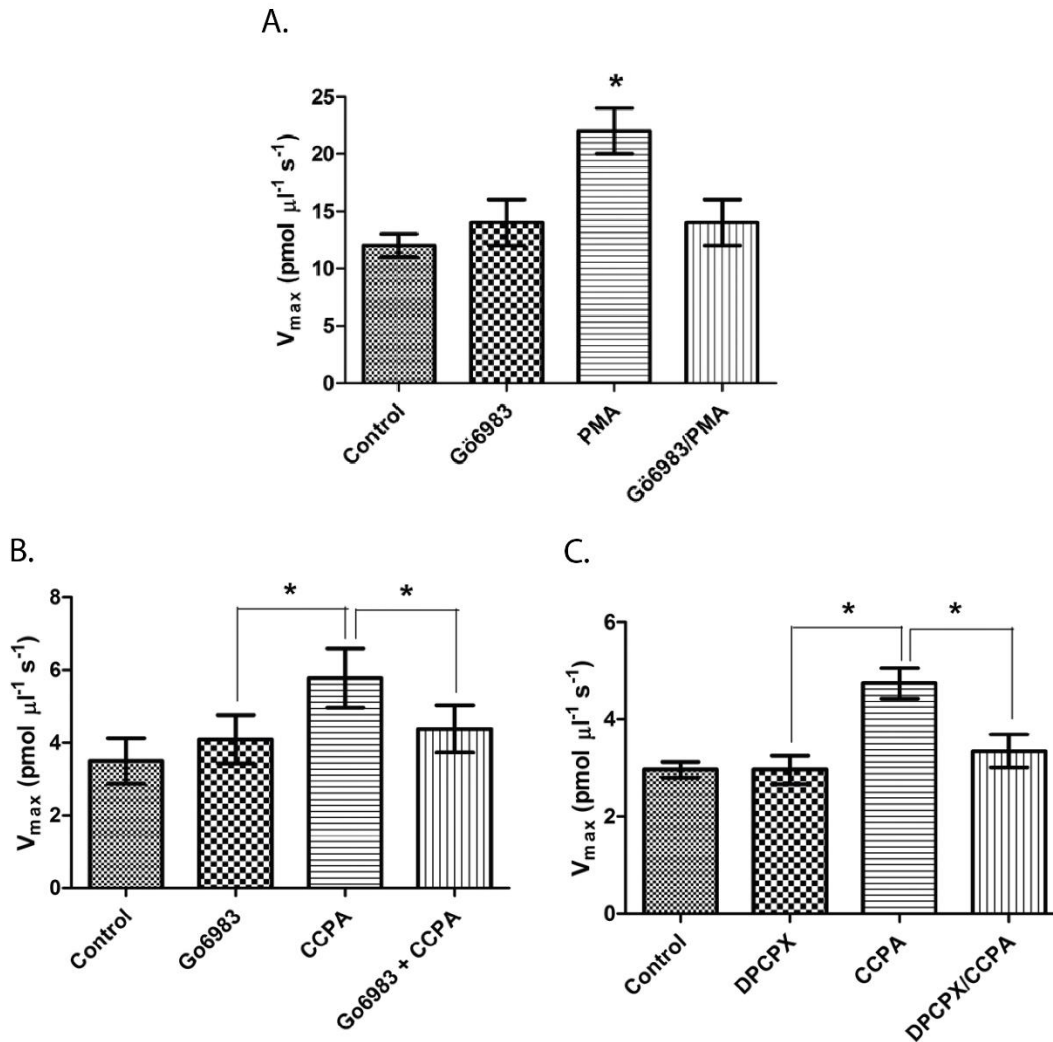


Figure 2.3: Summary of changes to uptake of 2-Chloroadenosine by ENT1 (changes in the V_{max}) in PK15-hENT1 cells as measured by radioligand uptake assays. In Panel A, GÖ6983, an inhibitor of PKC, does not cause changes to uptake rate by ENT1. Use of PMA, a PKC activator, does significantly increase uptake rate of 2-Chloroadenosine by ENT1. Pre-incubation with GÖ6983 attenuates the effect of PMA. In Panel B, stimulation at the A_1AR receptor by CCPA led to an increase in the V_{max} rate of 2-Chloroadenosine uptake by ENT1. This effect was attenuated with GÖ6983, an inhibitor of PKC. In Panel C, DPCPX, an antagonist of A_1AR on its own does not lead to any changes in the uptake rate of 2-chloroadenosine by ENT1. And in the presence of DPCPX, the increase in V_{max} caused by stimulation at A_1AR by CCPA is attenuated. Each point represents the mean \pm SEM from 5 independent experiments. Significantly different from data obtained in the absence of PMA treatment (Student's t-test for paired data, $P < 0.05$).

Figure 2.4 Graphical representation of Objective 1: Regulation of hENT1 expression at the plasma membrane

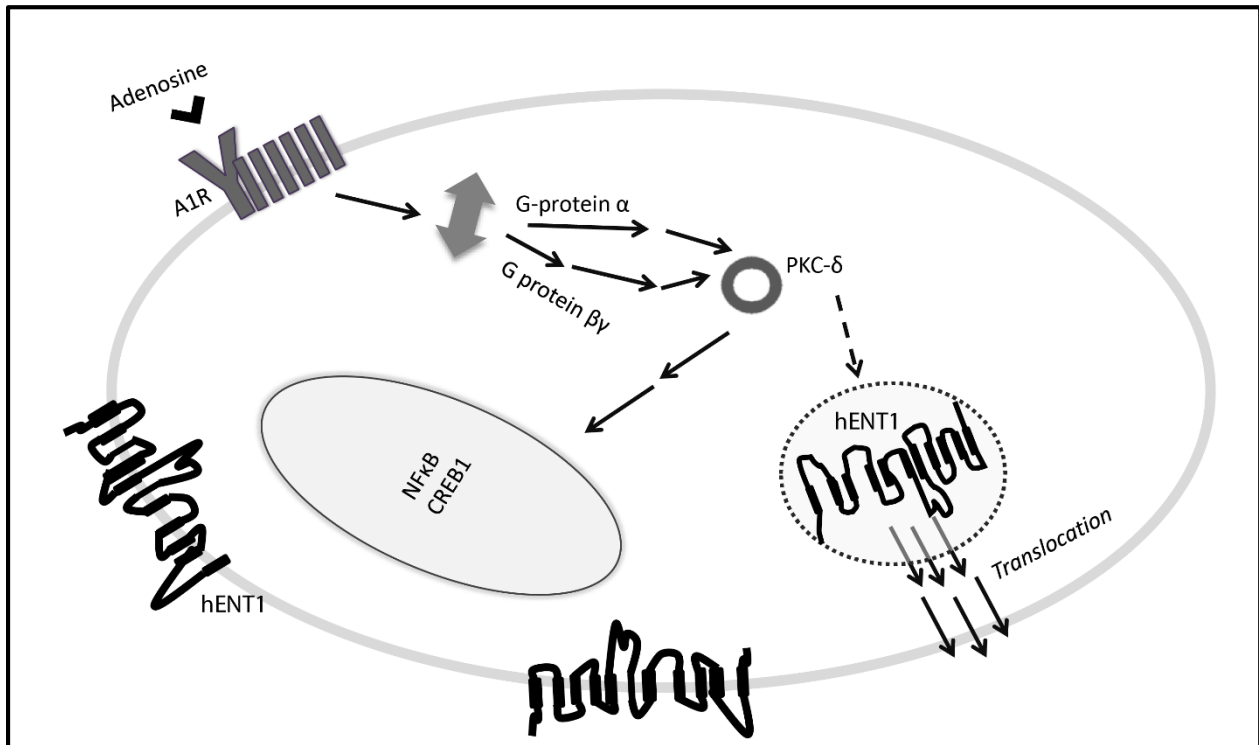


Figure 2.3: Stimulation of the adenosine receptor 1 (A₁AR) or activation of protein kinase C (PKC), which is downstream in the A₁AR signaling pathway, induces an increase in the amount of hENT1 protein at the plasma membrane. This increase in plasma membrane localized ENT1 is responsible for the changes in uptake activity of wild-type hENT1, as discussed with Figures 2.1 and 2.2. Moreover, modification at Serine 281, part of a canonical PKC phosphorylation site, is responsible for this phenomena.

2.2 Rationale and Hypothesis for Objective 2: hENT1 Complex

The presence of hENT1 oligomers has been suggested in the literature but not conclusively shown in intact cells. Based on structural and functional data available about ENT1, we hypothesize that hENT1 exists as a multimeric complex in intact cells.

For many other proteins, their oligomeric state impacts structural stability or function. Glucose transporter 1 (GLUT1), for example, functions in a monomeric, dimeric, and tetrameric state.

Although genetically dissimilar, ENT1 and GLUT1 share some structural characteristics such as multiple transmembrane domains (ENT1 has 11, and GLUT1 has 12), a cytosolic N terminus, a large intracellular loop and a single extracellular loop containing a glycosylation site.

Depending on the oligomeric state of GLUT1, its substrate binding and transport mechanism varies. A monomer interchangeably expresses its extracellular-facing and intracellular-facing conformations. In a dimer, the monomers can expose the substrate binding site to the extracellular and intracellular spaces simultaneously, and the dimer substrate kinetics do not show cooperativity between the monomers. In its tetrameric form, GLUT1 displays cooperative substrate binding and transport kinetics among the monomers^{125,126}. The function of other proteins also relies on their quaternary structure. For example, receptor tyrosine kinases, are activated by dimerizing at the plasma membrane to initiate downstream signaling cascades in various cancer phenotypes¹³⁰⁻¹³². Other enzymes, such as the metabolic enzyme glutaminase C, gain structural stability and exhibit varied kinetic properties in dimeric form¹³³. In order to fully understand the function and regulation of ENT1, all possible oligomeric compositions and their influence on transporter activity must be identified.

Radiation inactivation, photoaffinity labelling and inhibitor cooperativity studies have all suggested that ENT1 exists in non-monomeric populations. Radiation inactivation studies of human erythrocytes identified the NBMPR-sensitive (es) nucleoside transporter (now known as ENT1) and approximated its molecular mass to be 122 kDa. The majority of early photoaffinity labelling in various species, such as rats, pigs, guinea pigs, sheep and human, identified multiple peaks of ENT1, some at around 40 kDa to 50 kDa, and a higher mass peaks at 60 kDa to 80 kDa^{20,39,40,43}. It was later discovered that the molecular mass of an hENT1 monomer is 50.2 kDa, 55 kDa in the glycosylated form. As a membrane protein, ENT1 has many hydrophobic regions and is therefore prone to aggregate formation; this can explain the appearance of higher molecular mass ENT1's by photoaffinity labelling³⁹. Furthermore, in our lab, Francis Cunningham analyzed PK15-hENT1 cells by Blue Native Electrophoresis (BNE) and found ENT1 migrating to 130 kDa, adding further supportive evidence for higher-order ENT1 complex formation⁹⁰.

To test the hypothesis that ENT1 exists as a multimeric complex or oligomer, several biochemical and immunofluorescence experiments were conducted. Firstly, co-immunoprecipitation experiments using cell transfected with hENT1 with two different epitope tags was used to investigate association of hENT1 monomers into a dimeric state. This technique has been used to identify interacting pairs such as: carbonic anhydrase II (CAII) and sodium/proton (Na^+/H^+) exchanger (NHE1), syntaxin 1 with the dopamine transporter, and the dimerization of μ -opioid receptors^{76,96,134}. Chemical and immunofluorescence-based cross-linking experiments were used to address this hypothesis, including: co-immunoprecipitation, chemical cross-linking, and proximity ligation. Histone-histone associations and aspartate

receptor dimerization are two examples of associating proteins that have been analyzed by chemical cross-linking^{135,136}. Proximity ligation is an immunofluorescence technique which has been used successfully in studies looking at the interaction between various membrane receptors and other enzymes¹³⁷⁻¹³⁹.

By forming a complex with other proteins relevant in the processing or metabolism of the substrate, a transport protein complex can respond rapidly to changes in the cellular environment. One such example is carbonic anhydrase (CAII), a cytosolic protein that forms complexes with several membrane transporters such as anion exchanger 1 (AE1), sodium/proton exchanger (NHE1), or aquaporin to enhance transport function and respond to relevant stimuli^{134,140,141}. We suspect that enzymes responsible for the anabolism or catabolism of adenosine form a complex with ENT1 at the plasma membrane because of the rapid rate of adenosine metabolism and involvement of ENT1 in regulating adenosine signaling¹⁴². Enzymes of interest include, but are not limited to, adenosine kinase and adenosine deaminase. It has been shown that extracellular adenosine deaminase binds to and enhances A₁AR signalling, thus increasing second messenger production which may in turn directly or indirectly modify ENT1¹⁴³. The activities of 5'-ecto-nucleotidase and 5'-endo-nucleotidase have previously been shown not to couple with nucleoside transport, at least in astrocytes; however, further study is necessary as these enzymes contribute to regulating extracellular adenosine pools¹⁴⁴. It is important to remember that ENT1 has a variety of other nucleoside substrates, endogenous and exogenous, that it transports. Therefore, this study is open to any other proteins that may interact with hENT1, not only those involved in adenosine metabolism.

Investigation into potential ENT1 protein complexes began with mass spectrometry in-gel analysis experiments. To identify transiently interacting binding partners, cells were treated with Lomant's reagent for chemical cross-linking in the presence of the ENT1 inhibitor NBMPR, or the substrate uridine. NBMPR will be used in order to stabilize ENT1 in an inhibitor bound outward facing conformation. Similarly, uridine will be used to capture ENT1 in an inward-facing, substrate binding conformation. Adenosine is not used because, unlike uridine, it contains a primary amine that would quench the cross-linking reagent. This method of complex identification is a common form of preliminary complex analysis and used by many contributors to online databases for protein complexes¹⁴⁵⁻¹⁴⁷. The Alberta Proteomics and Mass Spectrometry Facility run by the Biochemistry department at the University of Alberta performs in-gel protein identification and their services were used for this study.

2.3 Specific Goals

1. Determine whether the increase in ENT1 activity by A₁AR stimulation and PKC activation through Serine 281 is due to changes in ENT1 expression at the plasma membrane using biochemical and immunofluorescence techniques.
2. Determine whether ENT1 exists as an oligomer in intact cells through biochemical and immunofluorescence approaches using lysed and intact cells.
3. Initiate the investigation into existence of an ENT1 complex by mass spectrometry analysis following chemical cross-linking of cells in the presence of relevant ENT1 inhibitors or substrates.

CHAPTER 3. MATERIALS AND METHODS

3.1 Materials

Modified Eagle Medium (MEM), sodium pyruvate, non-essential amino acids, Geneticin® (G418), LipofectAMINE™ 2000, penicillin/streptomycin, trypsin/EDTA, and culture-grade phosphate-buffered saline (PBS) were purchased from Invitrogen (Burlington, Ontario, Canada). Bovine growth serum (BGS), EZ-Link Sulfo-NHS-SS-Biotin, 3,3'-dithiobis [sulfosuccinimidylpropionate] (DTSSP), and dithiobis[succinimidylpropionate] (DSP), dimethyl sulfoxide (DMSO), dithiothreitol (DTT), streptavidin agarose resin, double frosted microscope slides, Bradford and BCA colorimetric protein assays were all supplied by Thermo Fisher Scientific (Waltham, MA, USA). Pig kidney epithelial nucleoside transporter deficient cells (PK15-NTD) were graciously provided by Dr. Ming Tse (Johns Hopkins University, Baltimore, MD, USA). The glycosylphosphatidyl-inositol-anchored green fluorescent protein (GPI-GFP) constructs and monoclonal rabbit anti-GFP antibody were obtained from Dr. Luc Berthiaume (University of Alberta, Edmonton, Canada). The HA-tagged anion exchanger 1 (HA-AE1) and carbonic anhydrase (CAII) constructs were obtained from Dr. Joseph Casey (University of Alberta, Edmonton, AB, Canada). Culture flasks and plates were purchased from Sarstedt (Nümbrecht, Germany). NBMPR and uridine were purchased from Sigma (Oakville, ON, Canada). Phorbol 12-myristate 13-acetate (PMA) and 4 α -PMA, 2-chloro-N(6)-cyclopentyladenosine (CCPA), were purchased from Tocris Bioscience (Ellisville, Missouri, USA). Mammalian protease inhibitor cocktail was supplied by Calbiochem (California, USA). BioRad PROTEAN tetra-cell system, PowerPac Universal, PROTEAN pre-cast 4-20% gradient gels, 2X Laemmli Sample Buffer, were from BioRad (Hercules, CA, USA). Normal chicken serum, rabbit

anti-MYC antibody were from Abcam (Cambridge, MA, USA). Donkey anti-goat IgG-HRP, donkey anti-rabbit IgG-HRP, goat anti GAPDH (V-18), rabbit anti Na⁺/K⁺-ATPase α (H-300) antibodies were from Santa Cruz Biotechnology Inc. (Dallas, TX, USA). Immobilon transfer membranes, mouse anti-MYC, rabbit anti-GLUT-1 antibodies were from Millipore (Temecula, CA, USA). Mouse anti-HA clone 16B12 antibody was from Cedarlane (Burlington, ON). Mouse anti-DYKDDDDK (FLAG-tag) antibody was from Clontech Laboratories (Mountain View, CA, USA). Sheep anti mouse IgG-HRP from Amersham made by GE Healthcare (Buckinghamshire, UK). Dynabeads Protein G, ProLong[®] Gold antifade reagent with DAPI, Alexa Fluor[®] 594 chicken anti mouse and Alexa Fluor[®] 488 chicken anti rabbit antibodies were from Life Technologies (Eugene, OR, USA). Proximity Ligation Assay kits were purchased from OLink Biosciences (Uppsala, Sweden). All other compounds used were of reagent grade.

3.2 Immunofluorescence Analysis of FLAG-ENT1 Colocalized to the Plasma Membrane

PK15-hENT1 and PK15-S281A-hENT1 cells were grown to 20% confluence on poly-L-lysine-treated 1.5 mm glass slides in Sarstedt six-well plates. Twenty four hours after seeding, cells were transfected with 1.5 μ g GPI-GFP DNA using LipofectAMINE 2000 Plus Reagent (optimized 1:4 ratio of DNA:lipofectamine reagent). On the experiment day, twenty-four hours post-transfection, cells were washed with Dulbecco's phosphate buffered saline (D-PBS: 137 mM NaCl, 6.3 mM Na₂HPO₄, 2.7 mM KCl, 1.5 mM KH₂PO₄, 0.5 mM MgCl₂•6H₂O, 0.9 mM CaCl₂•2H₂O) and treated with 100 nM of PMA, 4 α - PMA, CCPA, or 0.1% DMSO (vehicle control) in 2 ml HEPES Balanced Salt Solution (HBSS: 0.137 M NaCl, 5.4 mM KCl, 0.25 mM Na₂HPO₄, 0.44 mM KH₂PO₄, 1.3 mM CaCl₂, 1.0 mM MgSO₄, 4.2 mM NaHCO₃) at 37°C for 15 minutes. PMA has been used at 100 nM in other studies to increase hENT1 substrate uptake following just 15

minutes of incubation⁵⁰. (A concentration of 100 nM for CCPA was determined to be sufficient to produce a change in uptake function of ENT1 by Scott Hughes in the laboratory). All subsequent steps were performed at room temperature. Cells were washed twice in D-PBS, fixed in 10% zinc formalin for 12 minutes, and rinsed three times with D-PBS for 5 minutes. Cells were incubated in 2 ml of blocking/permeabilization buffer (D-PBS, 5% normal chicken serum, 0.3% Triton X-100) for 60 minutes. Cover slips were then inverted onto 100 μ l of primary antibody solution, 1:1000 mAB anti-FLAG (Clontech, Mountain View, CA, USA) and 1:5000 rabbit anti-GFP (EUSERA, Edmonton, AB, Canada), in buffer of D-PBS, 1% BSA, 0.1% Triton X-100 and incubated for 60 minutes at room temperature in a humidified chamber. Cover slips were rinsed three times in 2 ml of D-PBS for 5 minutes. Cover slips were incubated in 100 μ l of 1:500 secondary antibody (Alexa Fluor 594 chicken anti-mouse and Alexa Fluor 488 chicken anti-rabbit, Life Technologies, Eugene, OR, USA) in a dark, humidified chamber for 60 minutes. After three washes in D-PBS in the dark, cover slips were inverted and mounted on glass slides using Prolong Gold Antifade Reagent (Invitrogen, Burlington, ON, Canada) with 4'-6-diamidino-2-phenylindole (DAPI) to identify cell nuclei. DAPI reagent was allowed to set, in the dark, at room temperature overnight (~16 hours) and then the cover slips were sealed around the edges using Maybelline clear nail-polish (Color Show Nail Lacquer, Maybelline, NY). All images were acquired at the University of Alberta, Faculty of Medicine and Dentistry Cell Imaging Centre. Confocal Z-plane images were generated on IX-81 motorized inverted microscope (Olympus, Burlington, ON, Canada) with MS-2000 motorized XY stage with piezo Z insert that has 100 μ m travel (Advances Scientific Instrumentation, Eugene, OR, USA) and a SCU 10 spinning disk confocal scan-head (Yokagawa, Tokyo, Japan). Samples were observed and collected through a

63X PlanAPO oil immersion objective, with a numerical aperture of 1.42 (Quorum Technologies Inc., ON, Canada). A C9100-13 EM-CCD Digital Camera (Hamamatsu, Hamamatsu City, Japan) and Volocity Software (Perkin Elmer, Mississauga, ON, Canada) were used for image capture. Images displayed show a single, representative section of a Z-series taken through the entire cell with 0.3 μ m between planes. Pearson's coefficients representing colocalization of signal from hENT1 and the plasma membrane were determined using IMARIS software (©Bitplane), generously provided by Dr. Andrew Simmonds at the University of Alberta, Department of Cell Biology.

3.3 Cell Surface Processing by Biotinylation

PK15-hENT1 or PK15-S281A-hENT1 cells were rinsed with 4°C PBS, washed with 4°C Borate buffer (154 mM NaCl, 7.2 mM KCl, 1.8 mM CaCl₂, 10 mM boric acid, pH 9.0) and then incubated for 30 minutes at 4°C in Borate buffer, containing Sulpho-NHS-SS-Biotin (SNSB, 0.5 mg/ml, Pierce, IL, U.S.A). After washing three times with 4°C Quenching buffer (192 mM glycine, 25 mM Tris, pH 8.3), cells were solubilized for 20 minutes on ice in 500 μ l of IPB buffer (1% (v/v) IGEPAL CA-630, 5 mM EDTA, 150 mM NaCl, 0.5% (w/v) sodium deoxycholate, 10 mM Tris, pH 7.5), containing Complete Protease Inhibitor (Roche Applied Science, IN, USA). Cell lysates were centrifuged for 15 minutes at 13,200 x g and the supernatants recovered. For each sample, half of the supernatant was retained for later SDS-PAGE analysis (total protein, T). The remaining half of the supernatants were combined with 50 μ l of a 50% slurry of Immobilized Streptavidin Resin in PBS and incubated 16 hours at 4°C with gentle rotation. Samples were centrifuged for 2 minutes at 8,000 x g, and the supernatant collected (unbound protein, U). The T and U fractions of each sample were analyzed by SDS-PAGE and hENT1 was immuno-detected

using a primary mouse monoclonal anti-FLAG antibody (1:1000, CLONTECH, Mountain View, CA, USA) followed by 1:3000 sheep anti-mouse IgG-HRP secondary antibody (Amersham). A digital chemiluminescence camera captured images of the Western Blot. Densitometric quantitation of the bands was done using BioRad ImageLab software. The percentage of biotinylated protein was calculated as $(T-U)/T \times 100$.

3.4 Co-Immunoprecipitation Analysis

HEK293 cells were transiently transfected with vector (pcDNA 3.1 (-) plasmid), HA-hENT1, MYC-hENT1 or co-transfected with equal amounts of HA-hENT1 and MYC-hENT1 cDNA. Forty to forty-eight hours post-transfection, cells were lysed on ice in IPB buffer, containing protease inhibitors, for 20 minutes and centrifuged at 13,200×g for 15 minutes at 4°C. Half of the total protein lysate (T) was set aside and half (by volume) was incubated for 16 hours at 4°C with either 5 µl mouse monoclonal anti-HA 16B12 antibody or 5 µl rabbit polyclonal anti-MYC antibody and 50 µl Dynabeads protein G resin. Immunocomplexes were washed twice with 4°C IPB buffer, containing protease inhibitors, and once with 4°C PBS, pH 7.4, containing protease inhibitors, and centrifuged at 9,000 x g for 10 minutes prior to resuspension in 45 µl of 2× SDS-PAGE sample buffer with 2% v/v β-mercaptoethanol. Samples were heated at 65°C for 4 minutes prior to separation by SDS-PAGE and processed for immunoblotting as described above.

3.5 Extracellular Chemical Cross-Linking with DTSSP and Zinc Formalin

For cross-linking analysis of PK15-hENT1 cells, cells were grown to 80% confluence, washed with D-PBS buffer at 4°C, and incubated with 2 mM, or a range of concentrations from 1 mM to 7 mM, of 3,3'-dithiobis[sulfosuccinimidyl]propionate] (DTSSP) for 2 hours on ice at 4°C. Some

samples were pre-incubated with 100 nM PMA prior to cross-linking. The cross-linking reaction was stopped by 15 minutes of incubation with 20 mM Tris, pH=7.5. Cells were rinsed with D-PBS on ice, followed by lysis using IPB buffer with protease inhibitor for 20 minutes, as described above. Protein was quantified using Pierce™ BCA Protein Assay Kit. Equal mass of protein sample was incubated for 30 minutes at 37°C with 50 mM dithiothreitol (DTT) or untreated. Samples were then prepared and processed for Western Blot analysis as previously described. Alternatively, cells were cross-linked using 10% zinc formalin for 15 minutes at room temperature, lysed, and processed for Western Blot analysis as described above.

3.6 Proximity Ligation Assay

PK15-hENT1 cells were grown to 20% confluence on poly-L-lysine-treated glass coverslips. Twenty-four hours following transfection with MYC-hENT1 cDNA (for experimental condition and negative control), or HA-AE1 (anion exchanger 1) and CAII (carbonic anhydrase II) cDNA (positive control, as described in introduction). Cells were then washed with D-PBS, fixed, and permeabilized as previously described. Primary antibodies, all 1:500, were applied for 1 hour at 37°C using the inverted cover-slip method in a humidified chamber. Cells were washed 2x 5 minutes in D-PBS, and 1x 5 minutes in 50% Duolink Blocking Solution (Olink Biosciences)/50% D-PBS. PLA Plus and Minus probes were mixed together as described in the PLA Probe Protocol- probes were diluted 1:5 in the Duolink Antibody Buffer for a final volume of 40 µL per coverslip and incubated using the inverted cover slip method for 1 hour at 37°C in a humidified chamber. Cells were washed 2x 5 minutes in 1X Buffer A (0.01 M Tris, 0.15 M NaCl, 0.05% Tween 20). Ligation solution was diluted to 1X in milli-Q water and the ligase added at 1:40 dilution for a final volume of 40 µL per coverslip. Incubation occurred at 37°C for 30 minutes by inverted

coverslip method in a humidified chamber. Cells were washed 2x 2 minutes in 1X Buffer A. Amplification solution was diluted to 1X in milli-Q water and the polymerase was added at 1:80 dilution for a final volume of 40 μ L per coverslip. Incubation occurred at 37°C for 100 minutes by inverted coverslip method in humidified chamber. Cells were washed 2x 10 minutes in 1X Buffer B (0.2 M Tris, 0.1 M NaCl) and once for 1 minute in 0.01X Buffer B prior to mounting on glass slides using Prolong Antifade mounting media with DAPI. Sixteen hours following mounting media application, cover slips were sealed using clear nail-polish as previously described, prior to image collection. All images were acquired at the University of Alberta, Faculty of Medicine and Dentistry Cell Imaging Centre. Extended focus images were generated on IX-81 motorized inverted microscope (Olympus, Burlington, ON, Canada) with MS-2000 motorized XY stage with piezo Z insert that has 100 μ m travel (Advances Scientific Instrumentation, Eugene, OR, USA) and a SCU 10 spinning disk confocal scan-head (Yokagawa, Tokyo, Japan). Samples were observed and collected through a 40X air-lens and 63X PlanAPO oil immersion objective, with a numerical aperture of 1.42 (Quorum Technologies Inc., ON, Canada.) C9100-13 EM-CCD Digital Camera (Hamamatsu, Hamamatsu City, Japan) and Volocity Software (Perkin Elmer, Mississauga, ON, Canada) were used for image capture. Duolink Image Tool (free version) was used to analyze images and quantify red and blue signals.

3.7 Mass Spectrometry Analysis Sample Preparation

HEK293-T cells were grown in 10 cm plates and transfected with either FLAG-tagged hENT1 cDNA or empty vector (pcDNA 3.1 (-)) as control by calcium phosphate transfection method¹⁴⁸. Forty-eight hours post-transfection, cells were washed 2x with D-PBS and incubated for 10 minutes at room temperature with 1 mM uridine (a substrate of ENT1 that is not a primary

amine; solubilized in DMSO) or 100 nM NBMPR (ENT1 inhibitor, solubilized in DMSO). Dithiobis [succinimidylpropionate] (DSP), a cell-permeable cross-linker solubilized in DMSO, added to a final concentration of 2 mM in 8 mL final volume, with DMSO making up total of 8% final volume (below cell-toxicity levels of 10%). Cells were then incubated for 30 minutes at room temperature prior to quenching with 15 mM Tris buffer pH 7.5 for 15 minutes. Cells were washed in D-PBS and lysed for 20 minutes on ice with 300 μ L dodecyl maltoside (DDM) made as such: 0.08% w/v dodecylmaltoside in pH 7.4, 100 mM KCl, 10 mM Tris, 0.1 mM MgCl₂, 0.1 mM CaCl₂ with added protease inhibitor. Lysed samples were centrifuged at 16,000 x g for 10 minutes. The lysate was incubated with 50 μ L Dynabeads and 5 μ L mouse monoclonal anti-FLAG antibody (Clontech), rotating overnight (16 hours) at 4°C. Then, samples were washed 2x with 200 μ L DDM plus protease inhibitor and 500 μ L D-PBS plus protease inhibitor, and centrifuged at 9,000 x g for 10 minutes. The supernatant was removed and discarded and 40 μ L of 2X Laemmli Sample Buffer and 1 μ L of β -mercaptoethanol was added to each sample (Dynabeads, with proteins attached) prior to heating at 65°C for 4 minutes. Samples were loaded into a precast 4-20% gradient gel (BioRad) and separated until the sample buffer line was about 2 cm into the gel. Each lane was cut out using a sterile, fresh razor and submitted for In-Gel ID analysis to The Alberta Proteomics and Mass Spectrometry Facility operated by the Biochemistry department at the University of Alberta.

3.8 Data Analysis

Experiments were conducted at least four times and data presented as mean \pm S.E.M. or mean \pm 95% confidence interval, as specified, using GraphPad Prism v5.0. Statistical differences were assessed using Student's t-test for paired samples, one-way ANOVA with Tukey's post-test for

multiple comparisons, or nested two-level ANOVA, as indicated in results, with $P < 0.05$ denoting significance.

CHAPTER 4. RESULTS

4.1 Regulation of hENT1 by PKC Activation and A₁AR Stimulation

As the primary transporter of adenosine, hENT1 is an important factor in adenosine receptor-mediated signaling pathways. Previous pharmacological studies in our laboratory have explored how hENT1 function is affected through stimulation or inhibition of adenosine receptor 1 (A₁AR) signaling pathway and one downstream enzyme, protein kinase C (PKC). Computational analysis identified a potential PKC phosphorylation site at Serine 281. A similar site on the mouse ENT1 (mENT1), Serine 279, was confirmed to be phosphorylated by PKC using *in vitro* kinase assays⁷⁸. This site was mutated to produce a PK15-S281A-hENT1 stable mutant that was used for comparison to the wild type PK15-hENT1 in a series of experiments. For these experiments, phorbol 12-myristate 13-acetate (PMA), a PKC activator⁵⁰, 3-[1-[3-(dimethylamino)propyl]-5-methoxy-1*H*-indol-3-yl]-4-(1*H*-pyrrole-2,5,dione (Gö6983), a PKC inhibitor, 2-chloro-N(6)-cyclopentyladenosine (CCPA), a high-affinity A₁AR agonist¹⁴⁹, and 8-cyclopentyl-1,3-dipropylxanthine (DPCPX), an A₁AR antagonist¹⁵⁰, were used. PMA has been used in other studies to increase hENT1 substrate uptake following just 15 minutes of incubation with 100 nM of the activator⁵⁰. The broad spectrum PKC inhibitor Gö6983, was used at a 100 nM concentration which is approximately 10-fold higher than its IC₅₀ for inhibiting PKC isoforms δ and ϵ , having been previously implicated in regulating ENT1⁵⁰. In functional studies performed in our laboratory using these drugs, it was shown that in response to A₁AR stimulation and PKC activation, PK15-hENT1 cells have increased substrate uptake function as

indicated by an increase in initial uptake rate, V_{max} . This response is lost in PK15-S281A-hENT1 cells⁸³.

This section addresses the hypothesis that this increase in uptake rate (V_{max}) is due to an increase in the amount of hENT1 protein at the plasma membrane. Changes in plasma-membrane hENT1 following pharmacological stimulation of A_1AR and PKC was studied by immunofluorescence and biochemical approaches.

4.1.1 Immunofluorescence Analysis of hENT1 Localization

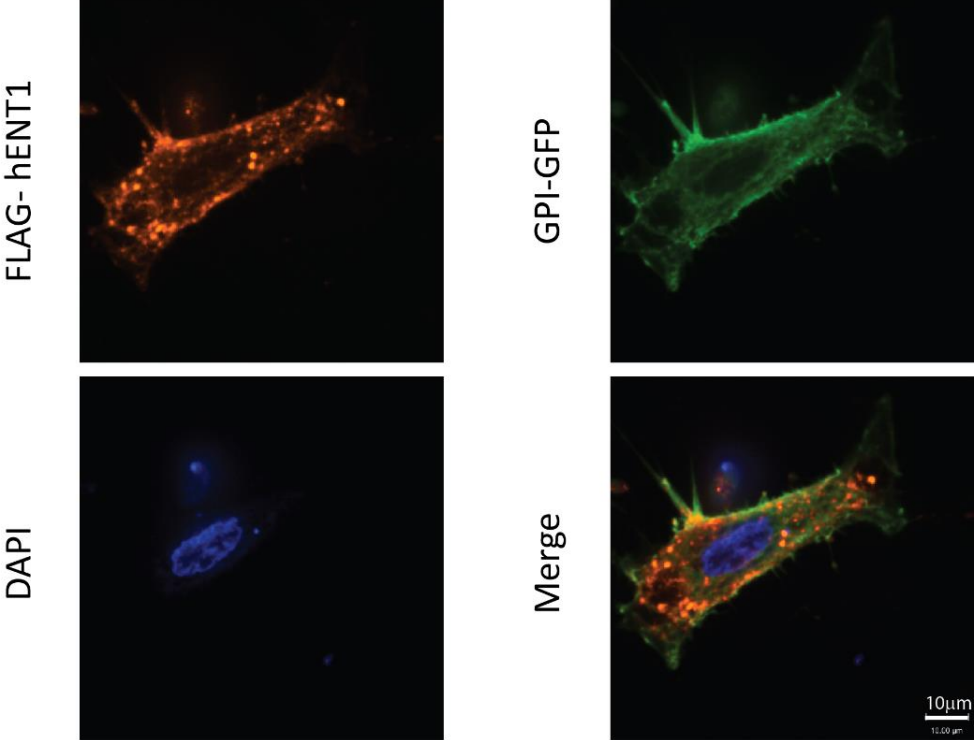
PK15-hENT1 and PK15-S281A-hENT1 were transfected with glycosylphosphatidylinositol (GPI-GFP), a plasma membrane marker, and were processed for immunocytochemical analysis following treatment with 100 nM PKC activator (PMA), its inactive analog (4α -PMA) as control, A_1AR agonist (CCPA) or 0.1% DMSO as vehicle control. Mouse monoclonal anti-FLAG and chicken anti-mouse Alexa594 antibodies were used to identify FLAG-tagged ENT1 proteins, as shown in figures 4.1-4.4 in red. Rabbit anti-GFP and chicken anti rabbit-Alexa488 antibodies were used to amplify the plasma membrane signal from GPI-GFP, which appears in green in figures 4.1-4.4.

Nuclei were stained with 4',6-diamidino-2-phenylindole (DAPI) in the mounting media.

Confocal images of cells were collected using a spinning disk confocal microscope with a 63X oil immersion lens. A representative slice, with the clearest view of the plasma membrane, from each condition is displayed below in Figures 4.1-4.4.

Figure 4.1 PK15-hENT1 Cells, +/- 100 nM PMA Treatment

A. PK15-hENT1, 4 α -PMA



B. PK15-hENT1, PMA

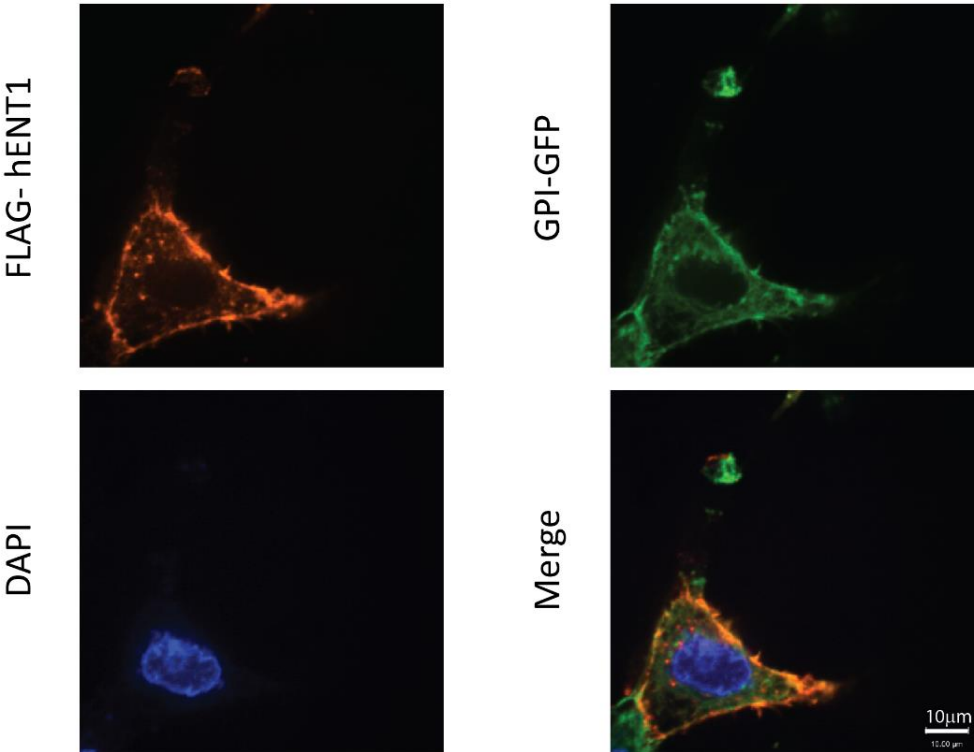
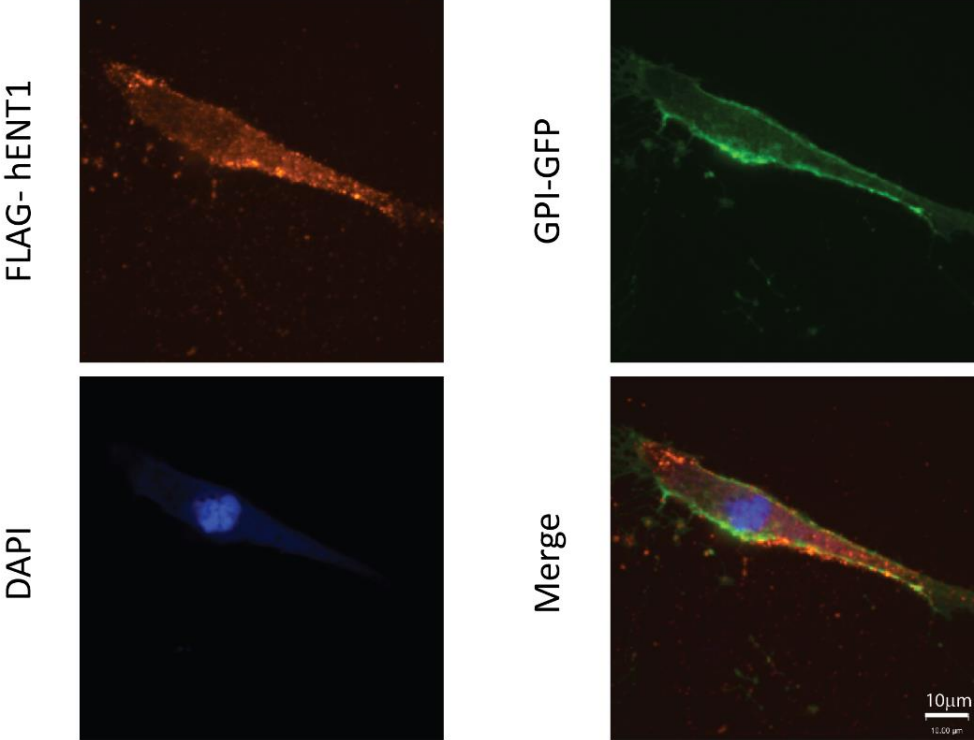


Figure 4.1: Confocal images of PK15-hENT1 cells incubated with the PKC activator PMA (panel B) or its inactive form 4 α -PMA (panel A). hENT1, the membrane marker GPI-GFP and nuclei are shown in red, green and blue, respectively. All images were acquired using constant exposure times and gains for every channel. Scale bars represent 10 μ m. In both panels A and B, FLAG-tagged wild-type ENT1 is localized near the plasma membrane as well as inside large intracellular occlusions. In the merged image in panel A, ENT1 is localized just below the plasma membrane in a puncta pattern and there is some overlap with GPI-GFP at the plasma membrane, indicated by apparent yellow staining. In the merged image in panel B, there is continuous yellow staining at the plasma membrane. The punctate pattern staining of ENT1 that appears in panel A is not prevalent in panel B.

Figure 4.2 PK15-S281A-hENT1 Cells, +/- 100 nM PMA Treatment

A. PK15-S281A-hENT1, 4 α -PMA



B. PK15-S281A-hENT1, PMA

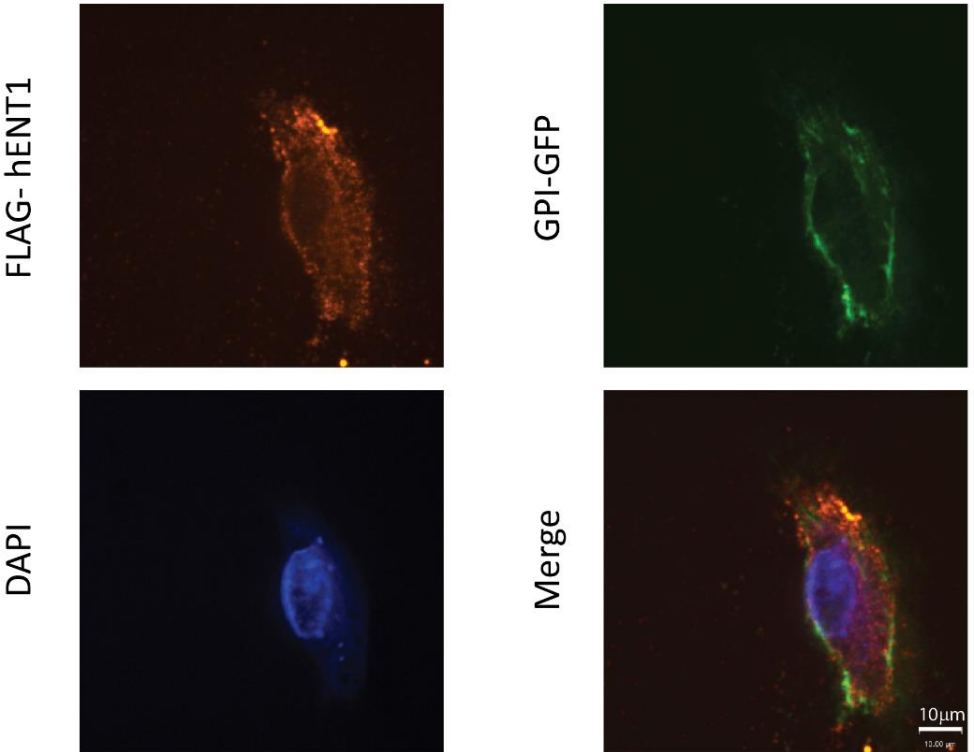
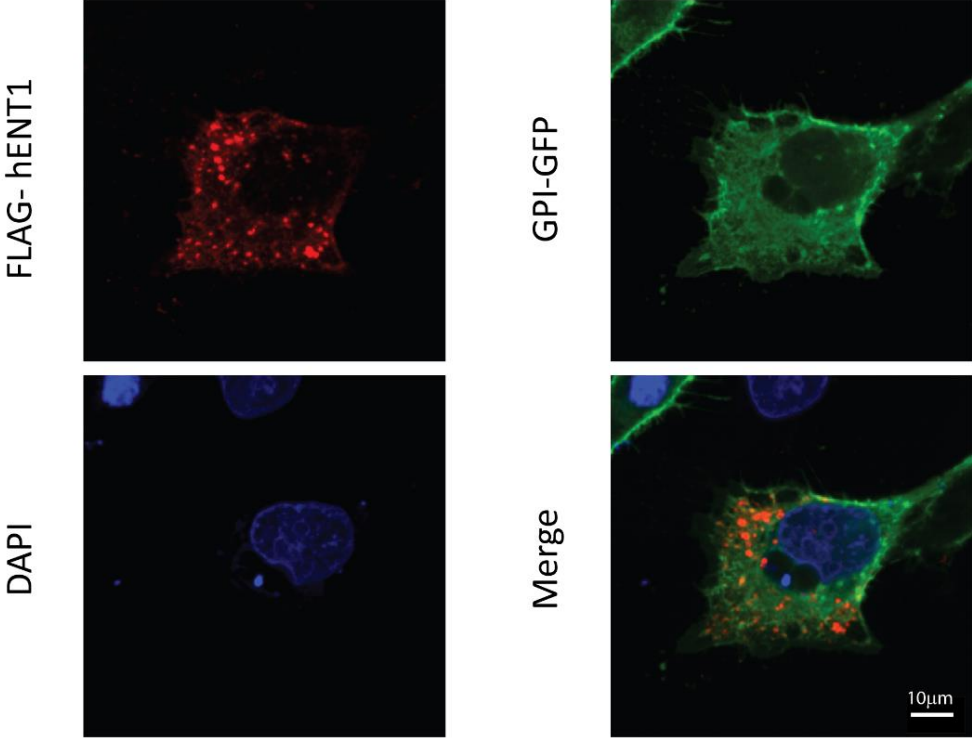


Figure 4.2: Confocal images of PK15-S281A-hENT1 cells incubated with the PKC activator PMA (panel B) or its inactive form 4 α -PMA (panel A). hENT1, the membrane marker GPI-GFP and nuclei are shown in red, green and blue, respectively. All images were acquired using constant exposure times and gains for every channel. Scale bars represent 10 μ m. In both panels A and B, ENT1 appears sparsely distributed throughout the cytoplasm and near the membrane in a puncta-pattern. The merged images of both panels A and B show very little yellow staining.

Figure 4.3 PK15-hENT1 Cells, +/- 100 nM CCPA Treatment

A. PK15-hENT1, 0.1% DMSO



B. PK15-hENT1, 100nM CCPA

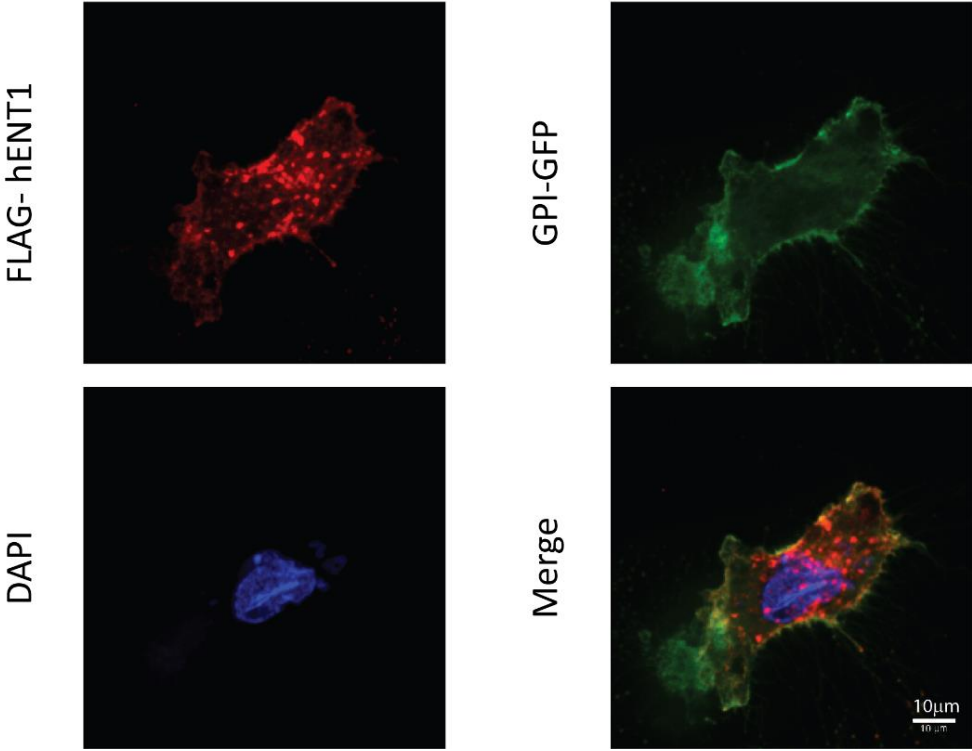
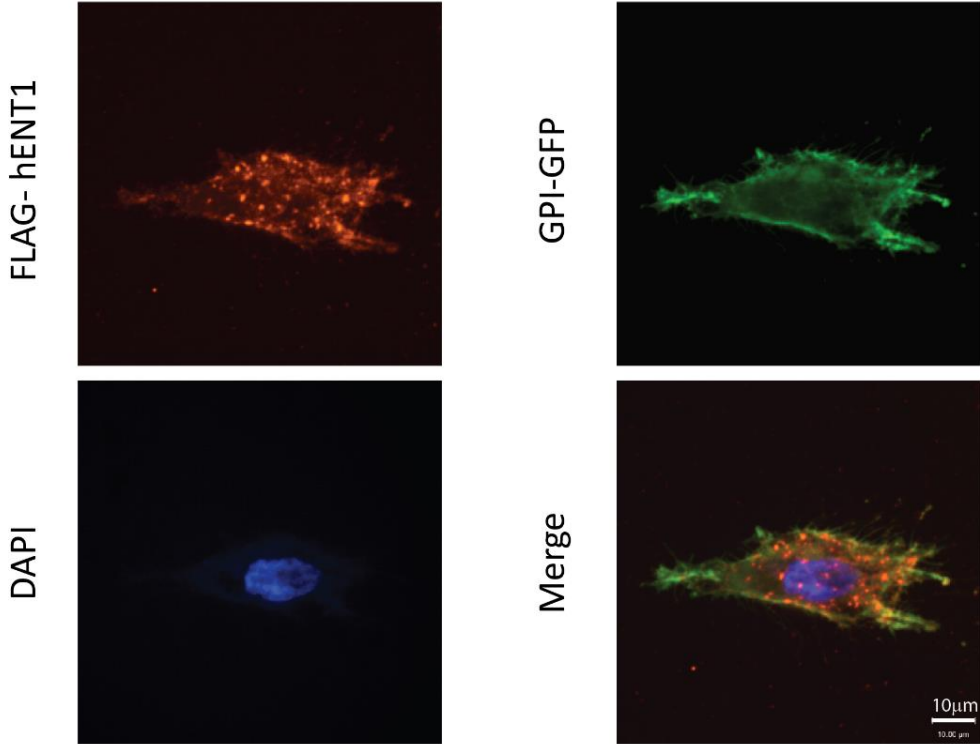


Figure 4.3: Confocal images of PK15-hENT1 cells incubated with the A₁AR stimulator, CCPA (panel B) or vehicle control, DMSO (panel A). hENT1, the membrane marker GPI-GFP and nuclei are shown in red, green and blue, respectively. All images were acquired using constant exposure times and gains for every channel. Scale bars represent 10 μm. In panels A and B, ENT1 appears primarily in large intracellular occlusions as well as in a puncta pattern along the plasma membrane. In the merged image in Panel B, some yellow staining is apparent at the plasma membrane.

Figure 4.4 PK15-S281A-hENT1 Cells, +/- 100 nM CCPA Treatment

A. PK15-S281A-hENT1, 0.1% DMSO



B. PK15-S281A-hENT1, 100nM CCPA

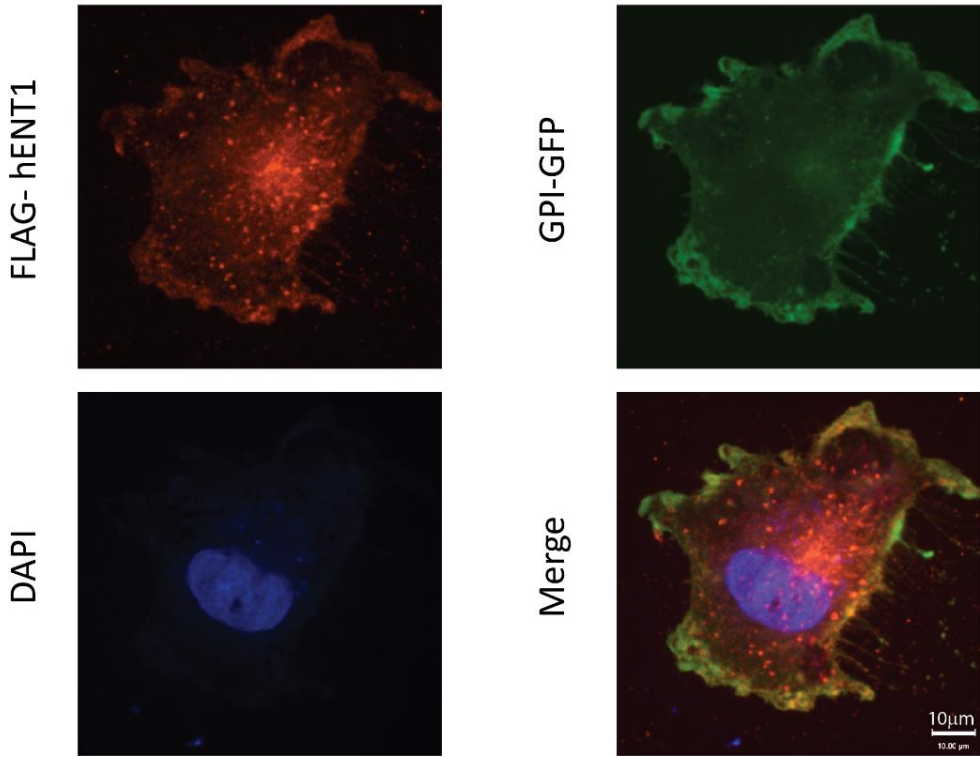


Figure 4.4: Confocal images of PK15-S281A-hENT1 cells incubated with the A₁AR stimulator, CCPA (panel B) or vehicle control, DMSO (panel A). hENT1, the membrane marker GPI-GFP and nuclei are shown in red, green and blue, respectively. All images were acquired using constant exposure times and gains for every channel. Scale bars represent 10 μm. In both panels A and B, ENT1 is localized primarily to intracellular occlusions and in puncta-pattern staining under the plasma membrane. Merged images in panels A and B show primarily separate red and green staining and some discontinuous yellow staining at the plasma membrane.

Generally, PK15-S281A-hENT1 cells appeared smaller in size than PK15-hENT1 cells. They do not grow as quickly or attain the same surface coverage, and fewer cells with intact nuclei are available for image capture. Both cell types contained large intracellular occlusions of ENT1 which varied in their size and quantity from cell to cell in both wild-type and mutant. As described in figures 4.1-4.4, ENT1 appears frequently in a punctate-pattern along/below the plasma membrane as well as in large intracellular occlusions. GPI-GFP is an effective plasma membrane marker and stains the membrane in a continuous fashion. The nuclei, shown in blue, are intact and indicative of healthy cells acquired for imaging.

Qualitatively, appearance of yellow staining indicates overlap between red and signals, which shows plasma-membrane localized ENT1, and is seen primarily in Panel B of Figure 4.1. In order to determine whether there were significant changes in overlap between hENT1 and the plasma membrane marker, Pearson's correlation coefficients, quantifying colocalization of red fluorescent signal (hENT1) with green signal (GPI), were measured using IMARIS V7.4 (©Bitplane) software.

Figure 4.5 Quantifying colocalization of hENT1 with plasma membrane marker, GPI-GFP

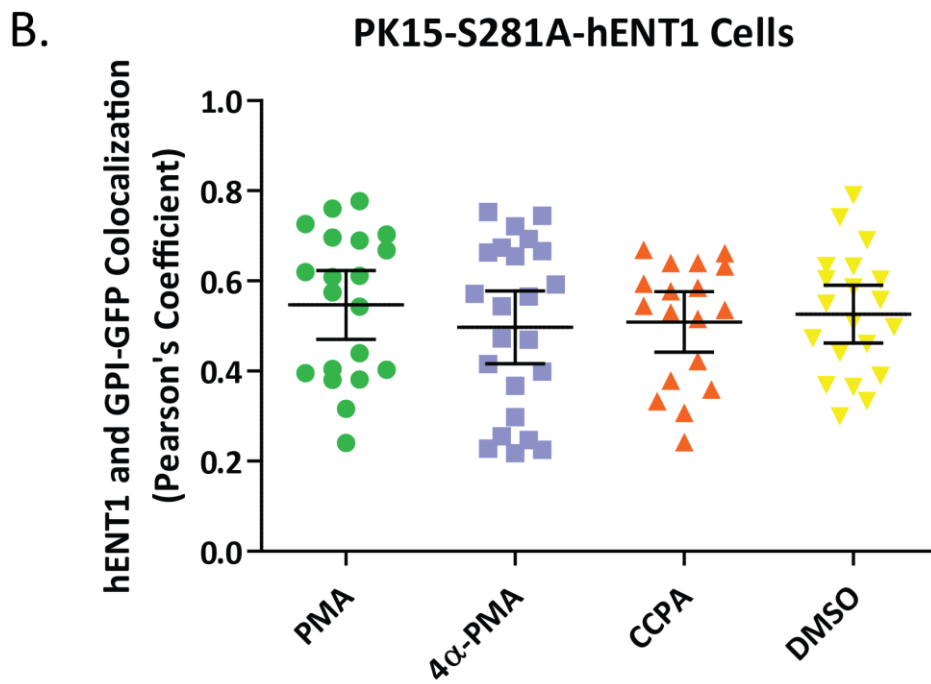
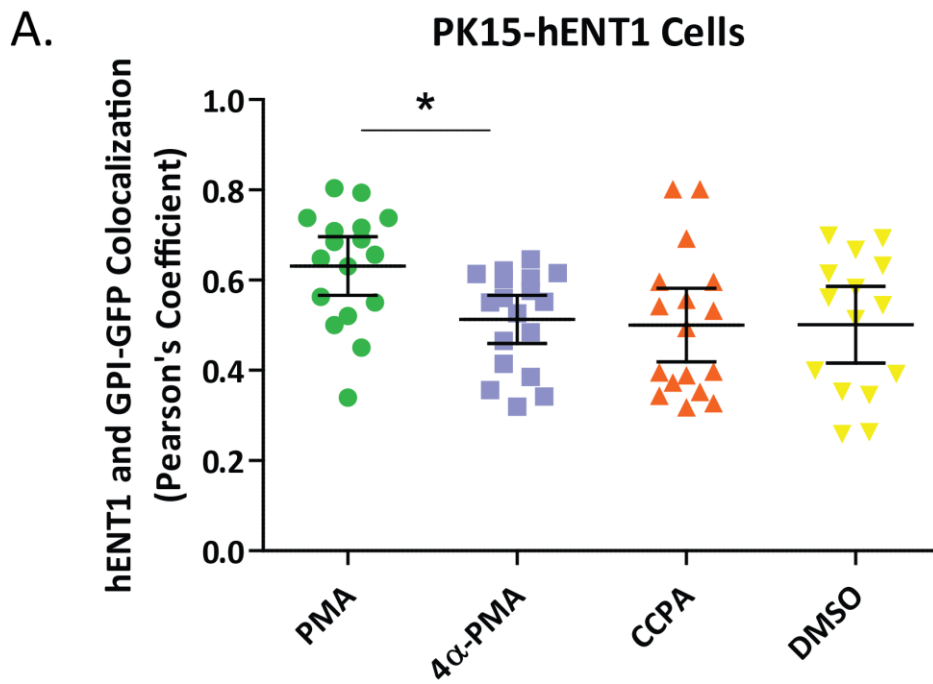


Figure 4.5: This figure shows Pearson's coefficients of FLAG-tagged hENT1 and GPI-GFP colocalization calculated using IMARIS software. Pearson's coefficient represents the relative amount of hENT1 at the plasma membrane. The graphs in Figure 4.5 below show replicate samples from five independent experiments (four samples were collected for quantitation from each experiment). The error bars represent 95% confidence intervals. Two-way nested ANOVA was used to compare PMA treatment to 4 α -PMA control treatment, and CCPA treatment to DMSO control, in each cell type, where $p < 0.05$ was considered significant. In PK15-hENT1 cells following PKC activation by PMA treatment (panel A), more hENT1 localized at the plasma membrane compared to 4 α -PMA control- Pearson's coefficients are 0.63 ± 0.03 and 0.51 ± 0.03 respectively, $p=0.02$. There was no change in colocalization following A₁AR stimulation by CCPA treatment in PK15-hENT1 cells (panel A); Pearson's coefficients for CCPA treated and DMSO control are 0.50 ± 0.04 and 0.50 ± 0.04 , respectively and $p=0.99$. There was no significant change in plasma membrane localization of S281A-hENT1 following either PKC activation or A₁AR stimulation by PMA ($p=0.36$) or CCPA ($p=0.70$) treatment, respectively, when compared to control (panel B).

To further investigate the observed changes (and lack thereof) in hENT1 localization, analysis of cell surface processing by biotinylation was also applied.

4.1.2 Cell Surface Processing by Biotinylation

PK15-hENT1 and PK15-S281A-hENT1 cells were used for cell surface processing studies. Cells were treated with 100 nM PMA, 4 α -PMA, CCPA, or 0.1% DMSO as described in section 3.3 and then incubated with Sulpho-NHS-SS-Biotin. Biotin binds only to protein exposed at the cell surface so when cells were then lysed, it was possible to separate the biotin-bound lysate (protein at the extracellular surface of the cell) from the unbound (intracellular protein) with streptavidin-agarose resin. Equal quantities of total and unbound protein, quantified by BCA assay, were subjected to SDS-PAGE. Mouse monoclonal anti-FLAG antibody was used to identify the protein of interest by Western Blot analysis.

Figure 4.6 Representative Western Blots of cell surface processing experiments

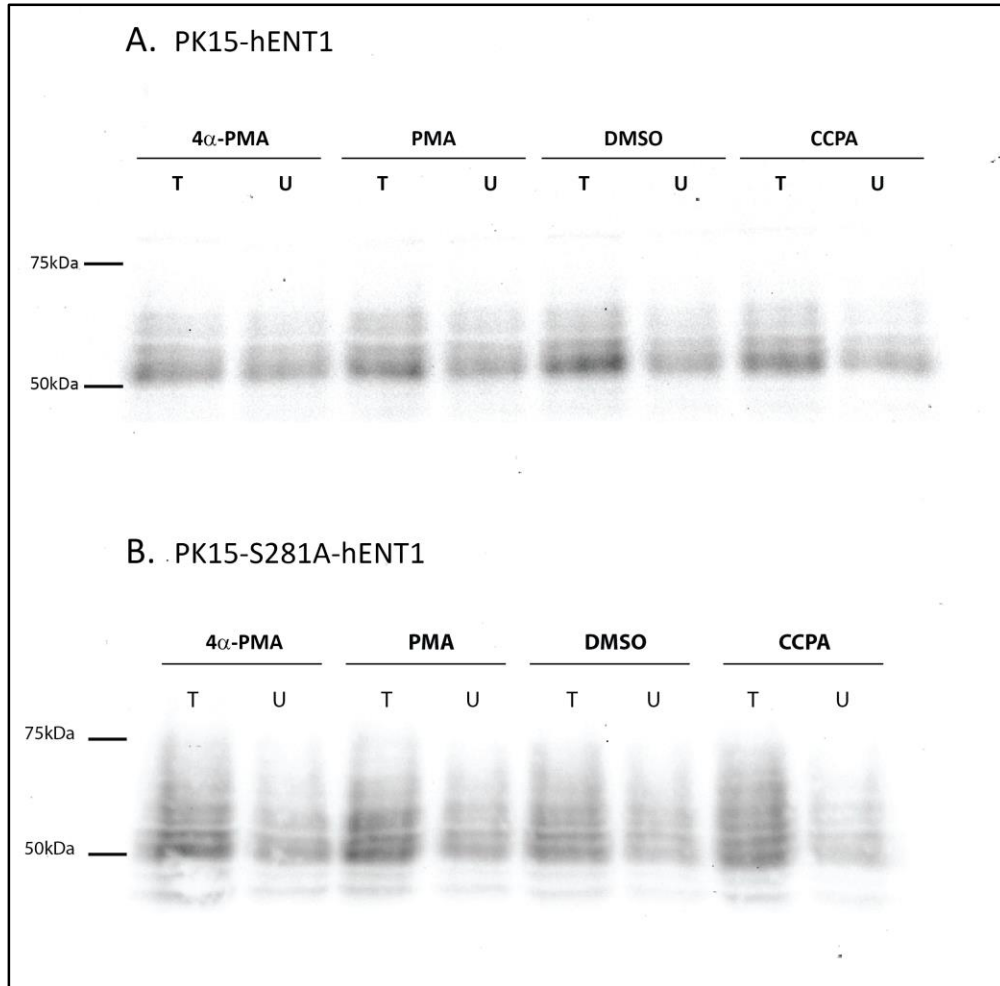


Figure 4.6: A representative Western Blot image captured using a digital chemiluminescence camera. Panel A shows PK15-hENT1 cells and panel B shows PK15-S281A-hENT1 cells. Total protein lysate is identified as 'T' and the intracellular protein/unbound by biotin is identified as 'U.' Multiple bands corresponding to FLAG-tagged ENT1 are apparent in both PK15-hENT1 and PK15-S281A-hENT1 samples. The relatively dense band at 50 kDa represents non-glycosylated ENT1. Three diffuse bands at and above 55 kDa represent ENT1 with various levels of glycosylation. Bands below 50 kDa, particularly visible in the PK15-S281A-hENT1 samples, correspond to the degradation product of ENT1 as seen previously in the literature³⁷.

The band density from digital western blot images was calculated using ImageLab software from ©Biorad. The software identifies the densest region of the band and sets band size according to an internal algorithm. The percentage of protein bound at the plasma membrane was calculated as follows:

$$\% \text{ Bound} = \frac{(\text{total protein} - \text{unbound protein})}{\text{total protein}} \times 100$$

Figure 4.7 shows the percentage of membrane bound hENT1 in PMA treated and CCPA treated conditions for both PLK15-hENT1 and PK15-S281A-hENT1 cells.

Figure 4.7 Quantifying hENT1 at the plasma membrane

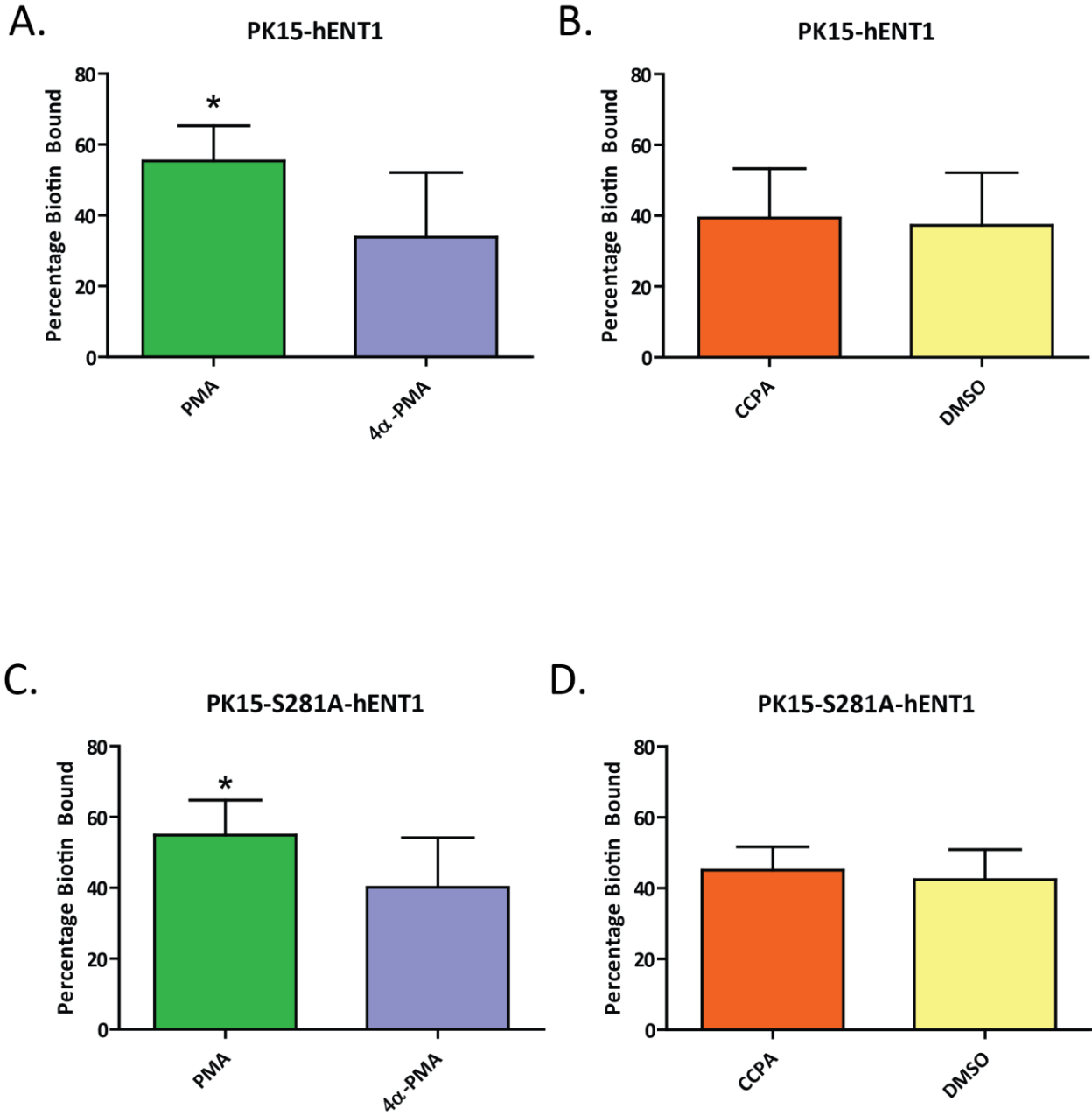


Figure 4.7: Bar graphs show the average percentage of hENT1 at the plasma membrane \pm 95% confidence interval. Panels A and B show n=6 cell surface processing experiments with PK15-hENT1 cells, PMA treatment and control in panel A and CCPA treatment and control in panel B. Panels C and D show n=4 experiments with PK15-S281A-hENT1 cells; panel C shows the PMA treatment and control and panel D shows the CCPA treatment and control. Each treatment group was compared to its treatment control by Student's t-test with a 95% confidence interval, where $P < 0.05$ is significant. In PK15-hENT1 cells, $55 \pm 3.9\%$ of hENT1 was plasma membrane bound in the PMA treated condition compared to $36 \pm 5.8\%$ in the 4α -PMA treated (control) cells, the difference is statistically significant as $p = 0.02$. Stimulation of the A_1 AR with CCPA showed no change compared to DMSO control in PK15-hENT1 cells, $39.4 \pm 5.4\%$ and $37.3 \pm 5.8\%$, respectively, $p = 0.79$. In PK15-S281A-hENT1 cells, PMA also caused an increase in plasma membrane localization of hENT1. There was a significant difference in plasma-membrane hENT1, $p = 0.03$, between PMA-treated ($54.9 \pm 3.1\%$) and control ($40.17 \pm 4.4\%$) cells. There was no change in PK15-S281A-hENT1 protein at the plasma membrane following CCPA treatment ($42.4 \pm 2.7\%$ control, $45.11 \pm 2.1\%$ + CCPA, $p = 0.46$).

Through immunofluorescence and cell surface processing experiments it was determined that there is an increase in hENT1 at the plasma membrane in PK15-hENT1 cells following activation of PKC but not through stimulation of A_1 AR. In PK15-S281A-hENT1 cells, stimulation through A_1 AR also did not result in any changes in hENT1 expression at the plasma membrane in both immunofluorescence and biotinylation studies. Activation of PKC in PK15-S281A-hENT1 cells did not result in an increase in plasma membrane-hENT1 when analyzed by immunofluorescence.

However, there was a marked increase in plasma-membrane localized ENT1 in PK15-S281A-hENT1 cells as determined by cell surface processing experiments (an increase from 40 to 55% protein at the plasma membrane following PMA treatment, $p=0.03$).

These experiments have shown that changes in hENT1 uptake function following stimulation at A₁AR (as shown in Figure 2.2) are not due to an increase in hENT1 at the plasma membrane.

Furthermore, the increase in transport function following PKC activation are only in part due to an increase in hENT1 protein at the plasma membrane (as shown in Figure 2.1). The discussion section 5.1 further delves into the significance of these findings.

4.2 Multimeric hENT1 Complex

Biochemical and immunofluorescent techniques were used to assess whether hENT1 monomers interact. Association of hENT1 was analyzed in transiently transfected HEK293 cells with MYC- and HA-tagged hENT1 through co-immunoprecipitation. In order to assess interaction in stably-expressing cells, PK15-hENT1 cells were used for chemical cross-linking analysis with cell impermeable reagent DTSSP and by immunofluorescence using a Proximity Ligation Assay.

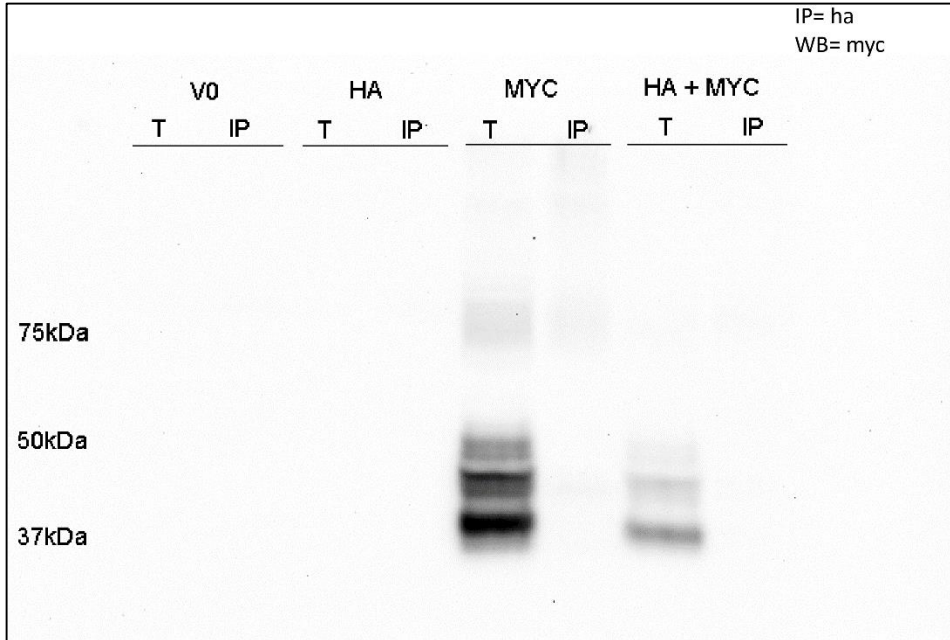
4.2.1 Co-Immunoprecipitation in HEK293 Cells

HEK293 cells were transfected with MYC-hENT1, HA-hENT1, co-transfected with both, or with empty vector. Following lysis, cells were immunoprecipitated using a monoclonal anti-HA antibody. The total lysate and immunoprecipitated samples were separated by SDS-PAGE and interrogated with a polyclonal anti-MYC antibody (Figure 4.8A). The converse experiment, immunoprecipitation with anti-MYC and Western Blot with anti-HA was also done (Figure 4.8B).

A digital chemiluminescence camera captured images of the Western Blot. Representative images are shown in Figure 4.8.

Figure 4.8 Co-Immunoprecipitation Western Blot

a. Immunoprecipitation with anti-HA antibody, Western Blot with anti-MYC antibody



b. Immunoprecipitation with anti-MYC Antibody, Western Blot with anti-HA antibody

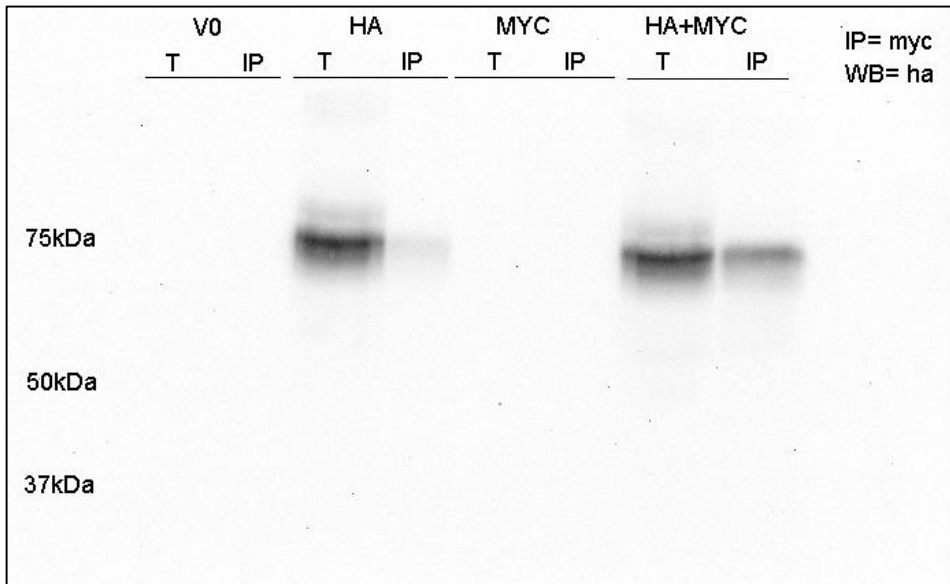


Figure 4.8: In panel A, a representative Western Blot of a co-immunoprecipitation experiment in which monoclonal anti-HA antibody was used for immunoprecipitation and a polyclonal anti-MYC antibody was used for probing is shown. No bands are visible in lanes 1-4. Lanes 1 and 2 are of vector transfected cells (V0), and no bands are expected as no MYC-tagged protein should exist in those samples. Lanes 3 and 4 are negative controls: cells transfected with HA-ENT1, immunoprecipitated (Lane 4 only) with anti- HA antibody, should not and did not contain any MYC-ENT1, suggesting that there is no cross-reactivity of anti-MYC antibody with the HA epitope, nor is there anything in the total lysate of HA-ENT1 transfected cells that an anti-MYC antibody can detect. The membrane was properly blocked to avoid non-specific antibody binding. Lane 5, total lysate from MYC-ENT1 transfected cells, is an effective positive control. MYC-ENT1 is apparent as a diffuse band at around 50 kDa and a sharp band just below 50 kDa. A sharp, saturated band just above 37 kDa is likely a degradation product³⁷. Lane 6 serves as another negative control, pulling down with anti-HA antibody did not result in MYC-ENT1 pull-down, suggesting that the anti-HA antibody does not cross-react. Lane 7, containing total lysate from cells co-transfected with MYC and HA-ENT1 contain HA-ENT1 in a series of three bands identical to those in lane 5 in their relative intensity, but not absolute intensity, as expected. Lane 8 was blank. Panel B shows the same experiment but with converse antibodies used for immunoprecipitation and Western Blot- polyclonal anti-MYC was used for immunoprecipitation and a monoclonal anti-HA antibody was used for the Western Blot. In this case, lanes 5 and 6 serve as negative control- they show that cells transfected with MYC-ENT1 do not have any HA-ENT1, that the background noise is low, and that the antibodies are specific. Lane 3 shows the positive control - total lysate from HA-ENT1 transfected cells contains HA-ENT1. Lanes 7 and 8

both show identical bands, varying slightly in saturation as expected. In co-transfected cells, HA-ENT1 is present following immunoprecipitation with anti-MYC antibody suggesting that the two ENT1 types (HA and MYC) associate. All HA-ENT1 bands appear at 75 kDa and only one band is present, not 3, as in Figure 4.8a. Higher than usual migration on Western Blot may be indicative of protein aggregation.

Bands corresponding to ENT1 are observed in the immunoprecipitated lane of the co-transfected cell lysate sample (Lane 8, Figure 4.8b) suggesting that MYC-hENT1 and HA-hENT1 are associating together in order for both proteins to be pulled down with an antibody selective for only one tag, MYC. Section 5.2 includes a discussion about the presence of single bands at 75 kDa in panel B, as well as a discussion of why these two converse experiments did not yield the same results.

4.2.2 PK15-hENT1 Cells Did Not Show Cross-Linking of ENT1

PK15-hENT1 cells were incubated with varying concentrations of DTSSP, a water-soluble cross-linker. The cross-linker reacts with primary amines within an 8 Å distance on the extracellular surface of the cell. DTT treatment following crosslinking was used to cleave the bond in half the samples prior to separation by SDS-PAGE. Zinc formalin was also used as a general cross-linker. Cross-linking with zinc-formalin and DTSSP was done in the presence and absence of PMA, following our knowledge that PMA treatment stimulates plasma membrane localization of hENT1.

Figure 4.9 Chemical cross-linking of PK15-hENT1 cells

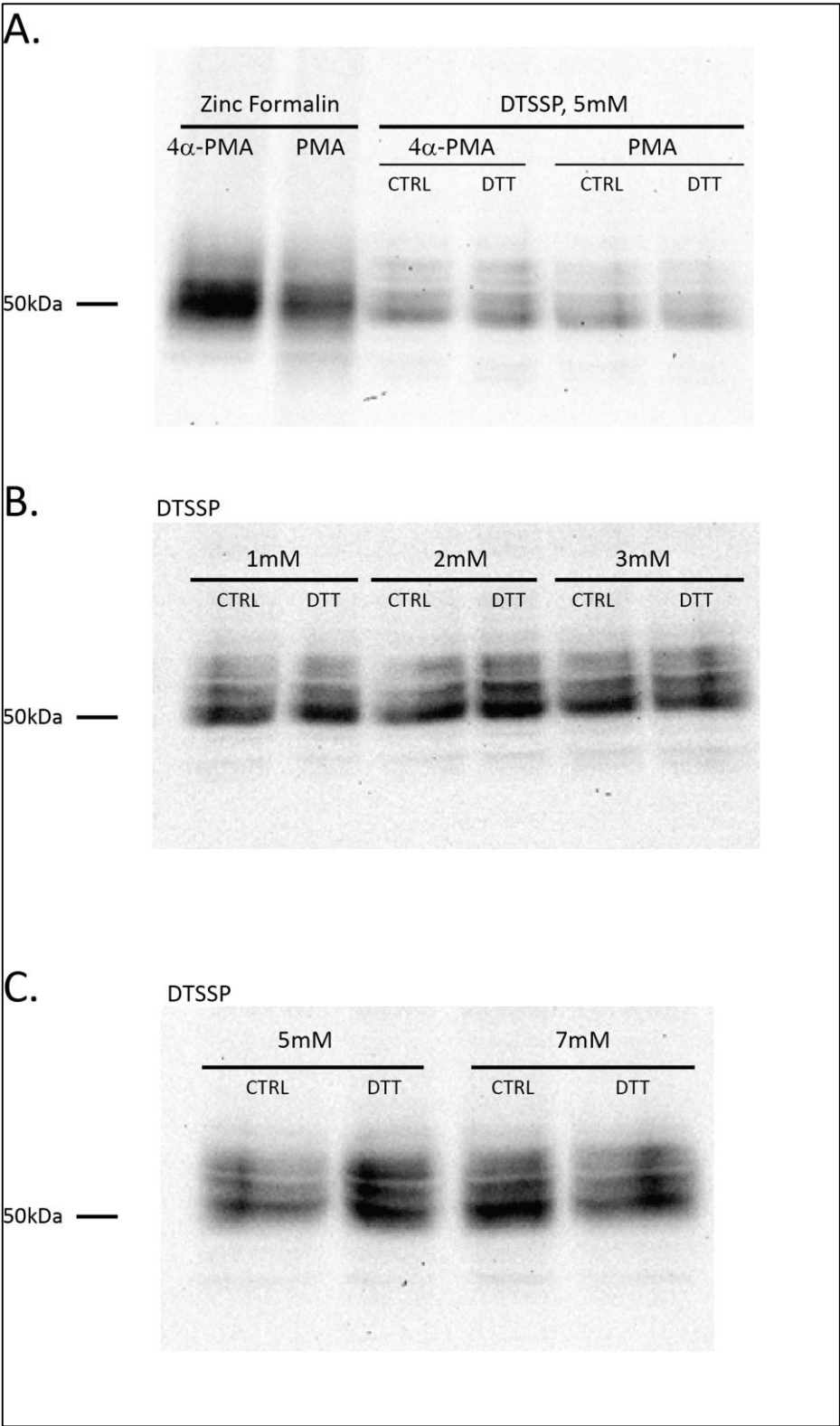


Figure 4.9: These are representative Western Blot images of several crosslinking experiments captured with a digital chemiluminescence camera. Panel A shows zinc formalin cross-linking as well as cross linking with 5 mM DTSSP in the presence of PMA. Figures B and C show the results of using varying concentrations of DTSSP. All three panels, A, B, and C, show very similar results. Three bands, varying in intensity, appear at and above 50 kDa and correspond to the non-glycosylated and glycosylated FLAG-tagged ENT1 protein. Very faint bands can be seen below 50 kDa, around 37 kDa, which is the degradation product of ENT1³⁷. If cross-linking of two ENT1's occurred, the control (CTRL) lanes would show higher order protein bands, and the corresponding DTT treated lanes would show the monomeric protein as is seen in all lanes in Figure 4.9. Zinc formalin and DTSSP did not crosslink hENT1 in PK15-hENT1 cells. For comparison, the crosslinking experiment was done with HEK293 cells transfected with MYC-hENT1, HA-hENT1, and co-transfected with both, as shown in Figure 4.10.

Figure 4.10 Chemical cross-linking of HEK293 cells expressing MYC- and HA- hENT1

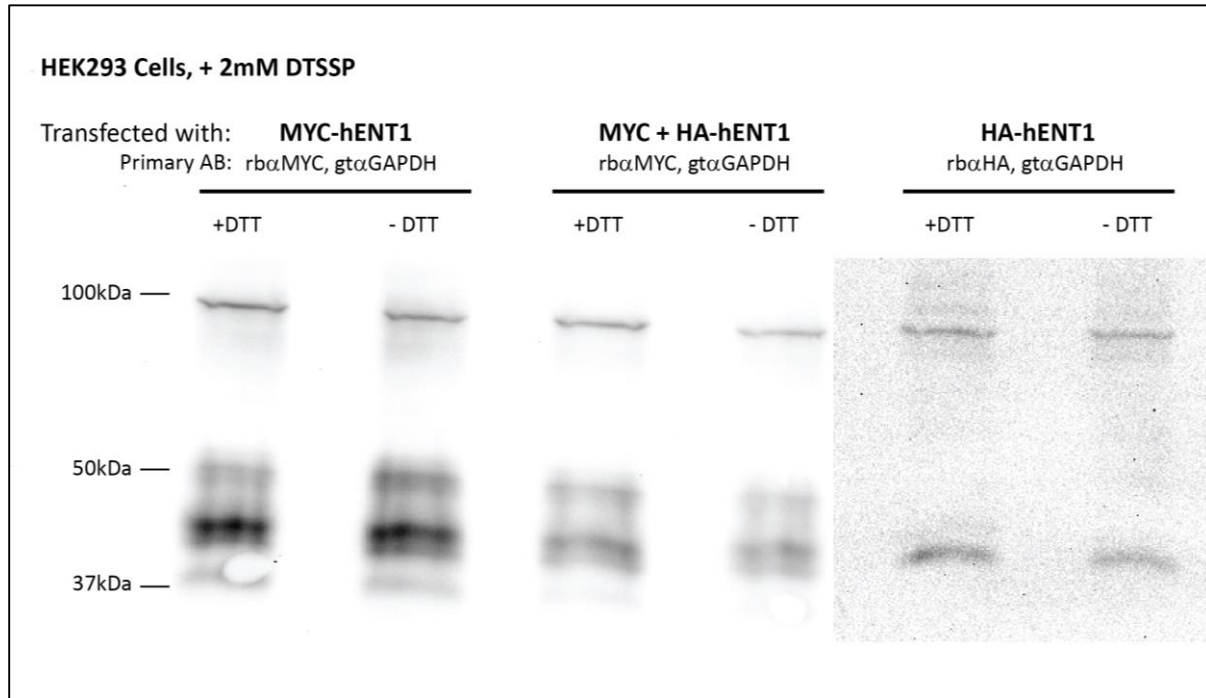


Figure 4.10: In transfected HEK293 cells, DTSSP did not crosslink hENT1. Lanes 1 and 2 show HEK293 cells transfected with MYC-hENT1, probed with rabbit anti-MYC and goat anti-GAPDH antibodies, where GAPDH serves as a loading control. Lanes 3 and 4 show HEK293 cells co-transfected with HA- and MYC-hENT1, probed with rabbit anti-MYC and goat anti-GAPDH antibodies. Lanes 5 and 6 show HEK293 cells transfected with HA-hENT1, probed with rabbit anti-HA and goat anti-GAPDH antibodies. Lanes are labelled as +DTT indicate that those samples were treated with DTT prior to SDS-PAGE loading to cleave the cross-linker and remove cross-linked products, whereas in the -DTT lane, samples do not undergo cleavage and represent the result of crosslinking with DTSSP. In all six lanes, hENT1 was observed just above 37 kDa, and around 50 kDa. These bands correspond to the degradation product and full sized hENT1 respectively. The 37 kDa band is the GAPDH control. The band at 100 kDa is an artifact and not related to the cross-linking event, as it is present in all lanes and there is no change in

band density within each pair of samples. If the 100 kDa band was a result of cross-linking between two ENT1 monomers, then the DTT would cleave a disulfide bond within the spacer arm of the sulfo-NHS-ester crosslinker and the 100 kDa band would not exist at equal density in the control (- DTT) and the +DTT lanes.

4.2.3 Proximity Ligation Assay in PK15-hENT1 Cells

PK15-hENT1 and the base PK15-NTD cells were used for this experiment. For the experimental condition and negative control, cells were transfected with MYC-hENT1, and for the positive control cells were transfected with HA-tagged anion exchanger 1 (AE1) and carbonic anhydrase II (CAII)¹⁴⁰. Monoclonal mouse anti-FLAG and rabbit anti-MYC antibodies were used for the experimental condition (Figure 4.11A), the positive control with monoclonal anti-HA and rabbit anti-CAII (Figure 4.11B), and the negative control with monoclonal anti-FLAG and rabbit anti-GLUT1 (Figure 4.11C). From then on, the Proximity Ligation Assay protocol was followed as outlined by Olink Bioscience.

Figure 4.11 Proximity Ligation Assay Images Showing hENT1 Monomer Interaction

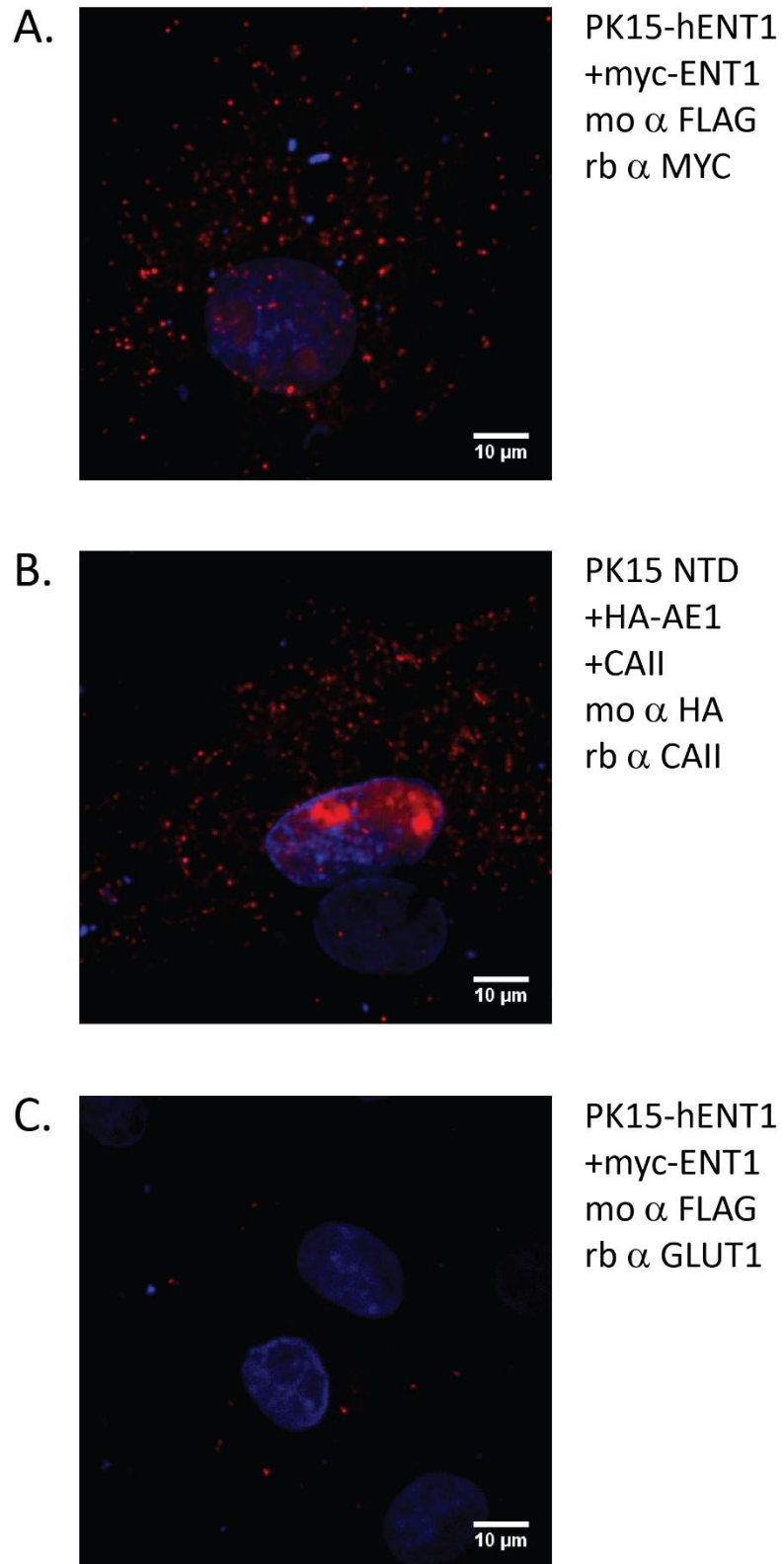


Figure 4.11: Panel A shows the experiment, PK15-hENT1 cells transfected with MYC-hENT1 and probed using primary antibodies anti-FLAG and anti-MYC. Panel B shows the positive control, PK15-NTD cells transfected with CAII and HA-AE1 probed with primary antibodies anti-CAII and anti-HA. Panel C shows the negative control, PK15-hENT1 cells transfected with MYC-hENT1 probed with anti-FLAG and anti-GLUT1 antibodies. All images were acquired using constant exposure times and gains for every channel. Scale bars represent 10 μm . In all panels, each red signal indicates a proximity event- two primary antibodies raised against different epitopes (differentiated by the species of the antibody) that are within 12 Å of each other. Each blue signal comes from DAPI-containing mounting media and indicates a nucleus.

Red and blue signals were quantified according to the instructions of the manufacturer and analyzed using Duolink Image Tool (©Olink Bioscience). The number of red signals (each signal corresponds to successful DNA polymerization/proximity event) was divided by the number of blue signals (nuclei) to determine the number of successful colocalization events per cell.

Represented below in Figure 4.12 is a summary of four independent proximity ligation assay experiments.

Figure 4.12 Quantitation of Proximity Ligation Assay

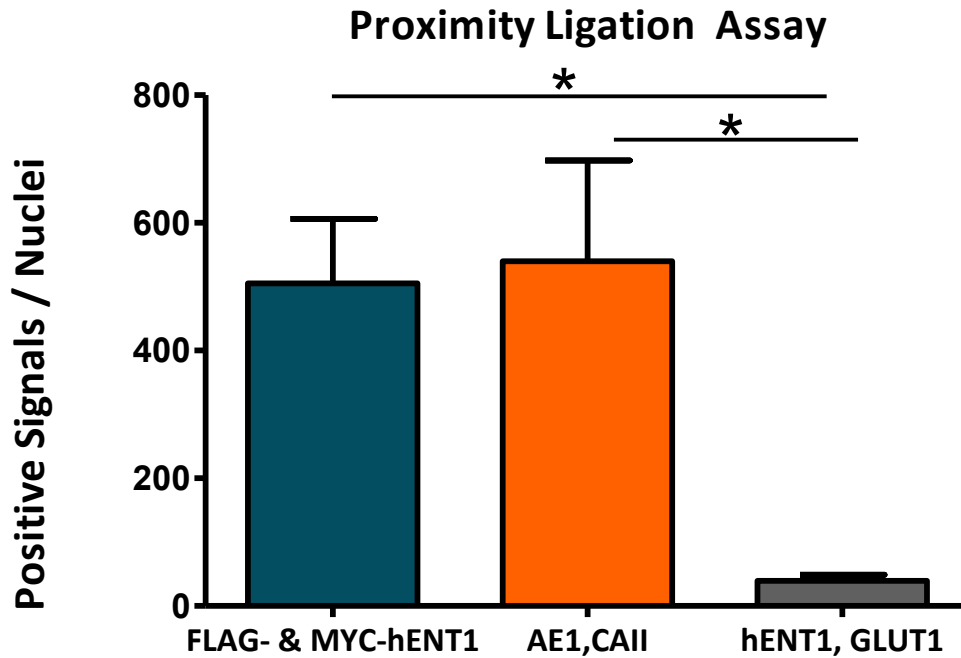


Figure 4.12: Twenty-four replicates from 4 independent experiments +SEM are summarized in Figure 4.12. One-Way ANOVA was used to compare the samples, and $p < 0.05$ was considered statistically significant. The positive control (HA-AE1 and CAII) and experimental condition (FLAG-hENT1 and MYC-hENT1) were not significantly different ($p > 0.05$), as they had on average 540 ± 157 and 505 ± 101 signals per cell respectively. The negative control (FLAG-hENT1 and GLUT1) had 39 ± 10 signals per cell, and this value is significantly different from both the positive control and experiment ($p < 0.05$). Tagged ENT1 monomers are shown to interact in intact cells at a rate significantly greater than the negative control, ENT1 and GLUT1.

4.2.4 Mass Spectrometry In-Gel ID

In order to initiate investigation into hENT1 complex formation and finding interacting protein partners, mass spectrometry in-gel identification experiments were performed. HEK293-T cells were transfected with FLAG-hENT1 cDNA, incubated with either 100 nM NBMPR or 1 mM uridine, and incubated with DSP- a cell permeable cross-linking reagent. Following immunoprecipitation with anti-FLAG antibody, the lysate was separated by SDS-PAGE and the bands excised for mass spectrometry.

Results from transfected and un-transfected cells of each condition were compared. A result was considered a ‘hit’ if it was unique to the hENT1-expressing cells and duplicated between experiments.

Table 4.1 Mass Spectrometry In-Gel ID Results

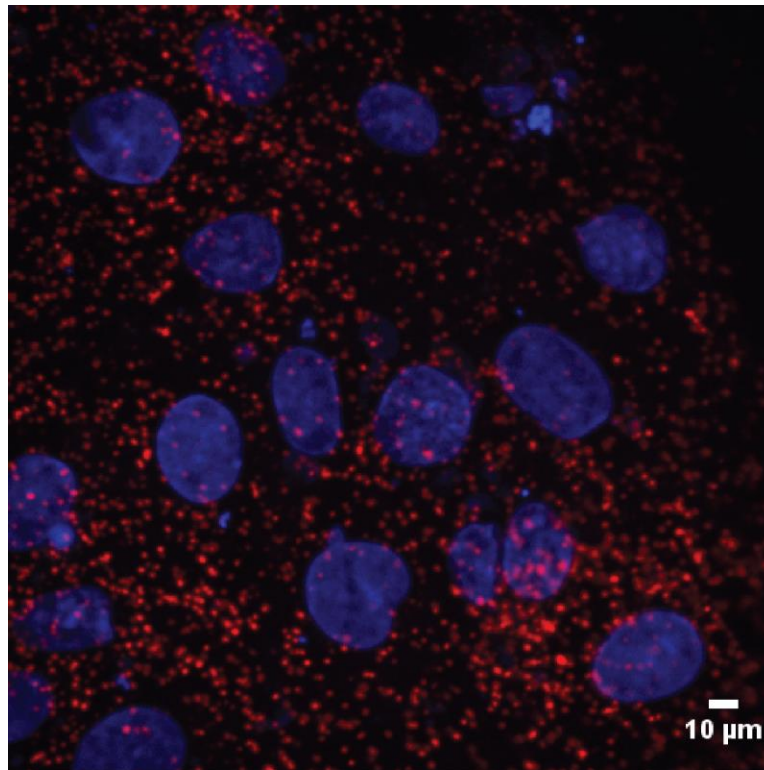
DUPLICATES	SAMPLES PRE-TREATED WITH URIDINE	SAMPLES PRE-TREATED WITH NBMPR
SODIUM/POTASSIUM-TRANSPORTING ATPASE SUBUNIT ALPHA-1 OS=HOMO SAPIENS GN=ATP1A1 PE=1 SV=1 - [AT1A1_HUMAN]	3 hits out of n= 4	2 hits out of n=4
CLATHRIN HEAVY CHAIN 1 OS=HOMO SAPIENS GN=CLTC PE=1 SV=5 - [CLH1_HUMAN]	2 hits out of n= 4	1 hit out of n = 4

Out of 4 independent experiments, the catalytic (alpha, α) subunit of Na⁺/K⁺-ATPase came up 3 and 2 times, with uridine and NBMPR pre-incubation, respectively. Clathrin heavy chain also appeared in several experiments.

4.2.5 Proximity Ligation of hENT1 and Na⁺/K⁺-ATPase

When first designing the proximity ligation assay experiment for identifying ENT1-ENT1 interactions, Na⁺/K⁺-ATPase was used as a negative control. PK15-hENT1 cells were probed with mouse monoclonal anti-FLAG and rabbit anti Na⁺/K⁺-ATPase alpha. Figure 4.13 is a representative image from these experiments.

Figure 4.13 Proximity Ligation Assay of PK15-hENT1_{FLAG} with Na⁺/K⁺-ATPase



PK15-hENT1 + MYC-hENT1
mo α FLAG, rb α Na⁺ K⁺ ATPase

Figure 4.13: a representative image from n=3 experiments of proximity ligation assay results from PK15-hENT1 cells transfected with MYC-hENT1 and probed with primary antibodies anti-FLAG and anti-Na⁺/K⁺-ATPase subunit α . In this set of experiments, FLAG-ENT1 and MYC-ENT1 interactions happened 154 ± 32 times, and FLAG-ENT1 and Na⁺/K⁺-ATPase interactions occurred 157 ± 21 times, $p > 0.05$. The absolute value of the number of interactions cannot be compared to Figures 4.11/4.12 as they were separate experiments and the data here were recorded at 40X magnification, not 63X.

These results support the in gel identification mass spectrometry assays, confirming that FLAG-hENT1 and endogenous Na⁺/K⁺-ATPase interact in intact cells.

CHAPTER 5. DISCUSSION

Nucleosides serve as signaling molecules to regulate biological functions as well as building blocks for energy carrier molecules and nucleic acid polymerization. The maintenance of nucleoside flux is therefore crucial to many cellular processes and is well regulated by several transport systems. The focus of this thesis is equilibrative nucleoside transporter 1 (ENT1). It has been shown that selective ENT1 inhibition reduces re-uptake of adenosine from the extracellular milieu, thereby potentiating anti-inflammation, vasodilation and other therapeutic effects of adenosine signaling³⁻⁶. Furthermore, ENT1 transports cytotoxic nucleoside analog drugs used for treatment of cancer and viral infection¹¹⁶. Despite proven clinical relevance in many areas, such as cancer, cardiovascular disease, diabetes, and various neuronal pathophysiologies, little is known about the regulation of ENT1 activity and ENT1 expression at the plasma membrane. This thesis addressed the following points: (1) regulation of ENT1 activity in response to protein kinase C activation (PKC) and adenosine receptor 1 stimulation (A₁AR), and (2) formation of an ENT1 complex at the plasma membrane.

5.1 A PKC-Mediated Mechanism is Partially Responsible for Increasing ENT1 Expression at The Plasma Membrane

Several studies have proposed that ENT1 may be regulated by protein kinases and observed cross-talk between adenosine receptors and nucleoside transport which altered transporter expression^{84,85}. Furthermore, predictive software such as NetPhos 2.0 server, identified a potential protein kinase C PKC phosphorylation site on ENT1 at Serine 281. Previously in our laboratory, *zero-trans* influx studies have been conducted using cells expressing wild-type ENT1

and a S281A-hENT1 mutant under conditions of A₁AR stimulation and PKC activation in order to study adenosine receptor/nucleoside transporter cross-talk and the effects of phosphorylation on activity, respectively. Both stimulation of A₁AR and direct activation of PKC increased hENT1 transport function (increase in V_{max} between untreated and treated cells) and this effect was abolished in PK15-S281A-hENT1 cells.

This thesis addressed the hypothesis that an increase in the amount of hENT1 protein at the plasma membrane is responsible for the observed increase in hENT1 uptake activity following PKC activation and A₁AR stimulation. Both PK15-hENT1 and PK15-S281A-hENT1 cells were treated with either PMA, a PKC activator, or CCPA, an A₁AR stimulator, prior to analysis of plasma-membrane localization. Plasma membrane localization was analyzed in two ways: (1) colocalization of FLAG-tagged hENT1 with a fluorescent membrane marker, GPI-GFP, and (2) cell surface biotinylation followed by semi-quantitative Western Blot analysis.

PKC activation by PMA resulted in an increase in plasma membrane localization of wild-type hENT1, observable by both colocalization and cell surface processing. No change in plasma membrane localization of S281A-hENT1 was observed by immunofluorescence colocalization. However, cell surface biotinylation experiments also showed that PK15-hENT1-S281A cells express more hENT1 at the plasma membrane following PKC activation. From these results, we conclude that an increase in plasma membrane localization is responsible for increased uptake function in PK15-hENT1 cells. However, this effect is not due entirely to direct activity by PKC at the S281A region of hENT1 and further investigation is necessary to determine what intermediary factors may be involved.

There was discrepancy between the two plasma membrane localization analysis methods with regards to PKC activation in PK15-S281A-hENT1 cells. By immunofluorescence colocalization analysis, the difference in colocalization coefficients between control treated and PMA treated cells was statistically insignificant, $p=0.36$. However, by cell surface biotinylation, in control-treated PK15-S281A-hENT1 cells 40% of hENT1 was localized to the plasma membrane compared to 55% following PMA treatment, $p=0.03$. This difference in results is due to the relative sensitivities of each method for this type of analysis. Confocal microscopy has a resolution of about 300 nm; therefore, quantitative data of protein-protein interactions occurring on an Ångström level acquired by this method is prone to noise. Furthermore, confocal analysis makes it clear that expression of hENT1 is heterogenous between cells plated on the same cover slip, even if they are stably transfected. One theory for this phenomenon is that ENT1 expression is known to vary through different stages in the cell cycle¹⁵¹. Many replicate samples were analyzed in order to decrease the signal to noise ratio and minimize the effect of heterogeneity. However, cell surface processing by biotinylation has a clear advantage in this regard because large volumes of lysed cells are used for analysis. Protein quantification prior to Western Blot analysis ensures that each well of the SDS-PAGE is loaded with equal amounts of protein. Therefore, we believe that cell surface processing by biotinylation is a more sensitive technique for this type of study and base our conclusions with regards to PK15-S281A-hENT1 cells on these results. PKC activation did indeed cause an increase in hENT1 at the plasma membrane in both PK15-hENT1 (wild type) and PK15-S281A-hENT1 cells.

The motivation for this hypothesis came from studies of ENT1 mediated radiolabelled permeant uptake which showed that PKC activation in PK15-S281A-hENT1 cells did not result in an

increase in transporter activity. The findings reported in this thesis regarding PK15-S281A-hENT1 cells show that an apparent increase in plasma membrane hENT1 does not necessarily result in an increase in transport activity. Therefore, it is not clear how much of the increase in uptake activity in PK15-hENT1 cells is due to the increase in plasma membrane localized transporter. Some of the change in activity must be due to some other change to ENT1 mediated through Serine 281, perhaps a modification that results in a more favorable conformation of transporter for uptake activity. Extensive study of the serotonin receptor (SERT), suggests that PKC regulation of this transporter's activity is biphasic- the first phase is independent of changes to trafficking/endocytosis and is due to intrinsic protein changes following the addition of a negatively charged modifier such as a phosphate group⁷⁹. Studies of norepinephrine transporters (NETs) have also reported both trafficking dependent and independent mechanisms of activity regulation by phosphorylation, suggesting a mechanism by which phosphorylation and dephosphorylation alters conformation of proteins at the cell surface¹⁵². Na⁺/K⁺-ATPase is also known to be regulated in a similar phosphorylation/dephosphorylation dependent manner that is independent of trafficking¹⁵³. Furthermore, there may be other proteins downstream of PKC activation. The interactions of these intermediate proteins with hENT1 may affect localization and not require an intact canonical PKC phosphorylation site in the Serine 281 region of hENT1.

Stimulation of A₁AR by CCPA did not induce an increase in plasma membrane localized hENT1 protein in either PK15-hENT1 or PK15-S281A-hENT1 cells as observed by both methodologies. These results in PK15-S281A-hENT1 cells support the uptake studies in which no change in activity was observed following A₁AR stimulation in these cells. PK15-hENT1 cells do respond to

A₁AR stimulation with an increase in uptake function (as seen by an increase in V_{max} of 2-chloroadenosine influx by ENT1), which is not matched with an increase in cell surface hENT1. We expected similar localization results following A₁AR stimulation as we observed following PKC activation because 1) stimulation of A₁AR leads to PKC activation, and 2) in radiolabeled permeant uptake studies, inhibition of PKC by GÖ6983 attenuated the effect of A₁AR stimulation on the V_{max} rate. A change in the maximal transport capacity of ENT1 (V_{max}) that is not reflected by a change in the number of ENT1 protein at the plasma membrane suggests that the rate of substrate translocation is increasing via modifications to existing ENT1 proteins at the plasma membrane. ENT1 is believed to follow an alternating access model of transport mechanics, an increase in the rate of change between outward facing and inward facing ENT1 conformations would result in an increased V_{max} as observed though zero-*trans* influx studies⁵². Other studies can be done to confirm if this is in fact the explanation for the results obtained. For example, equilibrium exchange transport studies can be used to look at changes in substrate (2-chloroadenosine or uridine) influx in cells pre-loaded with 2-chloroadenosine or uridine. In previous equilibrium exchange studies with uridine and 2-chloroadenosine, 2-chloroadenosine acted as a trans-inhibitor, lowering the rate of conformation change of the loaded carrier (containing uridine) in comparison to the empty carrier¹⁵⁴. If A₁AR-signalling-induced phosphorylation of ENT1 modifies ENT1's translocation efficiency, then in a similar equilibrium exchange experiment as described earlier could be performed with and without treatment with CCPA to stimulate A₁AR. If the translocation efficiency of 2-chloroadenosine is enhanced upon phosphorylation, then the trans-inhibition effects of 2-chloroadenosine on uridine transport may be attenuated. A possible reason for why direct PKC activation results in

a change in hENT1 localization and A₁AR stimulation does not is that there are several downstream pathways of A₁AR stimulation, therefore, not every A₁AR stimulated by CCPA will lead to PKC activation whereas PMA activation of PKC is direct and immediate. Also, kinases such as PKC are diffused throughout the cell cytosol and stimulation of A₁AR may only lead to an activation of PKC in certain regions of the cell. The spatial distribution of kinases as well as secondary messengers, such as cAMP, have been observed and can be regulated by sequential activation of various G-protein coupled receptors¹⁵⁵. This spatial regulation leads to the propagation of a selected signaling cascades as demonstrated with selective stimulation/inhibition at the prostaglandin (PGE₂) and β-adrenergic receptors¹⁵⁵. A₁AR stimulation, although it activates PKC downstream, is affecting hENT1 activity in a way that does not involve changes to hENT1 expression at the plasma membrane.

5.2 hENT1 Forms Dimers in Intact Cells

In the literature and in our own laboratory, the appearance of hENT1 with a higher molecular mass suggests ENT1 complex formation or oligomerization. This thesis provides evidence of ENT1-monomer association and quantifies monomer interactions in intact cells.

Co-immunoprecipitation of MYC- and HA- tagged proteins showed that hENT1 monomers are capable of association. Qualitative Western Blot probed with anti-HA antibody showed that total lysate and the anti-MYC immunoprecipitated fractions from co-transfected cells contained HA-tagged ENT1, as shown in Figure 4.8b. This showed that MYC- and HA- ENT1 proteins associate and maintain contact through the immunoprecipitation process. The converse experiment using a monoclonal anti-HA antibody for immunoprecipitation and polyclonal anti-

MYC antibody for Western Blot probing did not produce the expected hENT1 band at 50 kDa in lane 8 (co-transfected, immunoprecipitated samples) as shown in Figure 4.8a. The monoclonal anti-HA antibody, unlike the polyclonal anti-MYC antibody, is selective for a single epitope and not ideal for immunoprecipitation; therefore, immunoprecipitation with the polyclonal anti-MYC and Western Blot probing with anti-HA, as in Figure 4.8b, was a more appropriate experimental design. Clearly, antibody selection is a critical step for this assay. Furthermore, co-immunoprecipitation studies have some limitations: (1) provide a qualitative assessment only, (2) experiments done on a transiently transfected cell system, and (3) association is assessed following lysis of the cell and there may be false positive results. A transiently transfected system means that MYC-/HA- hENT1 is transcribed from a plasmid with a proliferative, CMV promoter, forcing the cell to produce an excess amount of hENT1 protein which may associate superfluously. hENT1, like other plasma membrane proteins, is prone to hydrophobic collapse and aggregation due to the hydrophobic, membrane-spanning regions. Excess expression of this protein in a transiently transfected system would increase the chances of aggregation following lysis. Hydrophobic collapse and aggregation may offer an explanation for the appearance of 75 kDa bands in Figure 4.8b, which demonstrate a shift up in molecular mass of hENT1. A moderate lysis buffer, IPB (does not contain SDS) was used and samples were heated to 65°C prior to SDS-PAGE loading instead of 100°C in order to minimize these effects. In conclusion, although qualitatively useful, simple and supporting of our hypothesis, this technique cannot stand alone as evidence for interaction of hENT1.

The follow-up experiment, a chemical cross-linking of PK15-hENT1 cells using DTSSP, a cell impermeable cross-linker, did not show higher-molecular mass forms of ENT1. PK15-hENT1

cells were used as hENT1 is stably expressed at physiologically relevant quantities, as a counter to the excessive expression of hENT1 by transient transfection in co-immunoprecipitation studies. DTSSP has an eight-atom spacer arm and reacts with primary amines, lysine (Lys/K), at pH 7-9. This method has been used previously to establish the dimeric structure of the SLC4A11 protein, a Na⁺/OH⁻ transporter^{156,157}. However, there are some drawbacks: (1) the monoclonal anti-FLAG antibody used has a relatively low-affinity, (2) stably expressed FLAG-hENT1 may be at a low relative quantity compared to other proteins, and (3) the spacer arm is limited by the availability of lysines to cross-link in the appropriate quantities and orientation. We took several measures to address these drawbacks. Firstly, anti-FLAG antibodies from different sources, including Sigma, Lifetein, and Santa Cruz, were assessed before committing to the Clontech anti-FLAG antibody as it produced the clearest Western Blot results. Then, a transiently transfected cell system was used with HA- and MYC-tagged hENT1. Also, based on knowledge from immunofluorescence colocalization and cell surface processing data, PK15-hENT1 cells were treated with PMA prior to cross-linking to induce an increase in the amount of hENT1 at the plasma membrane. In HEK293 cells transiently transfected with HA- and MYC-tagged hENT1, no cross-linking of hENT1 was observed. Ultimately, chemical cross-linking did not provide evidence to support the hypothesis. This is most likely due to a lack of appropriately spaced lysines in the extracellular region of hENT1, as experiments were done to address low expression of hENT1 and antibody affinity issues. There are four lysines on the predicted exofacial surface of hENT1, as can be seen in Figure 1.3. Lysine 58 is located within the first extracellular loop, lysine 131 is at the predicted membrane interface of loop 2, and lysines 315 and 379 are in loops 4 and 5 respectively. Assuming that the conformation of the

protein is as predicted (Figure 1.3), loops 2, 4, and 5 are significantly shorter and less flexible than loop 1, possibly limiting the chance of amide bond formation with a crosslinking reagent and another lysine. There is no 3D structural information currently available to confirm the predicted model and relative orientations of lysine residues.

Another method frequently used to assess interaction between two proteins is the proximity ligation assay (PLA). This assay visualizes and allows for the quantification of interaction events between two proteins¹⁵⁸. Analysis of PK15-hENT1 transfected with MYC-hENT1 cells showed that FLAG- and MYC-tagged hENT1 monomers exist within detection-proximity¹³⁸. The number of interactions between FLAG- and MYC-hENT1 (505±101 interactions per cell) was significantly greater than the interactions between the negative control, FLAG-ENT1 and glucose transporter 1, GLUT1 (39±10 interactions per cell), $p < 0.05$. In contrast, the number of interactions between hENT1 molecules was not statistically different from the positive control- HA-tagged anion exchanger 1 (HA-AE1) and carbonic anhydrase II (CAII) (540±157 interactions per cell), a known interacting pair at the plasma membrane¹⁴⁰. This experiment supports the hypothesis that in intact cells, hENT1 proteins interact and likely associate in a dimeric state. This immunofluorescent crosslinking technique is not limited by the amount or relative orientation of specific amino acids on the extracellular surface of hENT1 like chemical crosslinking by DTSSP, as discussed previously. Another major advantage of the technique is the ability to visualize and quantify each interaction^{137,138}. PLA has been used to assess the interactions of other proteins in cells as well as tissues. This assay has been used in several studies to assess receptor tyrosine kinase dimerization and even to make assessments about relapse and survivability from clinical samples^{132,139}. Moreover, specific brain regions of rats were injected

with μ -opioid agonists and antagonists, analyzed by PLA, and it was determined that μ -receptors heterodimerize with α_{2A} -adrenoreceptors with varying frequency in response to these drugs⁹⁶. Similar studies (identifying changes in interaction following drug treatments) are planned for hENT1. Preliminary studies on this topic were conducted to observe changes in dimerization in response to adenosine receptor 1 stimulation. As discussed previously, it was determined that the increase in transport activity of hENT1 in response to A₁AR stimulation could not be accounted for by changes in the number of transporter proteins at the plasma membrane. Perhaps changes in relative quantities of hENT1 populations of varied oligomeric structure profoundly affect activity. The results are not shown in Chapter 4 as, after three experiments, no significant results or trends were seen to indicate that there is a change in interaction of hENT1's following A₁AR stimulation. These data are inconclusive because, as discussed in Section 5.1, a major current concern is heterogeneous expression levels of hENT1 among PK15-hENT1 cells on the same cover slip. The relative expression of FLAG-hENT1 also appeared to impact the amount of MYC-hENT1 that cells transiently express. Only some cells are able to express both constructs. This may be due to excess hENT1 transcripts available for the translation machinery and/or internal regulation by the cell to limit production of hENT1 protein. Moreover, hENT1 is subject to cell-cycle dependent regulation of expression¹⁴. This heterogeneity of expression must be addressed, potentially by applying cell cycle synchronizing agents either prior or post-transfection, before experimentation in this direction may continue^{159,160}. It should also be noted that ENT1 uptake function following A₁AR stimulation by CCPA is increased by only 30% (Figure 2.1). Even if changes in oligomerization account for the entirety of that functional difference, observing such a small difference ($\leq 30\%$) with a proximity

ligation assay will require a more stable base-line of ENT1 expression, so the error between replicates and experiments can be adequately reduced.

Another immunofluorescence study was designed to assess changes in interaction between MYC-hENT1 and HA-hENT1 in HEK293 cells with the intent of a preliminary analysis of hENT1 oligomer stoichiometry. Cells were transfected with changing ratios of MYC-hENT1 to HA-hENT1 cDNA. The hypothesis was that Pearson's colocalization coefficient for MYC-hENT1 and HA-hENT1 would increase as the ratio between the amounts of transfected cDNA neared 1:1. However, several iterations of the experiment and subsequent analysis shows that this methodology is not best-suited to address this question. Colocalization coefficients were derived in two ways. The first method was by using IMARIS v8.3, Bitplane Inc, to reconstruct 3D images of the cells from Z-stacks and look at colocalization of green (corresponding to MYC-hENT1) to red (corresponding to HA-hENT1) signal in a given 3D space (known as a voxel). Colocalization analysis using IMARIS showed little difference in colocalization between the negative control (MYC-SLC4A1 and HA-AE1) and positive control (HA-AE1 and CAII). We thought this may be due to all the proteins assessed following the same secretory pathway, therefore significant overlap in the endoplasmic reticulum and Golgi apparatus would lead to a false-positive colocalization coefficient. Using Volocity software to calculate colocalization allowed for the isolation of the plasma membrane region by hand as a region of interest (ROI) in order to dismiss intracellular 'noise'. By this method, the trends in the results were similar to those acquired by IMARIS- the positive and negative controls fail to show a significant difference from each other or the experimental condition. Therefore, the significant results that were observed from the first experiment of this kind cannot be trusted. Upon further deliberation, we

conclude that the resolution offered by this method is not adequate to discern the expected small changes in interaction. Colocalization of two proteins can certainly be qualitatively and quantified assessed by these methods when the expected changes are more distinct. A better methodology would be to use fluorescence resonance energy transfer (FRET) microscopy, which detects interacting proteins within 100 Å and has been used in protein oligomerization stoichiometry studies¹²⁹. This technique uses live cells, which would allow for better assessment of minute changes in interactions over a period of time and better account for fluctuations in plasma membrane localization of hENT1.

Clearly, identifying hENT1 monomer interactions in intact cells opens many new avenues for study, including determining if larger order oligomers exist and what their stoichiometry may be. Furthermore, existence of hENT1 in multiple states contributes to the popular hypothesis that there are multiple populations of hENT1 with varied behaviours^{45,58,161}.

5.2.1 Interacting Partners of hENT1

A secondary hypothesis for why hENT1 is frequently found at an increased molecular mass is that hENT1 forms a multi-protein complex. This complex, and potential various interacting partners, may also contribute to the presence of multiple hENT1 populations which result in varied trafficking and response to stimuli¹⁶¹. Preliminary investigation into this hypothesis is described in this thesis and identified sodium potassium ATPase (Na⁺/K⁺-ATPase) as a potential interacting partner of hENT1. Similar analyses, involving chemical cross-linking followed by mass spectrometry, has been applied to other systems and is recommended for the construction of a comprehensive database of protein complexes^{146,147}.

The final experimental design that was settled on used HEK293-T cells, crosslinked with DSP following incubation with NBMPR or uridine to observe proteins interacting with ENT1 primarily when it is in an inhibitor or substrate bound conformation. The $\alpha 1$ subunit of Na^+/K^+ -ATPase was a hit in 3 out of 4 uridine pre-incubated, and 2 out of 4 NBMPR pre-incubated analyses (Table 4.1). A result was considered a 'hit' if it was unique to the hENT1-expressing cells (in comparison to un-transfected cells) and duplicated between experiments. Prior to this study, ENT1 had not been identified as a potential interacting partner for Na^+/K^+ -ATPase and does not appear in various protein-protein interaction databases, including String10 (<http://string-db.org/>), The BioGRID v3.4 (<http://thebiogrid.org/>), the Database for Interacting Proteins (DIP) (<http://dip.doe-mbi.ucla.edu/dip/Main.cgi>), and IntAct Molecular Interaction Database which cites a variety of databases (<http://www.ebi.ac.uk/intact/>)¹⁶²⁻¹⁶⁴. For this reason, Na^+/K^+ -ATPase and FLAG-hENT1 pairing was initially used as a negative control in proximity ligation assays in PK15-hENT1 cells. When the assay yielded positive hits, it was concluded that this was a false positive due to non-specific binding of the rabbit anti Na^+/K^+ -ATPase antibody. In light of new evidence from mass spectrometry results, these images (in Figure 4.13) have been recovered as supportive evidence for interaction between hENT1 and Na^+/K^+ -ATPase α subunit. Na^+/K^+ -ATPase is a large membrane protein made up of two to three subunits- the catalytic α subunit, a smaller glycoprotein β subunit necessary for proper membrane-localization, and occasionally a γ subunit that modulates pump activity¹⁶⁵. Na^+/K^+ -ATPase establishes the membrane potential of cells by pumping potassium ions in and sodium ions out of the cell. Na^+/K^+ -ATPase is known to interact with many membrane and cytosolic proteins and, through many of these interactions, Na^+/K^+ -ATPase initiates several downstream signaling cascades¹⁶⁶.

One of the signal transduction methods identified for Na⁺/K⁺-ATPase involves the binding of Src family of kinases which effectively turn the Na⁺/K⁺-ATPase into a membrane tyrosine kinase¹⁶⁶. Other interactions involve Na⁺/K⁺-ATPase in the regulation of cellular metabolism, formation of tight junctions, and Ca²⁺ regulation¹⁶⁶. A potential interaction between hENT1 and Na⁺/K⁺-ATPase is worth further investigation to determine how these two membrane proteins influence one another's activity, if at all.

All relevant signal transduction mechanism involving Na⁺/K⁺-ATPase occur through the α subunit. There are four isozymes of the 110 kDa- α subunit, and isozymes α_2 , α_3 , and α_4 are 78-87% similar to α_1 ; the ATP1A1 gene encodes the α_1 subunit¹⁶⁷. The α_1 subunit, like hENT1, is ubiquitously expressed in human tissues. Also like hENT1, α_1 is regulated by PKC. PKC-mediated phosphorylation causes a significant change in the amount of α_1 subunit present at the plasma membrane through clathrin-mediated endocytosis of the protein^{168,169}. We have shown that PKC activation increases the amount of ENT1 at the plasma membrane. The similarities between these two proteins are likely coincidental; however, through structural similarities or regulatory mechanisms, these proteins may be targeted to similar plasma membrane environments known as lipid rafts¹⁷⁰.

No significant similarity between hENT1 and Na⁺/K⁺-ATPase β_1 , β_2 , or β_3 was found using protein BLAST (BLASTP 2.2.32 NCBI); however, β subunit is known to form homodimers and intercellular interactions with β subunits of neighboring cells^{171,172}. The motifs responsible for α and β unit heterodimerization and β/β homodimerization have been identified. Na⁺/K⁺-ATPase β/β homodimerization occurs through glycine zipper (GxxxGxxxG) motifs¹⁷³. There are two GxxxG motifs on hENT1 which have been investigated as the basis of hENT1 dimerization by

Frances Cunningham in the Hammond laboratory and are described in her thesis work⁹⁰. As part of that work, stable constructs of mutant GxxxG motifs, G163L and G445L, were constructed; however, these mutants were not functional and not expressed, respectively, and therefore unavailable for further study. The G163 and G445 to leucine mutations may be too disruptive to the structure of the protein, and suggested further study would mutate the glycine to alanine or serine mutants. If the new mutants are expressed and functional, they can be used to further investigate hENT1 dimerization and also potential interaction with Na⁺/K⁺-ATPase.

The α/β heterodimer interactions through a conserved heptad: YX₃YXXLX₃F¹⁷³. The specific heptad responsible for Na⁺/K⁺-ATPase α/β heterodimerization has not been identified as a common interface for subunit interaction and is not present in ENT1. There is a somewhat similar motif of FYxYYxxL starting at F231 (Phe-Tyr-Arg-Tyr-Tyr-Glu-Glu-Leu-Lys). Hydrophobicity studies predict that this region is part of the long intracellular loop between TMD 6 and 7. However, Network Protein Sequence Analysis (NPS) identified the region between E230-K239 as having a potential amphiphilic, alpha-helical structure. Such a structure could facilitate interaction between two proteins at the plasma membrane. Nevertheless, the presence of this amphiphilic helix is just a prediction and the secondary structure of the intracellular loop has not been described in the literature; therefore, any potential 'motifs' in this region are purely speculative. Likely, the interaction interface between ENT1 and Na⁺/K⁺-ATPase α subunit is dissimilar to the α/β subunit interacting domains but it could be of value to create mutants of these regions in ENT1 and see if there are changes to association between ENT1 and Na⁺/K⁺-ATPase α subunit. Na⁺/K⁺-ATPase is a ubiquitously expressed protein that has shown to alter its

function and signal transduction capabilities in response to binding/interacting with other proteins, therefore, the potential interaction with hENT1 is worth investigating as it may uncover a new role for hENT1 in signal transduction pathways of the cell.

There is one other consistent hit from these mass-spectrometry experiments- the clathrin heavy chain. Clathrin-mediated endocytosis mechanisms have been identified in the recycling of ENT1⁴⁵. Moreover, enhanced endocytosis following inhibitor binding to hENT1 has also been observed⁴⁸. Therefore, these findings support what has been previously reported in the literature for hENT1.

5.3 Conclusions

This thesis provides new evidence for hENT1 regulation by protein kinase C and the nature of hENT1 expression at the plasma membrane. Direct activation of PKC induces an increase in hENT1 localized to the plasma membrane which may be responsible for some of the increase in transport function observed by radioligand uptake experiments. However, PKC activation in cells expressing hENT1 with a mutation in the canonical PKC phosphorylation site (PK15-S281A-hENT1) also induced an increase in plasma membrane localization. This suggests that PKC does not act solely via direct modification at Serine 281; another ENT1 serine/threonine residue may be involved, or an intermediate factor may be responsible for this effect. Stimulation at A₁AR did not show any change in plasma membrane localization of hENT1. Therefore, further research into how stimulation at A₁AR results in an increase in transport function is required. These findings further illustrate that regulation of hENT1 is complex and that many intermediate factors are still unknown. Understanding the regulatory pathways of hENT1

trafficking and activity is crucial to the proper development and use of selective drugs to inhibit hENT1, such as NBMPR, draflazine, and dipyridamole, as well as inhibitors discovered after-the-fact such as tyrosine receptor kinase inhibitors used in cancer therapy.

hENT1 protein-protein interactions, including potential oligomerization, have long been proposed in the literature based on findings of high-molecular mass hENT1 entities by several methods including photoaffinity labelling, radiation inactivation, and non-denaturing gel electrophoresis^{39-41, 88-90}. These entities vary in size and among species^{20,39-43}. This thesis qualitatively assessed the potential for hENT1 monomer interaction and quantified these interactions in intact cells. Furthermore, preliminary studies into hENT1 complex formation identified one unexpected binding partner, the α subunit of Na⁺/K⁺-ATPase. Na⁺/K⁺-ATPase is known to interact with many other proteins and through these interactions direct various cellular signaling cascades¹⁶⁶. Other plasma membrane proteins experience different functional activity based on oligomeric state, such as GLUT1, or exist in multiple populations that exhibit variations in trafficking and stimuli-response, such as NHE3^{49,95}. New areas of research can be pursued following these findings, including determining whether higher order hENT1 oligomers or hetero-oligomers of hENT1/hENT2 exist, the functional differences between different oligomeric states, and the functional effect of interaction with Na⁺/K⁺-ATPase.

This work contributes to the field of basic knowledge about hENT1 function, membrane transporter function in general, and opens new channels of research for hENT1. These and related further findings are crucial to developing new hENT1-targeting therapies.

REFERENCES

1. Murray, A. W. The Biological Significance of Purine Salvage. *Annu. Rev. Biochem.* **40**, 811–826 (1971).
2. Klinger, M., Freissmuth, M. & Nanoff, C. Adenosine receptors: G protein-mediated signalling and the role of accessory proteins. *Cell. Signal.* **14**, 99–108 (2002).
3. Dunwiddie, T. & Fredholm, B. Adenosine A1 receptors inhibit adenylate cyclase activity and neurotransmitter release and hyperpolarize pyramidal neurons in rat hippocampus. *J. Pharmacol. Exp. Ther.* **249**, 31–37 (1989).
4. Cronstein, B. N. Adenosine, an endogenous anti-inflammatory agent. *J Appl Physiol* **76**, 5–13 (1994).
5. Belardinelli, L., *et al.* The A2A Adenosine Receptor Mediates Coronary Vasodilation. *J. Pharmacol. Exp. Ther.* **284**, 1066–1073 (1998).
6. Liu, G. S., *et al.* Protection against infarction afforded by preconditioning is mediated by A1 adenosine receptors in rabbit heart. *Circulation* **84**, 350–356 (1991).
7. Pastor-Anglada, M., Cano-soldado, P., Errasti-murugarren, E. & Casado, F. J. SLC28 genes and concentrative nucleoside transporter (CNT) proteins. *Xenobiotica* (2008).
8. Gray, J. H., Owen, R. P. & Giacomini, K. M. The concentrative nucleoside transporter family, SLC28. *Pflugers Arch.* **447**, 728–34 (2004).
9. Pastor-Anglada, M., Errasti-Murugarren, E., Aymerich, I. & Casado, F. J. Concentrative nucleoside transporters (CNTs) in epithelia: from absorption to cell signaling. *J. Physiol. Biochem.* **63**, 97–110 (2007).
10. Johnson, Z. L., Cheong, C.-G. & Lee, S.-Y. Crystal structure of a concentrative nucleoside transporter from *Vibrio cholerae* at 2.4 Å. *Nature* **483**, 489–93 (2012).
11. Beal, P. R., *et al.* The equilibrative nucleoside transporter family, SLC29. *Pflugers Arch. Eur. J. Physiol.* **447**, 735–743 (2004).
12. Yao, S. Y. M., *et al.* Functional and Molecular Characterization of Nucleobase Transport by Recombinant Human and Rat Equilibrative Nucleoside Transporters 1 and 2. *Biochemistry* **277**, 24938–24948 (2002).
13. Yao, S. Y., *et al.* Molecular cloning and functional characterization of nitrobenzylthioinosine (NBMPR)-sensitive (es) and NBMPR-insensitive (ei) equilibrative nucleoside transporter proteins (rENT1 and rENT2) from rat tissues. *J. Biol. Chem.* **272**, 28423–30 (1997).
14. Baldwin, S. A., *et al.* Functional characterization of novel human and mouse equilibrative nucleoside transporters (hENT3 and mENT3) located in intracellular membranes. *J. Biol. Chem.* **280**, 15880–7 (2005).
15. Hsu, C.-L., *et al.* Equilibrative nucleoside transporter 3 deficiency perturbs lysosome function and macrophage homeostasis. *Science* **335**, 89–92 (2012).
16. Liu, B., *et al.* Equilibrative nucleoside transporter 3 depletion in β -cells impairs mitochondrial function and promotes apoptosis: Relationship to pigmented hypertrichotic dermatosis with

- insulin-dependent diabetes. *Biochim. Biophys. Acta* **1852**, 2086–95 (2015).
17. Zhou, M., Xia, L., Engel, K. & Wang, J. Molecular determinants of substrate selectivity of a novel organic cation transporter (PMAT) in the SLC29 family. *J. Biol. Chem.* **282**, 3188–95 (2007).
 18. Barnes, K., *et al.* Distribution and functional characterization of equilibrative nucleoside transporter-4, a novel cardiac adenosine transporter activated at acidic pH. *Circ. Res.* **99**, 510–9 (2006).
 19. Kwong, F. Y., *et al.* Purification of the human erythrocyte nucleoside transporter by immunoaffinity chromatography. *Biochem. J.* **255**, 243–9 (1988).
 20. Kwong, F. Y. P., Tse, C.-M. M., Jarvis, S. M., Choy, M. Y. M. & Young, J. D. Purification and reconstitution studies of the nucleoside transporter from pig erythrocytes. *Biochim. Biophys. Acta - Biomembr.* **904**, 105–116 (1987).
 21. Pennycooke, M., Chaudary, N., Shuralyova, I., Zhang, Y. & Coe, I. R. Differential expression of human nucleoside transporters in normal and tumor tissue. *Biochem. Biophys. Res. Commun.* **280**, 951–9 (2001).
 22. Griffith, D. A. & Jarvis, S. M. Nucleoside and nucleobase transport systems of mammalian cells. *Biochim. Biophys. Acta - Rev. Biomembr.* **1286**, 153–181 (1996).
 23. Antonioli, L., Blandizzi, C., Pacher, P. & Haskó, G. Immunity, inflammation and cancer: a leading role for adenosine. *Nat. Rev. Cancer* **13**, 842–57 (2013).
 24. Löffler, M., Morote-Garcia, J. C., Eltzschig, S. A., Coe, I. R. & Eltzschig, H. K. Physiological roles of vascular nucleoside transporters. *Arterioscler. Thromb. Vasc. Biol.* **27**, 1004–13 (2007).
 25. Vickers, M. F., *et al.* Functional production and reconstitution of the human equilibrative nucleoside transporter (hENT1) in *Saccharomyces cerevisiae*. Interaction of inhibitors of nucleoside transport with recombinant hENT1 and a glycosylation-defective derivative (hENT1/N48Q). *Biochem. J.* **339** (Pt 1, 21–32 (1999).
 26. Sundaram, M., *et al.* Topology of a human equilibrative, nitrobenzylthioinosine (NBMPR)-sensitive nucleoside transporter (hENT1) implicated in the cellular uptake of adenosine and anti-cancer drugs. *J. Biol. Chem.* **276**, 45270–5 (2001).
 27. Aseervatham, J., Tran, L., Machaca, K. & Boudker, O. The Role of Flexible Loops in Folding, Trafficking and Activity of Equilibrative Nucleoside Transporters. *PLoS One* **10**, e0136779 (2015).
 28. Visser, F., *et al.* Mutation of residue 33 of human equilibrative nucleoside transporters 1 and 2 alters sensitivity to inhibition of transport by dilazep and dipyridamole. *J. Biol. Chem.* **277**, 395–401 (2002).
 29. Sundaram, M., *et al.* Equilibrative Nucleoside Transporters: Mapping Regions of Interaction for the Substrate Analogue Nitrobenzylthioinosine (NBMPR) Using Rat Chimeric Proteins †. *Biochemistry* **40**, 8146–8151 (2001).
 30. SenGupta, D. J. & Unadkat, J. D. Glycine 154 of the equilibrative nucleoside transporter, hENT1, is important for nucleoside transport and for conferring sensitivity to the inhibitors nitrobenzylthioinosine, dipyridamole, and dilazep. *Biochem. Pharmacol.* **67**, 453–8 (2004).
 31. SenGupta, D. J., *et al.* A Single Glycine Mutation in the Equilibrative Nucleoside Transporter Gene, hENT1, Alters Nucleoside Transport Activity and Sensitivity to Nitrobenzylthioinosine †.

- Biochemistry* **41**, 1512–1519 (2002).
32. Park, J. S. & Hammond, J. R. Cysteine residues in the transmembrane (TM) 9 to TM11 region of the human equilibrative nucleoside transporter subtype 1 play an important role in inhibitor binding and translocation function. *Mol. Pharmacol.* **82**, 784–94 (2012).
 33. Hammond, J. R. & Zarenda, M. Effect of detergents on ligand binding and translocation activities of solubilized/reconstituted nucleoside transporters. *Arch. Biochem. Biophys.* **332**, 313–22 (1996).
 34. Girke, C., *et al.* High yield expression and purification of equilibrative nucleoside transporter 7 (ENT7) from *Arabidopsis thaliana*. *Biochim. Biophys. Acta - Gen. Subj.* **1850**, 1921–1929 (2015).
 35. Rehan, S. & Jaakola, V.-P. Expression, purification and functional characterization of human equilibrative nucleoside transporter subtype-1 (hENT1) protein from Sf9 insect cells. *Protein Expr. Purif.* **114**, 99–107 (2015).
 36. Kwong, F. Y., *et al.* Mammalian nitrobenzylthioinosine-sensitive nucleoside transport proteins. Immunological evidence that transporters differing in size and inhibitor specificity share sequence homology. *J. Biol. Chem.* **267**, 21954–60 (1992).
 37. Visser, F., *et al.* Residues 334 and 338 in transmembrane segment 8 of human equilibrative nucleoside transporter 1 are important determinants of inhibitor sensitivity, protein folding, and catalytic turnover. *J. Biol. Chem.* **282**, 14148–57 (2007).
 38. Schwarz, F. & Aebi, M. Mechanisms and principles of N-linked protein glycosylation. *Curr. Opin. Struct. Biol.* **21**, 576–82 (2011).
 39. Shi, M. M., Wu, J.-S. R., Lee, C.-M. & Young, J. D. Nucleoside transport. Photoaffinity labelling of high-affinity nitrobenzylthioinosine binding sites in rat and guinea pig lung. *Biochem. Biophys. Res. Commun.* **118**, 594–600 (1984).
 40. Wu, J. S. & Young, J. D. Photoaffinity labelling of nucleoside-transport proteins in plasma membranes isolated from rat and guinea-pig liver. *Biochem. J.* **220**, 499–506 (1984).
 41. Gati, W. P., *et al.* Photoaffinity labelling of a nitrobenzylthioinosine-binding polypeptide from cultured Novikoff hepatoma cells. *Biochem. J.* **236**, 665–70 (1986).
 42. Almeida, A. F., Jarvis, S. M., Young, J. D. & Paterson, A. R. Photoaffinity labelling of the nucleoside transporter of cultured mouse lymphoma cells. *FEBS Lett.* **176**, 444–8 (1984).
 43. Hammond, J. R. & Johnstone, R. M. Solubilization and reconstitution of a nucleoside-transport system from Ehrlich ascites-tumour cells. *Biochem. J.* **262**, 109–18 (1989).
 44. Lai, Y., Tse, C.-M. & Unadkat, J. D. Mitochondrial expression of the human equilibrative nucleoside transporter 1 (hENT1) results in enhanced mitochondrial toxicity of antiviral drugs. *J. Biol. Chem.* **279**, 4490–7 (2004).
 45. Nivillac, N. M. I., Bacani, J. & Coe, I. R. The life cycle of human equilibrative nucleoside transporter 1: from ER export to degradation. *Exp. Cell Res.* **317**, 1567–79 (2011).
 46. Liang, L. & Johnstone, R. M. Evidence for an internal pool of nucleoside transporters in mammalian reticulocytes. *Biochim. Biophys. Acta - Biomembr.* **1106**, 189–196 (1992).
 47. Guma, A., Zierath, J. R., Wallberg-Henriksson, H. & Klip, A. Insulin induces translocation of GLUT-4

- glucose transporters in human skeletal muscle. *Am J Physiol Endocrinol Metab* **268**, E613–622 (1995).
48. Torres, M., Delicado, E. G., Dolores Fideu, M. & Teresa Miras-Portugal, M. Down-regulation and recycling of the nitrobenzylthioinosine-sensitive nucleoside transporter in cultured chromaffin cells. *Biochim. Biophys. Acta - Biomembr.* **1105**, 291–299 (1992).
 49. Cha, B., Kenworthy, A., Murtazina, R. & Donowitz, M. The lateral mobility of NHE3 on the apical membrane of renal epithelial OK cells is limited by the PDZ domain proteins NHERF1/2, but is dependent on an intact actin cytoskeleton as determined by FRAP. *J. Cell Sci.* **117**, 3353–65 (2004).
 50. Coe, I., Zhang, Y., McKenzie, T. & Naydenova, Z. PKC regulation of the human equilibrative nucleoside transporter, hENT1. *FEBS Lett.* **517**, 201–5 (2002).
 51. Pedersen, N. B., Carlsson, M. C. & Pedersen, S. F. Glycosylation of solute carriers: mechanisms and functional consequences. *Pflugers Arch.* (2015). doi:10.1007/s00424-015-1730-4
 52. Ward, J. L., Sherali, A., Mo, Z.-P. & Chung-Ming, T. Kinetic and Pharmacological Properties of Cloned Human Equilibrative Nucleoside Transporters, ENT1 and ENT2, Stably Expressed in Nucleoside Transporter-deficient PK15 Cells. *J. Biol. Chem.* **275**, 8375–8381 (2000).
 53. Nivillac, N. M. I., *et al.* Disrupted plasma membrane localization and loss of function reveal regions of human equilibrative nucleoside transporter 1 involved in structural integrity and activity. *Biochim. Biophys. Acta* **1788**, 2326–34 (2009).
 54. Lee, E.-W., Lai, Y., Zhang, H. & Unadkat, J. D. Identification of the mitochondrial targeting signal of the human equilibrative nucleoside transporter 1 (hENT1): implications for interspecies differences in mitochondrial toxicity of fialuridine. *J. Biol. Chem.* **281**, 16700–6 (2006).
 55. Jarvis, S. M., Hammond, J. R., Paterson, A. R. P. & Clanachan, A. S. Nucleoside transport in human erythrocytes. A simple carrier with directional symmetry in fresh cells, but with directional asymmetry in cells from outdated blood. *Biochem. J.* **210**, 457–461 (1983).
 56. Jarvis, S. M. & Young, J. D. Nucleoside translocation in sheep reticulocytes and fetal erythrocytes: a proposed model for the nucleoside transporter. *J. Physiol.* **324**, 47–66 (1982).
 57. Jarvis, S. M., Janmohamed, S. N. & Young, J. D. Kinetics of nitrobenzylthioinosine binding to the human erythrocyte nucleoside transporter. *Biochem. J.* **216**, 661–667 (1983).
 58. Hammond, J. R. Kinetic analysis of ligand binding to the Ehrlich cell nucleoside transporter: pharmacological characterization of allosteric interactions with the [3H]nitrobenzylthioinosine binding site. *Mol. Pharmacol.* **39**, 771–9 (1991).
 59. Jones, K. W. & Hammond, J. R. Interaction of the mioflazine derivative R75231 with the nucleoside transporter: evidence for positive cooperativity. *Eur. J. Pharmacol. Mol. Pharmacol.* **246**, 97–104 (1993).
 60. Casillas, T., Delicado, E. G., Garcia-Carmona, F. & Miras-Portugal, M. T. Kinetic and allosteric cooperativity in L-adenosine transport in chromaffin cells. A mnemonical transporter. *Biochemistry* **32**, 14203–14209 (1993).
 61. Hou, Z., Orr, S. & Matherly, L. H. Post-transcriptional regulation of the human reduced folate carrier as a novel adaptive mechanism in response to folate excess or deficiency. *Biosci. Rep.* **34**,

- (2014).
62. Eltzschig, H. K., *et al.* HIF-1-dependent repression of equilibrative nucleoside transporter (ENT) in hypoxia. *J. Exp. Med.* **202**, 1493–505 (2005).
 63. Desai, A., *et al.* Adenosine A2A receptor stimulation increases angiogenesis by down-regulating production of the antiangiogenic matrix protein thrombospondin 1. *Mol. Pharmacol.* **67**, 1406–13 (2005).
 64. Eltzschig, H. K. & Collard, C. D. Vascular ischaemia and reperfusion injury. *Br. Med. Bull.* **70**, 71–86 (2004).
 65. Chaudary, N., Naydenova, Z., Shuralyova, I. & Coe, I. R. Hypoxia regulates the adenosine transporter, mENT1, in the murine cardiomyocyte cell line, HL-1. *Cardiovasc. Res.* **61**, 780–8 (2004).
 66. Chaudary, N., Naydenova, Z., Shuralyova, I. & Coe, I. R. The adenosine transporter, mENT1, is a target for adenosine receptor signaling and protein kinase Cepsilon in hypoxic and pharmacological preconditioning in the mouse cardiomyocyte cell line, HL-1. *J. Pharmacol. Exp. Ther.* **310**, 1190–8 (2004).
 67. Aymerich, I., Pastor-Anglada, M. & Casado, F. J. Long term endocrine regulation of nucleoside transporters in rat intestinal epithelial cells. *J. Gen. Physiol.* **124**, 505–12 (2004).
 68. Guillén-Gómez, E., *et al.* New role of the human equilibrative nucleoside transporter 1 (hENT1) in epithelial-to-mesenchymal transition in renal tubular cells. *J. Cell. Physiol.* **227**, 1521–8 (2012).
 69. Liu, Z.-Q., *et al.* Prognostic value of human equilibrative nucleoside transporter1 in pancreatic cancer receiving gemcitabine-based chemotherapy: a meta-analysis. *PLoS One* **9**, e87103 (2014).
 70. Clarke, M. L., Mackey, J. R., Baldwin, S. A., Young, J. D. & Cass, C. E. in *Clinically Relevant Resistance in Cancer Chemotherapy* 27–47 (2002).
 71. Takagaki, K., *et al.* Gene-expression profiling reveals down-regulation of equilibrative nucleoside transporter 1 (ENT1) in Ara-C-resistant CCRF-CEM-derived cells. *J. Biochem.* **136**, 733–40 (2004).
 72. Leisewitz, A. V, *et al.* Regulation of ENT1 expression and ENT1-dependent nucleoside transport by c-Jun N-terminal kinase. *Biochem. Biophys. Res. Commun.* **404**, 370–5 (2011).
 73. Cohen, P. The origins of protein phosphorylation. *Nat. Cell Biol.* **4**, E127–30 (2002).
 74. Ashcroft, M., Kubbutat, M. H. & Vousden, K. H. Regulation of p53 function and stability by phosphorylation. *Mol. Cell. Biol.* **19**, 1751–8 (1999).
 75. Grimard, V., *et al.* Phosphorylation-induced conformational changes of cystic fibrosis transmembrane conductance regulator monitored by attenuated total reflection-Fourier transform IR spectroscopy and fluorescence spectroscopy. *J. Biol. Chem.* **279**, 5528–36 (2004).
 76. Foster, J. D., Pananusorn, B. & Vaughan, R. A. Dopamine transporters are phosphorylated on N-terminal serines in rat striatum. *J. Biol. Chem.* **277**, 25178–86 (2002).
 77. Cervinski, M. A., Foster, J. D. & Vaughan, R. A. Syntaxin 1A regulates dopamine transporter activity, phosphorylation and surface expression. *Neuroscience* **170**, 408–16 (2010).
 78. van Balkom, B. W. M., *et al.* The role of putative phosphorylation sites in the targeting and shuttling of the aquaporin-2 water channel. *J. Biol. Chem.* **277**, 41473–9 (2002).

79. Reyes, G., *et al.* The Equilibrative Nucleoside Transporter (ENT1) can be phosphorylated at multiple sites by PKC and PKA. *Mol. Membr. Biol.* **28**, 412–26 (2011).
80. Jayanthi, L. D., Samuvel, D. J., Blakely, R. D. & Ramamoorthy, S. Evidence for biphasic effects of protein kinase C on serotonin transporter function, endocytosis, and phosphorylation. *Mol. Pharmacol.* **67**, 2077–87 (2005).
81. Jayanthi, L. D., Annamalai, B., Samuvel, D. J., Gether, U. & Ramamoorthy, S. Phosphorylation of the norepinephrine transporter at threonine 258 and serine 259 is linked to protein kinase C-mediated transporter internalization. *J. Biol. Chem.* **281**, 23326–40 (2006).
82. Coe, I. R., Yao, L., Diamond, I. & Gordon, A. S. The Role of Protein Kinase C in Cellular Tolerance to Ethanol. *J. Biol. Chem.* **271**, 29468–29472 (1996).
83. Grden, M., *et al.* High glucose suppresses expression of equilibrative nucleoside transporter 1 (ENT1) in rat cardiac fibroblasts through a mechanism dependent on PKC-zeta and MAP kinases. *J. Cell. Physiol.* **215**, 151–60 (2008).
84. Hughes, S. J., Cravetchi, X., Vilas, G. & Hammond, J. R. Adenosine A1 receptor activation modulates human equilibrative nucleoside transporter 1 (hENT1) activity via PKC-mediated phosphorylation of serine-281. *Cell. Signal.* **27**, 1008–18 (2015).
85. Bone, D. B. J., Robillard, K. R., Stolk, M. & Hammond, J. R. Differential regulation of mouse equilibrative nucleoside transporter 1 (mENT1) splice variants by protein kinase CK2. *Mol. Membr. Biol.* **24**, 294–303
86. Stolk, M., Cooper, E., Vilk, G., Litchfield, D. W. & Hammond, J. R. Subtype-specific regulation of equilibrative nucleoside transporters by protein kinase CK2. *Biochem. J.* **386**, 281–9 (2005).
87. Fernández Calotti, P., *et al.* Modulation of the human equilibrative nucleoside transporter1 (hENT1) activity by IL-4 and PMA in B cells from chronic lymphocytic leukemia. *Biochem. Pharmacol.* **75**, 857–65 (2008).
88. Ellory, C. Radiation inactivation for molecular size determinations. *Trends Biochem. Sci.* **4**, N99–N100 (1979).
89. Jarvis, S. M., Young, J. D. & Ellory, J. C. Nucleoside transport in human erythrocytes. Apparent molecular weight of the nitrobenzylthioinosine-binding complex estimated by radiation-inactivation analysis. *Biochem. J.* **190**, 373–6 (1980).
90. Clive J. Young, J. D. J. S. M. E. Radiation inactivation of the human erythrocyte nucleoside and glucose transporters. *Biochim. Biophys. Acta* **855**, 312–315 (1986).
91. Cunningham, F. STRUCTURE-FUNCTION ANALYSIS OF THE HUMAN EQUILIBRATIVE NUCLEOSIDE TRANSPORTER 1. (University of Western Ontario, 2011).
92. Lemmon, M. A., *et al.* Glycophorin A dimerization is driven by specific interactions between transmembrane alpha-helices. *J. Biol. Chem.* **267**, 7683–9 (1992).
93. Adams, P. D., Engelman, D. M. & Brünger, A. T. Improved prediction for the structure of the dimeric transmembrane domain of glycophorin A obtained through global searching. *Proteins* **26**, 257–61 (1996).
94. MacKenzie, K. R., Prestegard, J. H. & Engelman, D. M. A transmembrane helix dimer: structure and implications. *Science* **276**, 131–3 (1997).

95. Russ, W. P. & Engelman, D. M. The GxxxG motif: a framework for transmembrane helix-helix association. *J. Mol. Biol.* **296**, 911–9 (2000).
96. Zottola, R. J., *et al.* Glucose Transporter Function Is Controlled by Transporter Oligomeric Structure. A Single, Intramolecular Disulfide Promotes GLUT1 Tetramerization. *Biochemistry* **34**, 9734–9747 (1995).
97. Sun, G.-C., *et al.* GPCR dimerization in brainstem nuclei contributes to the development of hypertension. *Br. J. Pharmacol.* **172**, 2507–18 (2015).
98. Choi, D.-S., *et al.* The type 1 equilibrative nucleoside transporter regulates ethanol intoxication and preference. *Nat. Neurosci.* **7**, 855–61 (2004).
99. Chen, J., *et al.* The type 1 equilibrative nucleoside transporter regulates anxiety-like behavior in mice. *Genes. Brain. Behav.* **6**, 776–83 (2007).
100. Shan, D., Haroutunian, V., Meador-Woodruff, J. H. & McCullumsmith, R. E. Expression of equilibrative nucleoside transporter type 1 protein in elderly patients with schizophrenia. *Neuroreport* **23**, 224–7 (2012).
101. Xu, Z., *et al.* ENT1 inhibition attenuates epileptic seizure severity via regulation of glutamatergic neurotransmission. *Neuromolecular Med.* **17**, 1–11 (2015).
102. Warraich, S., *et al.* Loss of equilibrative nucleoside transporter 1 in mice leads to progressive ectopic mineralization of spinal tissues resembling diffuse idiopathic skeletal hyperostosis in humans. *J. Bone Miner. Res.* **28**, 1135–49 (2013).
103. Al-Massaied, A. L. & Craik, J. D. Decreased nucleoside transport and hENT1 transporter expression in beta-thalassemia major. *Med. Princ. Pract.* **18**, 180–6 (2009).
104. Robin, E., Sabourin, J., Marcillac, F. & Raddatz, E. Involvement of CD73, equilibrative nucleoside transporters and inosine in rhythm and conduction disturbances mediated by adenosine A1 and A2A receptors in the developing heart. *J. Mol. Cell. Cardiol.* **63**, 14–25 (2013).
105. Zimmerman, M. A., *et al.* Equilibrative nucleoside transporter (ENT)-1-dependent elevation of extracellular adenosine protects the liver during ischemia and reperfusion. *Hepatology* **58**, 1766–78 (2013).
106. Rose, J. B., *et al.* Absence of equilibrative nucleoside transporter 1 in ENT1 knockout mice leads to altered nucleoside levels following hypoxic challenge. *Life Sci.* **89**, 621–30 (2011).
107. Murray, C. L. Global, regional, and national age–sex specific all-cause and cause-specific mortality for 240 causes of death, 1990–2013: a systematic analysis for the Global Burden of Disease Study 2013. *Lancet* **385**, 117–71 (2014).
108. Rose, J. B., *et al.* Equilibrative nucleoside transporter 1 plays an essential role in cardioprotection. *Am. J. Physiol. Heart Circ. Physiol.* **298**, H771–7 (2010).
109. Mubagwa, K. Adenosine, adenosine receptors and myocardial protection An updated overview. *Cardiovasc. Res.* **52**, 25–39 (2001).
110. Luo, F., *et al.* Extracellular adenosine levels are associated with the progression and exacerbation of pulmonary fibrosis. *FASEB J.* (2015). doi:10.1096/fj.15-274845
111. Driver, A. G., Kukoly, C. A., Ali, S. & Mustafa, S. J. Adenosine in bronchoalveolar lavage fluid in

- asthma. *Am. Rev. Respir. Dis.* **148**, 91–7 (1993).
112. Huang, M., Wang, Y., Cogut, S. B., Mitchell, B. S. & Graves, L. M. Inhibition of nucleoside transport by protein kinase inhibitors. *J. Pharmacol. Exp. Ther.* **304**, 753–60 (2003).
 113. Damaraju, V. L., Kuzma, M., Mowles, D., Cass, C. E. & Sawyer, M. B. Interactions of multitargeted kinase inhibitors and nucleoside drugs: Achilles heel of combination therapy? *Mol. Cancer Ther.* **14**, 236–45 (2015).
 114. Wittfeldt, A., *et al.* Ticagrelor enhances adenosine-induced coronary vasodilatory responses in humans. *J. Am. Coll. Cardiol.* **61**, 723–7 (2013).
 115. Armstrong, D., *et al.* Characterization of the adenosine pharmacology of ticagrelor reveals therapeutically relevant inhibition of equilibrative nucleoside transporter 1. *J. Cardiovasc. Pharmacol. Ther.* **19**, 209–19 (2014).
 116. van den Berg, T. N. A., *et al.* Ticagrelor Does Not Inhibit Adenosine Transport at Relevant Concentrations: A Randomized Cross-Over Study in Healthy Subjects In Vivo. *PLoS One* **10**, e0137560 (2015).
 117. Jordheim, L. P., Durantel, D., Zoulim, F. & Dumontet, C. Advances in the development of nucleoside and nucleotide analogues for cancer and viral diseases. *Nat. Rev. Drug Discov.* **12**, 447–64 (2013).
 118. Naderkhani, E., Erber, A., Škalko-Basnet, N. & Flaten, G. E. Improved permeability of acyclovir: optimization of mucoadhesive liposomes using the phospholipid vesicle-based permeation assay. *J. Pharm. Sci.* **103**, 661–8 (2014).
 119. Spratlin, J., *et al.* The absence of human equilibrative nucleoside transporter 1 is associated with reduced survival in patients with gemcitabine-treated pancreas adenocarcinoma. *Clin. Cancer Res.* **10**, 6956–61 (2004).
 120. Pastor-Anglada, M. & Pérez-Torras, S. Nucleoside transporter proteins as biomarkers of drug responsiveness and drug targets. *Front. Pharmacol.* **6**, 13 (2015).
 121. Endres, C. J., *et al.* The role of the equilibrative nucleoside transporter 1 (ENT1) in transport and metabolism of ribavirin by human and wild-type or Ent1-/- mouse erythrocytes. *J. Pharmacol. Exp. Ther.* **329**, 387–98 (2009).
 122. Iikura, M., *et al.* ENT1, a ribavirin transporter, plays a pivotal role in antiviral efficacy of ribavirin in a hepatitis C virus replication cell system. *Antimicrob. Agents Chemother.* **56**, 1407–13 (2012).
 123. Parker, M. D., *et al.* Identification of a nucleoside/nucleobase transporter from *Plasmodium falciparum*, a novel target for anti-malarial chemotherapy. *Biochem. J.* **349**, 67–75 (2000).
 124. Aran, J. M. & Plagemann, P. G. W. Nucleoside transport-deficient mutants of PK-15 pig kidney cell line. *Biochim. Biophys. Acta - Biomembr.* **1110**, 51–58 (1992).
 125. Blom, N., Gammeltoft, S. & Brunak, S. Sequence and structure-based prediction of eukaryotic protein phosphorylation sites. *J. Mol. Biol.* **294**, 1351–62 (1999).
 126. Grenz, A., *et al.* Equilibrative nucleoside transporter 1 (ENT1) regulates postischemic blood flow during acute kidney injury in mice. *J. Clin. Invest.* **122**, 693–710 (2012).
 127. Henry, P., Demolombe, S., Pucéat, M. & Escande, D. Adenosine A1 stimulation activates delta-

- protein kinase C in rat ventricular myocytes. *Circ. Res.* **78**, 161–5 (1996).
128. Liu, A. M. F. & Wong, Y. H. G16-mediated activation of nuclear factor kappaB by the adenosine A1 receptor involves c-Src, protein kinase C, and ERK signaling. *J. Biol. Chem.* **279**, 53196–204 (2004).
 129. Minelli, A., Bellezza, I., Collodel, G. & Fredholm, B. B. Promiscuous coupling and involvement of protein kinase C and extracellular signal-regulated kinase 1/2 in the adenosine A1 receptor signalling in mammalian spermatozoa. *Biochem. Pharmacol.* **75**, 931–41 (2008).
 130. Luderman, K. D., Chen, R., Ferris, M. J., Jones, S. R. & Gnegy, M. E. Protein kinase C beta regulates the D₂-like dopamine autoreceptor. *Neuropharmacology* **89**, 335–41 (2015).
 131. Heldin, C.-H. Dimerization of cell surface receptors in signal transduction. *Cell* **80**, 213–223 (1995).
 132. Ullrich, A. & Schlessinger, J. Signal transduction by receptors with tyrosine kinase activity. *Cell* **61**, 203–212 (1990).
 133. Baan, B., Pardali, E., ten Dijke, P. & van Dam, H. In situ proximity ligation detection of c-Jun/AP-1 dimers reveals increased levels of c-Jun/Fra1 complexes in aggressive breast cancer cell lines in vitro and in vivo. *Mol. Cell. Proteomics* **9**, 1982–90 (2010).
 134. Møller, M., *et al.* Small angle X-ray scattering studies of mitochondrial glutaminase C reveal extended flexible regions, and link oligomeric state with enzyme activity. *PLoS One* **8**, e74783 (2013).
 135. Li, X., Alvarez, B., Casey, J. R., Reithmeier, R. A. F. & Fliegel, L. Carbonic anhydrase II binds to and enhances activity of the Na⁺/H⁺ exchanger. *J. Biol. Chem.* **277**, 36085–91 (2002).
 136. Thomas, J. & Kornberg, R. The study of histone--histone associations by chemical cross-linking. *Methods Cell Biol.* (1977).
 137. Milligan, D. L. & Koshland, D. E. Site-directed cross-linking. Establishing the dimeric structure of the aspartate receptor of bacterial chemotaxis. *J. Biol. Chem.* **263**, 6268–75 (1988).
 138. Gajadhar, A. & Guha, A. A proximity ligation assay using transiently transfected, epitope-tagged proteins: application for in situ detection of dimerized receptor tyrosine kinases. *Biotechniques* **48**, 145–52 (2010).
 139. Söderberg, O., *et al.* Direct observation of individual endogenous protein complexes in situ by proximity ligation. *Nat. Methods* **3**, 995–1000 (2006).
 140. Spears, M., *et al.* In situ detection of HER2:HER2 and HER2:HER3 protein-protein interactions demonstrates prognostic significance in early breast cancer. *Breast Cancer Res. Treat.* **132**, 463–70 (2012).
 141. Reithmeier, R. A. A membrane metabolon linking carbonic anhydrase with chloride/bicarbonate anion exchangers. *Blood Cells. Mol. Dis.* **27**, 85–9 (2001).
 142. Vilas, G., *et al.* Increased water flux induced by an aquaporin-1/carbonic anhydrase II interaction. *Mol. Biol. Cell* **26**, 1106–1118 (2015).
 143. Moser, G. H., Schrader, J. & Deussen, A. Turnover of adenosine in plasma of human and dog blood. *Am J Physiol Cell Physiol* **256**, C799–806 (1989).

144. Ciruela, F., *et al.* Adenosine deaminase affects ligand-induced signalling by interacting with cell surface adenosine receptors. *FEBS Lett.* **380**, 219–23 (1996).
145. Lai, K. M. & Wong, P. C. Metabolism of extracellular adenine nucleotides by cultured rat brain astrocytes. *J. Neurochem.* **57**, 1510–5 (1991).
146. Bennett, K. L., *et al.* Chemical cross-linking with thiol-cleavable reagents combined with differential mass spectrometric peptide mapping--a novel approach to assess intermolecular protein contacts. *Protein Sci.* **9**, 1503–18 (2000).
147. Sinz, A. Chemical cross-linking and mass spectrometry to map three-dimensional protein structures and protein-protein interactions. *Mass Spectrom. Rev.* **25**, 663–82 (2006).
148. Ruepp, A., *et al.* CORUM: the comprehensive resource of mammalian protein complexes. *Nucleic Acids Res.* **36**, D646–50 (2008).
149. Graham, F. L. & van der Eb, A. J. A new technique for the assay of infectivity of human adenovirus 5 DNA. *Virology* **52**, 456–467 (1973).
150. Klotz, K.-N., *et al.* 2-Chloro-N6-[3H]cyclopentyladenosine ([3HCCPA]) ?a high affinity agonist radioligand for A1 adenosine receptors. *Naunyn-Schmiedebergs Arch. Pharmacol.* **340**, 679–683 (1989).
151. Martinson, E. A., Johnson, R. A. & Wells, J. N. Potent adenosine receptor antagonists that are selective for the A1 receptor subtype. *Mol. Pharmacol.* **31**, 247–52 (1987).
152. Pressacco, J., Wiley, J. S., Jamieson, G. P., Erlichman, C. & Hedley, D. W. Modulation of the equilibrative nucleoside transporter by inhibitors of DNA synthesis. *Br. J. Cancer* **72**, 939–42 (1995).
153. Apparsundaram, S., Sung, U., Price, R. D. & Blakely, R. D. Trafficking-dependent and -independent pathways of neurotransmitter transporter regulation differentially involving p38 mitogen-activated protein kinase revealed in studies of insulin modulation of norepinephrine transport in SK-N-SH cells. *J. Pharmacol. Exp. Ther.* **299**, 666–77 (2001).
154. Sweeney, G. & Klip, A. Regulation of the Na⁺/K⁺-ATPase by insulin: why and how? *Mol. Cell. Biochem.* **182**, 121–33 (1998).
155. Jarvis, S. M., Martin, B. W. & Ng, A. S. 2-Chloroadenosine, a permeant for the nucleoside transporter. *Biochem. Pharmacol.* **34**, 3237–3241 (1985).
156. Liu, S., *et al.* Phosphodiesterases coordinate cAMP propagation induced by two stimulatory G protein-coupled receptors in hearts. *Proc. Natl. Acad. Sci. U. S. A.* **109**, 6578–83 (2012).
157. Vilas, G. L., *et al.* Oligomerization of SLC4A11 protein and the severity of FECD and CHED2 corneal dystrophies caused by SLC4A11 mutations. *Hum. Mutat.* **33**, 419–28 (2012).
158. Jalimarada, S. S., Ogando, D. G., Vithana, E. N. & Bonanno, J. A. Ion transport function of SLC4A11 in corneal endothelium. *Invest. Ophthalmol. Vis. Sci.* **54**, 4330–40 (2013).
159. Söderberg, O., *et al.* Characterizing proteins and their interactions in cells and tissues using the in situ proximity ligation assay. *Methods* **45**, 227–32 (2008).
160. Jackman, J. & O'Connor, P. M. Methods for synchronizing cells at specific stages of the cell cycle. *Curr. Protoc. Cell Biol.* **Chapter 8**, Unit 8.3 (2001).

161. Rosner, M., Schipany, K. & Hengstschläger, M. Merging high-quality biochemical fractionation with a refined flow cytometry approach to monitor nucleocytoplasmic protein expression throughout the unperturbed mammalian cell cycle. *Nat. Protoc.* **8**, 602–26 (2013).
162. Vyas, S., Ahmadi, B. & Hammond, J. R. Complex effects of sulfhydryl reagents on ligand interactions with nucleoside transporters: evidence for multiple populations of ENT1 transporters with differential sensitivities to N-ethylmaleimide. *Arch. Biochem. Biophys.* **403**, 92–102 (2002).
163. Chatr-Aryamontri, A., *et al.* The BioGRID interaction database: 2015 update. *Nucleic Acids Res.* **43**, D470–8 (2015).
164. Xenarios, I., *et al.* DIP, the Database of Interacting Proteins: a research tool for studying cellular networks of protein interactions. *Nucleic Acids Res.* **30**, 303–5 (2002).
165. Orchard, S., *et al.* The MIntAct project—IntAct as a common curation platform for 11 molecular interaction databases. *Nucleic Acids Res.* **42**, D358–63 (2014).
166. Dempski, R. E., Lustig, J., Friedrich, T. & Bamberg, E. Structural arrangement and conformational dynamics of the gamma subunit of the Na⁺/K⁺-ATPase. *Biochemistry* **47**, 257–66 (2008).
167. Pierre, S. V & Xie, Z. The Na,K-ATPase receptor complex: its organization and membership. *Cell Biochem. Biophys.* **46**, 303–16 (2006).
168. Lingrel, J. B., Orłowski, J., Shull, M. M. & Price, E. M. Molecular genetics of Na,K-ATPase. *Prog. Nucleic Acid Res. Mol. Biol.* **38**, 37–89 (1990).
169. Efendiev, R., *et al.* Simultaneous phosphorylation of Ser11 and Ser18 in the alpha-subunit promotes the recruitment of Na⁽⁺⁾,K⁽⁺⁾-ATPase molecules to the plasma membrane. *Biochemistry* **39**, 9884–92 (2000).
170. Bertorello, A. M., *et al.* Analysis of Na⁺,K⁺-ATPase motion and incorporation into the plasma membrane in response to G protein-coupled receptor signals in living cells. *Mol. Biol. Cell* **14**, 1149–57 (2003).
171. Lorent, J. H. & Levental, I. Structural determinants of protein partitioning into ordered membrane domains and lipid rafts. *Chem. Phys. Lipids* (2015). doi:10.1016/j.chemphyslip.2015.07.022
172. Vagin, O., Tokhtaeva, E. & Sachs, G. The role of the beta1 subunit of the Na,K-ATPase and its glycosylation in cell-cell adhesion. *J. Biol. Chem.* **281**, 39573–87 (2006).
173. Clifford, R. J. & Kaplan, J. H. β -Subunit overexpression alters the stoichiometry of assembled Na-K-ATPase subunits in MDCK cells. *AJP Ren. Physiol.* **295**, F1314–F1323 (2008).
174. Barwe, S. P., Kim, S., Rajasekaran, S. A., Bowie, J. U. & Rajasekaran, A. K. Janus model of the Na,K-ATPase beta-subunit transmembrane domain: distinct faces mediate alpha/beta assembly and beta-beta homo-oligomerization. *J. Mol. Biol.* **365**, 706–14 (2007).

APPENDICES

NATURE PUBLISHING GROUP LICENSE TERMS AND CONDITIONS

Nov 13, 2015

This is a License Agreement between Xenia Cravetchi ("You") and Nature Publishing Group ("Nature Publishing Group") provided by Copyright Clearance Center ("CCC"). The license consists of your order details, the terms and conditions provided by Nature Publishing Group, and the payment terms and conditions.

All payments must be made in full to CCC. For payment instructions, please see information listed at the bottom of this form.

License Number	3747150111349
License date	Nov 13, 2015
Licensed content publisher	Nature Publishing Group
Licensed content publication	Nature Reviews Cancer
Licensed content title	Immunity, inflammation and cancer: a leading role for adenosine
Licensed content author	Luca Antonioli, Corrado Blandizzi, Pál Pacher, György Haskó
Licensed content date	Nov 14, 2013
Volume number	13
Issue number	12
Type of Use	reuse in a dissertation / thesis
Requestor type	academic/educational
Format	print and electronic
Portion	figures/tables/illustrations
Number of figures/tables/illustrations	1
High-res required	no
Figures	Figure 1, p844 (signalling through adenosine receptors)
Author of this NPG article	no
Your reference number	None
Title of your thesis / dissertation	Regulation and Quaternary Structure of Human Equilibrative Nucleoside Transporter 1
Expected completion date	Jan 2016
Estimated size (number of pages)	100
Total	0.00 CAD
Terms and Conditions	

Terms and Conditions for Permissions

Nature Publishing Group hereby grants you a non-exclusive license to reproduce this material for this purpose, and for no other use, subject to the conditions below: